INVESTIGATION OF THE RHEOLOGICAL AND WORKABILITY PROPERTIES OF CONSTRUCTION AND DEMOLITION WASTE BASED GEOPOLYMER MORTARS

İNŞAAT YIKINTI ATIKLARI KULLANILARAK TASARLANAN JEOPOLİMER BAĞLAYICILI HARÇLARIN REOLOJİK VE İŞLENEBİLİRLİK ÖZELLİKLERİNİN İNCELENMESİ

HÜSEYİN İLCAN

PROF. DR. MUSTAFA ŞAHMARAN
Supervisor

Submitted to
Graduate School of Science and Engineering of Hacettepe University
as a Partial Fullfillment to the Requirements for be Award of
the Degree of Master of Science in Civil Engineering

January 2021

ETHICS

In this thesis study, prepared in accordance with the spelling rules of Institute of Graduate School of Science and Engineering of Hacettepe University.

I declare that

- all the information and documents have been obtained in the base of the academic rules
- all audio-visual and written information and results have been presented according to the rules of scientific ethics
- in case of using others work, related studies have been cited in accordance with the scientific standards
- all cited studies have been fully referenced
- I did not do any distortion in the data set
- and any part of this thesis has not been presented as another thesis study at this or any other university.

20 /01 / 2021

HÜSEYİN İLCAN

YAYINLANMA FİKRİ MÜLKİYET HAKKLARI BEYANI

Enstitü tarafından onaylanan lisansüstü tezimin/raporumun tamamını veya herhangi bir kısmını, basılı (kağıt) ve elektronik formatta arşivleme ve aşağıda verilen koşullarla kullanıma açma iznini Hacettepe üniversitesine verdiğimi bildiririm. Bu izinle Üniversiteye verilen kullanım hakları dışındaki tüm fikri mülkiyet haklarım bende kalacak, tezimin tamamının ya da bir bölümünün gelecekteki çalışmalarda (makale, kitap, lisans ve patent vb.) kullanım hakları bana ait olacaktır.

Tezin kendi orijinal çalışmam olduğunu, başkalarının haklarını ihlal etmediğimi ve tezimin tek yetkili sahibi olduğumu beyan ve taahhüt ederim. Tezimde yer alan telif hakkı bulunan ve sahiplerinden yazılı izin alınarak kullanması zorunlu metinlerin yazılı izin alarak kullandığımı ve istenildiğinde suretlerini Üniversiteye teslim etmeyi taahhüt ederim.

Yükseköğretim Kurulu tarafından yayınlanan "***Lisansüstü Tezlerin Elektronik Ortamda Toplanması, Düzenlenmesi ve Erişime Açılmasına İlişkin Yönerge***" kapsamında tezim aşağıda belirtilen koşullar haricince YÖK Ulusal Tez Merkezi / H. Ü. Kütüphaneleri Açık Erişim Sisteminde erişime açılır.

☐ Enstitü / Fakülte yönetim kurulu kararı ile tezimin erişime açılması mezuniyet tarihimden itibaren 2 yıl ertelenmiştir.

☐ Enstitü / Fakülte yönetim kurulu gerekçeli kararı ile tezimin erişime açılması mezuniyet tarihimden itibaren .... ay ertelenmiştir.

☐ Tezim ile ilgili gizlilik kararı verilmiştir.

20 / 01 2020

HÜSEYİN İLCAN

ABSTRACT

INVESTIGATION OF THE RHEOLOGICAL AND WORKABILITY PROPERTIES OF CONSTRUCTION AND DEMOLITION WASTE BASED GEOPOLYMER MORTARS

HÜSEYİN İLCAN

Master of Science, Department of Civil Engineering

Supervisor: Prof. Dr. Mustafa ŞAHMARAN

January 2021, 164 pages

Being the most widely used construction material, concrete brings about considerable challenges. Portland cement (PC), main binding material for concrete, creates enormous negative impacts mainly due to the high energy requirement for its production and associated release of greenhouse gases. Production of PC and concrete encompasses a series of steps which require involvement of natural resources such as water, aggregates, clay, limestone and gypsum, which leads to detrimental effects for environment as well. Considering that, minimizing the usage of cementitious materials would clearly increase the environmental benefits such as reduced energy consumption, CO_2 emissions and raw material use. This therefore has led researchers to search for the development of environmentally-friendly construction materials. Efforts within the recent years resulted in novel concepts of new generation binder materials termed as alkali-activated materials or geopolymers, that are successful candidates to partially or fully substitute PC.

Geopolymers are inorganic polymers that are formed as a result of the reaction between aluminosilicate source materials (i.e. precursors) and alkaline activators (e.g. solutions of alkali-hydroxide/-silicate). Among different aluminosilicate precursors used in geopolymer technology, mineral admixtures such as blast furnace slag, fly ash, silica fume and metakaolin are prevalent while as different alkaline activators, sodium

hydroxide potassium hydroxide, calcium hydroxide, sodium silicate are used more commonly. However, these precursors are highly demanded given their successful utilization concrete mixtures as mineral admixtures for years. Therefore, increasing attention was started to be paid on aluminosilicate precursors that are not strongly demanded by concrete industry.

As a result of the urban transformation, which is mainly based on demolishment and reconstruction, millions of buildings are transformed each year upon completing their service life and/or reaching to a state that is dangerous to their dwellers and environment. What to do with the tremendous amounts of Construction and Demolition Waste (CDW) created is a question of huge debate globally and CDW mostly ends up being landfilled, which requires immense areas of storage and is very costly health-/economy-/environment-wise. One effective way for the proper CDW handling is to utilize CDW components in producing geopolymers. This is reasonable given the fact that CDW generation is a global problem and CDW can be easily found anywhere in the world.

In this study, it was aimed to analyze effects of activators type, usage rates and combinations on rheological and workability performance of CDW based geopolymer matrix. In that context, at first, mortar phase composed of wall and roof members including bricks, tiles, glass waste and concrete waste in which recycled aggregate was utilized, was investigated with empirical test methods. For detailed investigation, rheometer was used to understand rheological and workability characteristic of CDW based geopolymer in addition to empirical test methods. In that way, know-how about rheological and workability performance of CDW based geopolymer was formed as well as mechanical performance and it was made possible to select the correct activator according to the application needs by using the results of the thesis study.

Keywords: Alkali Activated Materials, Geopolymer, Construction and Demolition Waste, Rheology, Workability, Alkali Activator

ÖZET

İNŞAAT YIKINTI ATIKLARI KULLANILARAK TASARLANAN JEOPOLİMER BAĞLAYICILI HARÇLARIN REOLOJİK VE İŞLENEBİLİRLİK ÖZELLİKLERİNİN İNCELENMESİ

HÜSEYİN İLCAN

Yüksek Lisans, İnşaat Mühendisliği Bölümü
Tez Danışmanı: Prof. Dr. Mustafa ŞAHMARAN
Ocak 2021, 164 sayfa

En yaygın kullanılan yapı malzemesi olan beton, önemli zorlukları beraberinde getirir. Beton için ana bağlayıcı malzeme olan portland çimentosu (PÇ), üretimi için yüksek enerji gereksinimi ve buna bağlı sera gazı salınımı nedeniyle çok büyük olumsuz etkilere sebep olur. PÇ ve beton üretimi, su, agrega, kil, kireçtaşı ve alçıtaşı gibi doğal kaynakların dahil edilmesini gerektiren ve çevre için de zararlı etkilere yol açan bir dizi adımı kapsar. Çimento esaslı malzemelerin kullanımının en aza indirilmesi, indirgenmiş enerji tüketimi, CO2 emisyonları ve hammadde kullanımı gibi çevresel faydaları net bir şekilde artıracaktır. Bu nedenle, araştırmacıları çevre dostu inşaat malzemeleri geliştirmeye yöneltmiştir. Son yıllardaki çabalar, PÇ'yi kısmen veya tamamen ikame etmek için başarılı alternatif olan, alkali ile aktive edilmiş malzemeler veya jeopolimerler olarak adlandırılan yeni nesil bağlayıcı malzemelerin buluşuyla sonuçlandı.

Jeopolimerler, alüminosilikat içeren malzemeler (yani prekürsörler) ile alkali aktivatörler (örneğin alkali-hidroksit / -silikat çözeltileri) arasındaki reaksiyonun bir sonucu olarak oluşan inorganik polimerlerdir. Jeopolimer teknolojisinde kullanılan farklı alüminosilikat prekürsör arasında yüksek fırın cürufu, uçucu kül, silika dumanı ve metakaolin gibi mineral katkılar yaygınken, farklı alkali aktivatörler olarak sodyum hidroksit potasyum hidroksit, kalsiyum hidroksit, sodyum silikat daha yaygın olarak kullanılmaktadır.

Bununla birlikte, bu prekürsörler, beton karışımlarını yıllarca mineral katkı olarak başarılı bir şekilde kullandıkları için oldukça talep görmektedir. Bu nedenle, beton endüstrisi tarafından çok fazla talep edilmeyen alüminosilikat prekürsörlerine artan bir ilgi gösterilmeye başlandı.

Yıkıma ve yeniden yapılanmaya dayalı kentsel dönüşüm sonucunda her yıl milyonlarca bina hizmet ömürlerini tamamlayarak ve / veya sakinleri ve çevre için tehlikeli bir duruma geldiklerinde dönüştürülüyor. Oluşan muazzam miktarlardaki İnşaat ve Yıkıntı Atıklarıyla (İYA) ne yapılacağı küresel olarak büyük bir tartışma konusudur ve CDW çoğunlukla depolanır ve atık sahasına bırakılır, bu durumda sağlık / ekonomi / çevre açısından çok maliyetli olan muazzam depolama alanları gerektirir. İYA'yı doğru işlemenin etkili bir yolu, jeopolimerlerin üretiminde İYA tabanlı bileşenleri kullanmaktır. İYA üretiminin küresel olarak sorunlu bir konu olduğu ve İYA'nın dünyanın hemen her yerinde kolayca bulunabileceği göz önüne alındığında bu şekilde kullanmak mantıklıdır.

Bu çalışmada, aktivatör tipinin, kullanım oranlarının ve kombinasyonlarının CDW tabanlı jeopolimer matrisin reolojik ve işlenebilirlik performansı üzerindeki etkilerinin incelenmesi amaçlanmıştır. Bu kapsamda ilk olarak geri dönüştürülmüş agrega kullanılan tuğla, kiremit, cam atıkları ve beton atıkları içeren duvar ve çatı elemanlarından oluşan harç fazı deneysel test yöntemleriyle incelenmiştir. Ayrıntılı araştırma için, reometre, deneysel test yöntemlerine ek olarak CDW bazlı jeopolimerin reolojik ve işlenebilirlik özelliklerini anlamak için kullanılmıştır. Böylelikle mekanik performansın yanı sıra CDW bazlı jeopolimerin reolojik ve işlenebilirlik performansı hakkında bilgi birikim (know-how) oluşturulmuş ve tez çalışmasının sonuçları kullanılarak uygulama ihtiyaçlarına göre doğru aktivatörün seçilmesi mümkün olmuştur.

Anahtar Kelimeler: Alkali Aktif Malzemeler, Jeopolimer, İnşaat ve Yıkıntı Atıkları, Reoloji, İşlenebilirlik, Alkali Aktivatör

ACKNOWLEDGEMENT

First, I have to express my gratitude to Prof. Dr. Mustafa ŞAHMARAN, my supervisor for the patient guidance, encouragement, and valuable advice during my thesis study.

Also, I have to give thanks to Prof. Dr. İsmail Özgür YAMAN, Prof. Dr. İlhami DEMİR, Assoc. Prof. Dr. Mustafa Kerem KOÇKAR, Assoc. Prof. Dr. Gürkan YILDIRIM for giving me the opportunity to defend my master thesis.

I would like to express my gratitude to all my colleagues at Hacettepe University for their support and valuable friendship.

I gratefully would like to give thanks to TUBITAK BİDEB-2210 for providing scholarship during my graduate study.

Lastly, I would like to thank my family for generous support during the completion of this study. Especially, I wish to express my deepest gratitude to my wife, since she supported and helped me while working on thesis study. This accomplishment would not have been possible without them.

Endless thanks...

HÜSEYİN İLCAN
January 2021, Ankara

TABLE OF CONTENTS

LIST OF TABLES

LIST OF FIGURES

SYMBOLS AND ABBREVIATIONS

Abbreviations

BFS	Blast Furnace Slag
$Ca(OH)_2$	Calcium Hydroxide
CDW	Construction Demolition Wastes
CW	Concrete Waste
FA	Fly Ash
GBFS	Ground Granulated Blast Furnace Slag
GW	Glass Waste
HB	Hollow Brick
Na_2SiO_3	Sodium Silicate
NaOH	Sodium Hydroxide
RCB	Red Clay Brick
RT	Roof Tile
SEM	Scanning Electron Microscopy
XRD	X-ray Diffraction Analysis
3ITT	Three Interval Thixotropy Test
Γ	Flowability Index
RCA	Recycled Concrete Aggregate
SF	Silica Fume
CC	Calcined Clay
AAS	Alkali Activated Slag
AAM	Alkali Activated Material
GCW	Ground Concrete Waste
S/B	Sand /Binder
W/B	Water/Binder

1. INTRODUCTION

Cement and concrete are at the center of modern civilization, with their confidence in the environment built to allow a superior quality of life. Concrete is the second widely utilized material all over the world after water (Aïtcin, 2000) and is manufactured in volumes of over 10 billion tons annually. Since, concrete is cheap, easily accessible and has high performance properties that meet application requirement for construction activities. However, cement production has a ~ 8% share of global CO_2 emissions (Scrivener & Kirkpatrick, 2008; Olivier et al., 2012). The total emission of cement production, approximately 0.8 tons CO_2 equivalent per ton, is shared between the emissions from burning fossil fuels and the CO_2 released by the conversion of calcium carbonate into its oxide form (Gartner, 2004). So, production of cement resulting high amount of CO_2 emission that causes the temperature of the atmosphere to rise, hence global warming. In addition to CO_2 emission, cement production causes to sulfur dioxide, nitrogen oxide and carbon monoxide formation in atmosphere. These gases are significantly harmful for human health, especially for the elder people. Besides emission of hazardous gases as a results of cement production, natural resources can be faced with depletion by virtue of higher production of concrete. Since cement could be obtained by grinding natural limestone and clay mixture, to produce excessive amounts of cement, natural limestone and clay will be consumed extremely. Also, natural aggregates, that its crushing process highly energy intensive, will be consumed to meet required amount of concrete production. This increment will significantly reduce access to these natural resources to be used in the future.

As the global community produces gradually increasing amounts of concrete to satisfy the infrastructural requirements of the developing world (Taylor et al., 2006), alternative cement-like binders are urgently needed to be created and commercialized. Considering the non-environmentally friendly nature of cement production, and the rapid increase in its use, there is a need for an alternative building material to cement based systems.

In that context, geopolymers could be alternative to cement-based matrix. Since it can show similar performance with cement-based system in various application area with lower environmental impacts (Gartner E, 2004). Geopolymer can exhibit wide range of

engineering characteristics in terms of improved compressive strength, rapid or long setting time, thermal conductivity, fire resistance according to used materials as precursor and activator used. Utilization of geopolymer during last decades become more popular in specific application area instead of Portland-Cement based cementitious systems. Geopolymer could be described as final products of geopolymerization reaction which is covering dissolution and polycondensation events where alkaline activators are utilized to prepare adequate medium for dissolution of precursor and formation of final products. In conventional geopolymer, mostly FA, SF, BFS, MK are used as precursor since they are aluminosilicate sources and each of them except MK is industrial waste and has no value. In that way, waste become raw materials and could be used to produce building materials that can carry load in structure as concrete.

Construction demolition waste (CDW) is a rapidly increasing concern in many countries. Environmental aspects of wastes from the construction industry have drawn extensive attention. in recent decades. In addition, the development and creation of new industrial goods from recycled materials has become increasingly important in recent years. In that context, several investigations have been carried in recent years to discuss the feasibility of utilizing industrial waste materials as raw materials in the geopolymer binder production. Researches showed that CDW materials that containing alumina silicate and calcium, has potential to be used as precursor in geopolymer production. And researches proved that CDW based geopolymer reached similar compressive strength performance with OPC-based concrete. However, CDW-based geopolymer needs to be investigated more to be commercialized as Ordinary Portland Cement (OPC) based concrete.

With the development in usage of CDW based geopolymer in order to make world green again by using waste materials as raw materials in concrete technology, knowledge about rheology of geopolymer become more essential for different advanced construction application such as self-leveling, shotcrete, three dimensional (3D) additive manufacturing. Therefore, to apply geopolymer in a work area as wide as concrete, rheology of geopolymer must be known down to the last detail. By enlarging application area of CDW based geopolymer by means of enhancing its properties with the knowledge of its rheology and mechanical properties in details, requirement for new landfill area, contamination of earth and groundwater resource, CO_2 emission, hazardous dust and

greenhouse gasses could be reduced. In addition, there is not much information about rheologic performance of CDW-based geopolymer in literature. Therefore, in that thesis, workability and rheological properties of CDW-based geopolymer systems together with mechanical properties are investigated. In that context, empirical and advanced test equipment are used to clarify how rheological and mechanical properties of CDW-based geopolymer with usage of various activator type, dosage and combination, changes.

2. LITERATURE REVIEW

2.1. Conventional Cement and Concrete

The bonding stage that supply strength to a modern concrete is generally depend on Portland cement (Hewlett, 1998). Portland cement is considered to be a low-tech material by society, but it has actually been a complicated combination of several mineral phases that have been produced to meet impermeability, durability, strength and passivation to reinforcements exposed to thermal, mechanical and chemical stresses for years. These characterizations have been achieved by chemists, materials scientists and engineers over many years of both industrial and academic research and development.

Portland cement consists of an excellent homogenized and finely grinded blend of limestone or calcium carbonate and a suitable amount of clay or shale at a temperature of about 1500 ^{o}C. The first version of calcium silicate cements binder was manufactured by the Greeks and Romans who found that finely grinded volcanic ash when blended with lime and water generated a weather-resistant hardened matrix. This mechanism is called as the pozzolanic reaction and forms the foundation of the benefit of materials such as FA, SF and MK to the strength and performance of concrete in modern version.

In the middle of 18th century, John Smeaton found out some adulterated lime (contain proper silica and alumina levels) have hydraulic characteristic. It means it had reactive silicates and aluminates that has ability to interact with water to obtain durable hydrates that prevent the movement of water. In 1759, this material was utilized by Smeaton during building of the Eddystone Lighthouse.

The "Portland cement" was initially described by Joseph Aspdin in patent No 5022 (1824). This was describing the systems for producing fabricated stone by blending lime with clay in the phase of a slurry and calcining dollops of dried material in a shaft lime kiln. Although Joseph Aspdin did not become the first to manufacture a calcium silicate cement, the patent he owned makes him first researcher for the finding of "Portland cement". Some researchers had already been working on this topic concurrently or before, in particularly Louis Vicat in France.

Produced cements in the 19th century were having a different composite composition regarding modern Portland cements because the used equipment did not reach required temperatures to form tricalcium silicate (C_3S), the main constituent mineral of modern cements. The dicalcium silicate (C_2S), lower reactivity, was the only source of silicate available in the matrix. At the end of the 19th century, the invention of the rotary kiln that produced a homogeneous product with a sufficiently high temperature consistently fulfilled the conditions required to achieve the formation of C_3S. In the 20th century, the form of the binder changed a few in the way of its chemistry and mineral composition, yet there have been significant enhancement in manufacturing techniques that resulted in developed efficiency in energy, advanced quality control, lowered detrimental impact on environment, and diminished labor work load. It shall be considered that the development of rotary kiln technics in the beginning of 20th century concur with the development of cement standards in the UK and the USA. These standards considered the strength of a final product to evaluate performance of matrix (Newman, 2003).

In addition to this information, concrete is a man-made building material that resemble stone. The word "concrete" is coming from the Latin word "concretus" which means "to grow together". Concrete is defined as a composite material comprised of coarse-grained material (aggregate or filler) located in a hard material medium (binder) that fills the gap between aggregate and bonds them each other. Generally, 15-20% cement (by total weight) is used as a binding material for concrete production. Although important information about the history of cement is given above, the temperature specified in Aspdin's study was not sufficient to manufacture exact Portland cement. Isaac Johnson was the first person, who burned the raw materials to clinker temperature in 1845 in order to produce modern version of PC. Thereafter, PC usage spread rapidly to Europe and North America (Li, 2011).

65-85% aggregate (by total weight) is used as a filling material in concrete. Aggregates have been another major component of concrete and contain materials such as clay, gravel, slag sand, crushed stone, and shale. Portland cement based plain concrete was defined as the first-generation concrete. 2nd generation concrete represented to reinforced concrete with steel bars. Francois Coignet was the first innovator in the application of reinforced concrete (Day & McNeil, 1996). Coignet began his experiment with iron reinforced concrete (Encyclopaedia Britannica, 1991). Hennebique realized, at the end of

19th century, that reinforced concrete was further developed, and the performance could be enhanced if the steel were used in the tensile zone.

As a structural material, 28-day compressive strength has been the main design index for concrete. There were a few senses to choose compressive strength as the performance indicator index. The first was mainly used to resist the compressive force in a concrete structure. Second, measuring the compressive strength requires a relatively easy process. Finally, it was considered that other characteristic of concrete could be depended to compressive strength via matrix microstructure. So, high compressive strength has become a critical aspect of concrete development. In 1918, Duff Adams discovered that the compressive strength of a concrete and water/binder ratio are inversely proportional to each other. Therefore, it has been discovered that a high performance can be reached by lowering the w/b ratio. However, there is a minimum need on the amount of water to make a concrete workable; it has therefore been discovered that the w/b ratio reduction may be limited unless precautions are considered to enhance the workability of the concrete. Therefore, researches to develop high performance concrete in terms of strength was very slow and limited before the 1960s. At that moment, concrete having 30 MPa strength was accepted as high strength concrete (Li, 2011).

Since the 1960s, because of two parameters, the development of high strength performance concrete has showed significant progression, which are the invention of water reducing additives and the introduction of mineral additives such as SF, FA and BFS into the matrix. The water reducing additive has been a chemical additive that can allow concrete to maintain high workability during at low w/b ratio and secondly, the use of finer minerals that can give reaction with calcium hydroxide, in order to produce secondary hydration products making the concrete microstructure denser, has caused this strength increase.

In the 1990s, a new "concrete" with a 200 MPa compressive strength was found in France. Because of the high amount of SF involved, it was originally named as reactive powder concrete and, in a time, converted into ultra-high strength (performance) concrete (UHSC) (Richard & Cheyrezy, 1995). UHSC has performed a compressive strength of 800 MPa with the heating process. However, it had a very fragile structure, so fibers had to be included in the UHSC. After including the fine steel fibers, 50 MPa was achieved

in terms of a flexural strength. UHSC was first used on a pedestrian bridge constructed in Sherbrooke, Canada (Aitcin et al., 1998).

2.1.1. The effect of conventional cement and concrete on the environment

Considering its universal usage in construction, the enormous volume of cement production required to produce this excessive amount of concrete, 10 billion tons worldwide, has brought significant environmental issues. Foremost among these was the fact that cement production has a ~ 8% share of global CO_2 emissions (Scrivener & Kirkpatrick, 2008; Olivier et al., 2012). The total emission of cement production, about 0.8 tons CO_2 equivalent per ton, is shared between the emissions from burning fossil fuels and the CO_2 released by the conversion of calcium carbonate into its oxide form (Gartner, 2004).

The effects of various processes involved in cement production have been detailed in many environmental studies (von Bahr et al., 2003; Josa et al., 2004, 2007; Boesch & Hellweg, 2010; Valderrama et al., 2012). Current researches have proven that calcination process during cement production has a significant influence on environment (Chen et al., 2010; Cagiao et al., 2011). It demonstrates that the procedures associated with the procurement of raw materials and involved in the post-calcination (grinding process) refer less than 20% of the climate change effect. Emissions throughout heating are divided between chemical decarbonation and fuel consumption with ratio of %60 and 40%, respectively (Habert, 2014).

The following information on the subject was shared in the report of the International Energy Agency on "Low Carbon Transition in the Cement Industry" (International Energy Agency, 2018). Cement is used to make concrete for buildings and infrastructure that are important for quality of life, social and economic well-being. The cement industry is the third highest consumer of industrial energy, accounting for 7% of the global industrial energy use of 10.7 EJ (Exajoule). Rising global population and urbanization models increase the demand for cement and concrete together with infrastructure development needs. Cement production in the worldwide is projected to increase by 12-23% until 2050. Direct CO_2 emissions from the cement industry are projected to grow globally by 4% until 2050 under the IEA (International Energy Agency) Reference Technology Scenario (RTS), although global cement production show a 12% increase.

Apart from CO_2 emitting, the one of the main reasons of existing of sulfur dioxide, nitrogen oxide and carbon monoxide are also cement plants. The following impacts on health and the environment are associated with them. Nitrous oxide (NOx) can lead to many health problems and negative environmental impacts. Affected groups involve children, people with lung diseases such as asthma, and people exposure to these conditions, can damage lung tissue. High concentrations of sulfur dioxide (SO_2) can influence respiration and cause worsening of existing respiratory and cardiovascular diseases. Vulnerable populations involve asthmatics, people with emphysema or bronchitis, children and the elderly. A main contributor to acid accumulation or acid rain is also SO_2. By lowering the oxygen supply to the body's organs and tissues, carbon monoxide (CO) can cause damaging health. CO also cause to the generation of smoke (ground-level ozone) that can cause respiratory problems (EPA, 2019). In addition to the environmental impacts that occur during the entire production process, the use of natural resources such as limited amounts of aggregate and water increases with the use of concrete, and this increase will significantly reduce access to these natural resources to be used in the future.

As the global community produces gradually increasing amounts of concrete to satisfy the infrastructural requirements of the developing world (Taylor et al., 2006), alternative cement-like binders are urgently needed to be created and commercialized. Although concrete is cheap, easily accessible and has high performance properties, considering its undeniable damages on the environment and the rapid increase in its use, there is a need for an alternative building material to cement based systems.

2.2. Alternative Binder: Geopolymer

Currently, the primary application area of geopolymer is utilization as an alternative to Portland Cement to provide the enhancement of minimized CO_2 induced from building materials. The product obtained after the reaction of alkali activator solution with a solid aluminosilicate is commonly referred to as "geopolymer" after Davidovits (1991) but probably more aptly as an illustration of what is called "inorganic polymer", produces a synthetic alkaline aluminosilicate material (Van, 1970). The following information about geopolymer is given in another source; the term "geopolymer" was coined by the Professor Joseph Davidovits in the 1970s and is stated to be a solid material synthesized

by the reaction of an aluminosilicate precursor with an alkaline solution (Davidovits 1982a, 1991, 2008).

These materials were able to perform comparable to conventional cement-based binders in some different applications, but however had the advantage of dramatically decreased Greenhouse gas emissions (Gartner E, 2004). Geopolymers can display a broad range of properties and performance, containing improved mechanical performance, lower shrinkage, acid and fire resistance and low thermal conductivity, based on raw material sourcing and conditions of processing. However, despite these broad variety of widely lauded qualities, these features may not be inherent in each geopolymer matrix. Polymers should not be seen as a common solution for all issues of material selection and use, yet instead, as a solution that can be adapted with the right blend and processing design to optimize properties for a particular application and / or reduce cost. Although the term 'geopolymer' is commonly used to define reaction products that are crystallized by the formation of alkali aluminosilicates from alkali activator reaction, geopolymeric gels are also usually used; "low temperature aluminosilicate glass" (Rahier et al., 1996), "alkali activated cement" (Palomo & Lopez, 2003), "geocement " (Krivenko, 1994), "alkali bonded ceramic", "inorganic polymer concrete" (Sofi et al., 2006) and "hydroceramic" (Bao et al., 2005) as well (Duxson et al., 2006). In spite of this diversity of expressions, all of the terms identify materials formation using the identical chemistry; it could be defined as a complicated matrix of bound alkali mediated dissolution and precipitation reactions in a liquid substratum. Although they are named very differently, the “geopolymer” and “inorganic polymer” are becoming more and more common in academic research.

While many macroscopic properties of geopolymer prepared from various sources of aluminosilicate are identical, their microstructure and physical, mechanical, chemical and thermal features vary considerably according to their raw material sources. Ordinary images demonstrating geopolymer microstructures formed from MK and Class F FA are shown in Figure 2.1. Significant variations between these geopolymers' microstructures have been observed. For example, systematic variations in the activator composition and associated with mechanical strength were investigated in the microstructure of geopolymers derived from MK (Rowles & O'connor, 2003; Duxon et al., 2005, 2006). It has been observed that as the Si / Al ratio augment, the microstructure becomes more

homogeneous with small pores than large porosity. This observation has been considered to be associated with a strict relation with Young's modulus and increment in compressive strength (Duxson et al., 2005). No influence on the micro-structure of the change of alkali cations from Na to K was immediately seen (Duxson et al., 2006).

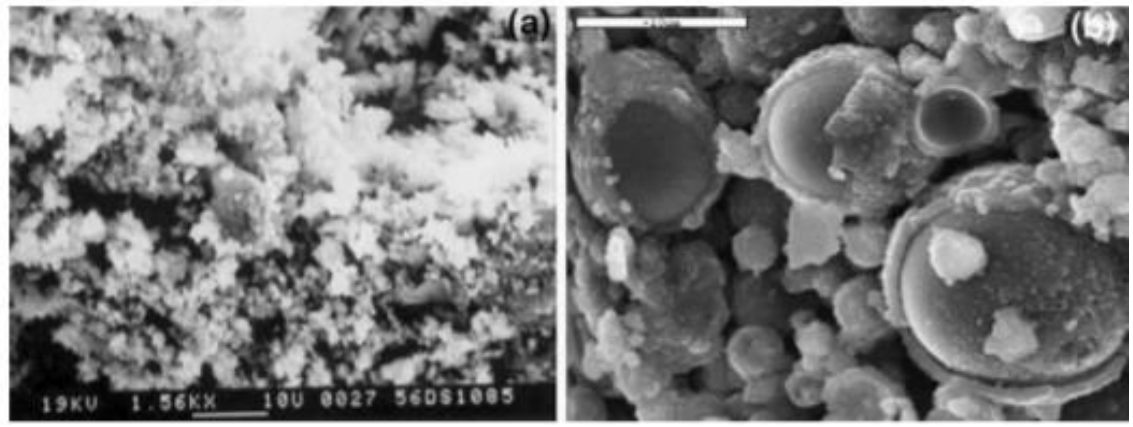

Figure 2.1. (a) Metakaolin synthetized by 8 M NaOH, (b) Volatile Ash synthetized by 8 M NaOH (Duxson et al., 2006)

Variations are clearly apparent in the features of geopolymers synthetized from various raw materials, in spite of the similarity in molecular structure and nanostructure. Geopolymers based on fly-ash are typically more durable and high strength. These properties have also led to the claim that FA systems' binding step and reaction mechanisms are inherently different from those of geopolymers based on MK. Although the dissolution properties of FA and inherent differences in phase composition lead to obtain geopolymers with different properties, it was observed that the identical silicon and aluminum bond and the identical gel phase binder were exist in both systems and in both molecular and microstructure. Therefore, the variations found in the literature in setting actions, microstructure and property formation are reconciled in the conceptual model of geopolymer reaction provided in Figure 2.2 (Duxon et al., 2006).

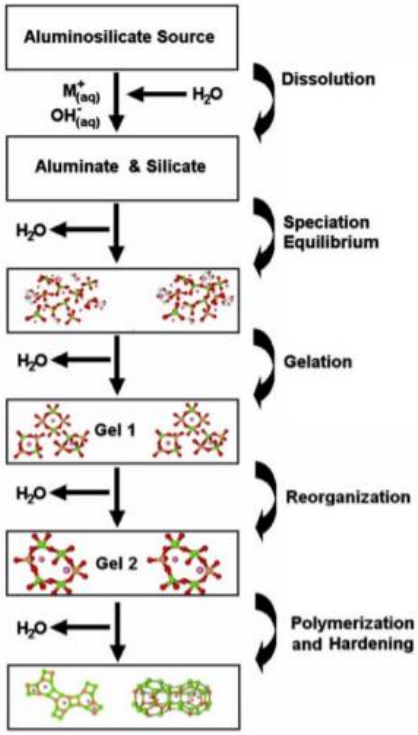

Figure 2.2. Geopolymerization Model (Duxson et al., 2006)

A general reaction process of the alkali activated materials consisting of reactive silica and alumina was published by Glukhovsky (1959) in the 1950s. The mechanism was split into three steps by the Gluhhovsky model: (a) destruction–coagulation; (b) coagulation condensation; (c) condensation–crystallization. In the near future, the Glukhovsky theori has been researched and expanded by numerous researchers and accumulated knowledge of zeolite synthesis has been applied to describe the geopolymerization mechanism (Fernandez et al., 2005; Provis et al., 2005a, 2005b; Fernandez-Jimenez et al., 2006; Van Deverter et al., 2006). The mechanism of reaction shown in Figure 2.2 describes the basic processes involved in converting a source of aluminosilicate into a synthetic aluminosilicate alkali. It should be stated that, for the sake of simplification, the potential necessity for the processing of raw materials, grinding, any kind of treatment, etc. to change the aluminum reactivity in the matrix were not given. Although demonstrated linearly, these progresses were highly interconnected and take place simultaneously. Aluminate and silicate types were produced by the dissolution of the aluminosilicate source through alkaline hydrolysis (consuming water). It was worth noting that the dissolution of particles at the surface leading the release in solution of aluminate and silicate (in monomeric form) was generally considered to be the process responsible for the conversion during geopolymerization of particles. This hypothesis has had a

significant scientific value depend on the literature defining alkaline dissolution and is therefore given in Figure 2.2. However, under the elevated alkaline and inadequately dissolved conditions prevailing during geopolymerization, the exact particle-to-gel process of conversion has never really been confirmed. Once in solution, the dissolution-released strains that may contain silicate already present in the activating solution have been introduced into the aqueous phase. Thus, a complicated mixture of silicate, aluminate and aluminosilicate types was created, and the balance of speciation in these solutions has been thoroughly investigated (Swaddle et al., 1994, Swaddle, 2001).

At high pH, the dissolution of amorphous aluminosilicates is fast, which quickly forms a supersaturated solution of aluminosilicate. Such case lead in the development of a gel in intense solutions as the oligomers by condensation create large networks in the liquid phase. This mechanism led water out which during dissolution is nominally consumed. Therefore, water acts as a reaction medium, yet then remains in the pores in the gel. This kind of gel structure, with the aluminosilicate binder and water forming the two phases, is commonly referred to as two-phase. A continuous gel formation time of the supersaturated aluminosilicate solution varied significantly with Processing conditions for raw materials and composition of solutions and conditions for synthesis (Aiello et al., 1991, Ivanova et al., 1994). After gelation, as the interconnection of the gel network enhances, the system continues to reorder and reorganize, leading the three-dimensional aluminosilicate structure likely referred to geopolymers. Briefly, this is the presence of different "gel" phases consistent with latest experimental results (Fernandez-Jimenez et al., 2006, Provis and Van Deventer, 2007) and numerical modeling for both MK and FA based geopolymers (Provis, 2006) are depicted in Figure 2.2. The aluminosilicate material nucleation or dissolution and the development of polymeric species are largely based on thermodynamic and kinetic parameters and include the first two steps described by Glukhovsky. Growth is defined as the stage where nuclei get a critical size and the production of crystals begins. The microstructure and pore dispersion of the material, that are crucial in deciding several physical features, are predicted to determine these structural rearrangement processes (Duxon et al., 2005).

As mentioned earlier, Glukhovsky suggested a general mechanism consisting of three phases for activation reactions in these materials: (a) destruction–coagulation; (b) coagulation condensation; (c) condensation–crystallization. In the first stage, when the Si

- O - Si bonds are broken by the OH ions in the alkaline activator, the reaction starts. The ions have redistributed their electronic densities circumstances of silicon atoms, which weaken the Si - O - Si bonds, leading them prone to break. This attack reveals the silanol (–Si - OH) and sialate (–Si - O–) species. The presence of the alkaline cation neutralized the leading negative charge, while the generation of Si - O^- - Na^+ bonds prevented the conversion to siloxane (Si - O - Si).

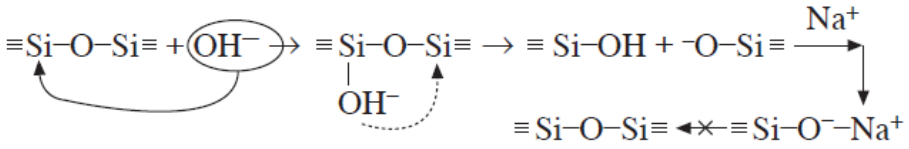

OH- groups affected Si-O-Al bonds in the similar process: dissolved aluminum species create complicated species, primarily Al (OH) 4- anions.

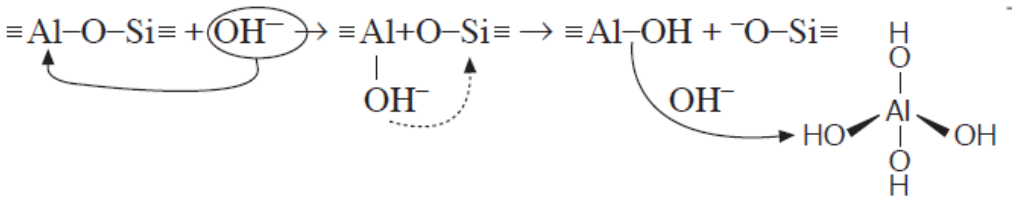

In the second step, concentration of ionic species promotes contact between decomposed products and polycondensation has begun leading to solidified structures. Mutually, silica monomers contact to produce dimers (forming Si-O-Si bonds) that react to form polymers with other monomers. OH ions catalyze this step. The clusters created in consequences of polymerization of silicic acid start to develop in each directions and form colloids. Aluminates are also involved in polymerization, isomorphically displacing silicon tetrahedra. While alkali metal catalyzes the reaction in the first step, it behaves as a structural component in the second.

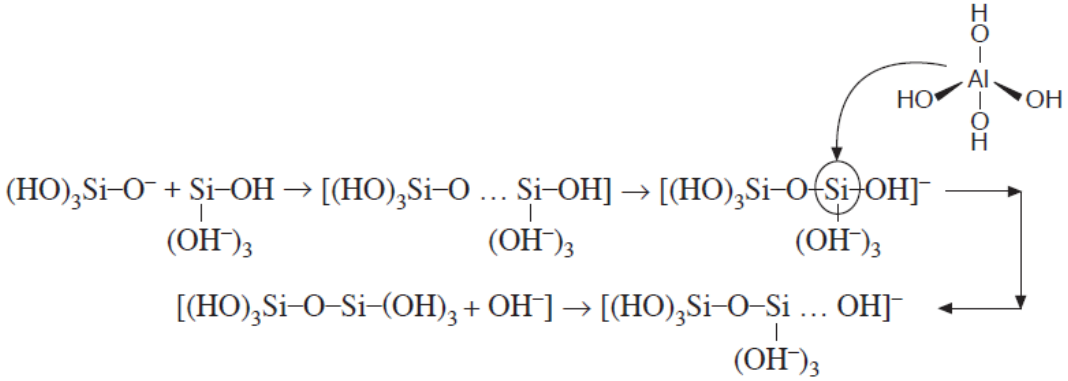

Finally, in the third stage, the particles in the first solid phase causes the reaction product to precipitate. The formulation of those products related to the mineralogy and chemical properties of raw resources, the used activator and the curing condition. While generally following the steps described above, the progress related with alkaline activation of MK and FA can also differ.

Multiple researchers later updated this model (Fernández-Jiménez et al., 2005b; Duxson et al., 2007b; Shi et al., 2011). Based on the developed model, N - A - S - H gel production involves an array of steps that could be summarized as noted below. When the aluminosilicate source meets the alkaline solution, it dissolves in various types, mainly silica and alumina monomers. Such monomers react to produce dimers, and these formed dimers react to form trimers, tetramers and related structures with other monomers. When the solution is saturated, the aluminosilicate gel, N - A - S - H gel starts to form. This gel is originally rich in Al (Fernández-Jimenez et al., 2006). This could be clarified by its formation in the early steps of the reaction (first hours) with a high Al^{3+} ion presence in an alkaline environment, as reactive aluminum dissolves faster than silicon. The reason for this is that Al - O bonds are weaker than Si - O bonds. During the reaction steps, the original source of aluminosilicate dissolves more Si - O groups, and the concentration of silicon in the reaction environment and its ratio in the medium of N - A - S - H gel continues to increase over time (Gel 2). This structural rearrangement has an active role in specifying the ultimate content of the polymer and in the pore microstructure and dispersion in the material, which is effective in improving many of the physical properties of the resulting cement.

The major product formed by the alkali activation is an amorphous alkali aluminosilicate hydrate (Mn- (SiO_2) -AlO_2) n. wH_2O) called as N - A - S - H gel (Palomo et al., 2005) (see Figure 2.3). An alkali element is indicated by the 'M' given in the formula. "n" stands for the degree of polymerization.

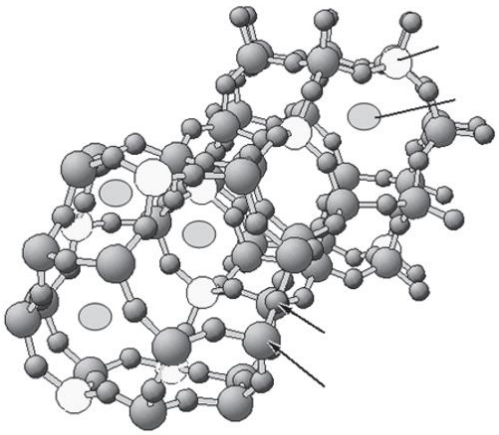

Figure 2.3. Representation of an N - A - S - H gel (Pacheco-Torgal et al., 2017)

2.2.1. Geopolymer Binders

The three most common classes of raw materials used in geopolymerization are BFS, CC (MK) and FA. Each of these has been intensively investigated in Portland cement-based systems as an additional cement material (ACI Committee 226 1987; Bouzoubaâ et al., 1999; Sabir et al. 2001; Richardson, 2004). In geopolymer synthesis, CC (generally MK) have been used considerably broadly, but existing plate-like particle morphologies have been identified to lead a more need for water that is not feasible in applications of geopolymer concrete. For two-part geopolymerization, other kinds of raw materials have also been utilized, involving several synthetic powder (Hos et al 2002; Gordon et al., 2005); yet, utilizations of them are not common (Provis & Van Deverter, 2009). SiO_2, Al_2O_3 and CaO amounts of these three main geopolymer binders are given in Figure 2.4. In addition, the content of SF is given this figure. Although SF is not used as widely as the other three, it is used in geopolymeric systems.

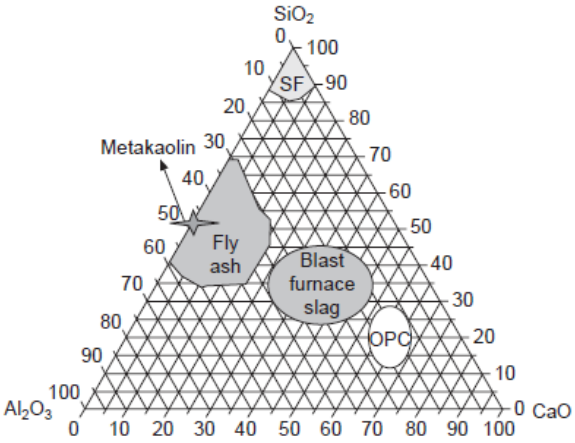

Figure 2.4. Chemical composition of MK, FA, BFS, Portland Cement, and SF.

2.2.1.1. Metakaolin (calcined clay)

MK itself is characterized as a relatively complex material formed at temperatures ranging from 500-800 °C by calcination of kaolinite clay based raw materials (MacKenzie et al 1985; Rocha and Klinowski 1990; Badogiannis et al 2005; Granizo et al 2007). Although the fact that it is derived from the layered kaolinite structure by removing hydroxyl groups means it should remain in a line to some extent, the structure of MK seems to be distorted in X-ray analysis. The MK utilized in matrix differ significantly in terms of particle size, content and crystallinity of the kaolinite where they are taken. In the use of MK for geopolymer manufacturing, each of these factors is essential, and it means that there is little likelihood that a particular "recipe" will exist that is most suitable for geopolymers produced from a broad variety of sources. Research about alkaline activation has increased exponentially following the author Davidovits (1979), who enhanced and patented alkali activation of MK (Rashad, 2013). These new forms of binders, alkali activation of aluminosilicate sources, can be known as third generation cement after lime and PC. To minimize CO_2 emission, alkaline activation of MK is suggested. Alkaline activation of MK is associated with hardening mullet at temperatures below 100 °C (Davidovits, 1982, 1991; Granizo et al., 1997; Krivenko, 1997) and it provides strength cementitious materials to gain strength. The specific surface and content of the kaolin and the kind and intensity of the activator are directly influential on the content, structure and characteristic of the final output goods as a result of activation of the MK.

Granizo et al. (2007) indicated that an amorphous hydrated sodium aluminosilicate is the reacting result of MK activation with Na_2SiO_3 + NaOH solutions. Some researchers (Granizo et al., 1997, 2004) stated that the output of MK activation with NaOH solutions is N-A-S-H gel with superior strength performance. Granizo et al. (2000) investigated various molarity of NaOH to activate 2 kinds of MK with different solution / solid ratios. They found out that the product as a result of MK alkali activation was essentially an amorphous sodium aluminosilicate. As Na_2O concentration increased and MK fineness increased, total heat released increased. Insoluble residues (IR) of mixtures composed coarse MK were higher than fine MK. As Na_2O increased in medium, IR decreased exponentially. Thus, as the NaOH concentration increased, the reaction degree increased.

Davidovits (1985) defined the alkaline activation of MK with a polymerization model like that proposed to define the development of zeolites (Duxson et al., 2007) or zeolite precursors from alkaline aluminosilicate solutions. Rahier et al. (1997) stated that the formed material is amorphous and cement-like when the activator is a combination of NaOH and water glass, but its structure and chemical content can vary from that of the product generated when sodium hydroxide is utilized solely. The influence of NaOH molarity and the existence of Na_2SiO_3 activators on the development of crystal phases from MK-based geopolymers was investigated by Zhang et al. (2009).

The hydration procedure of MK geopolymer activated via potassium silicate was studied by Yunsheng et al. (2007). They announced that in the early steps of hydration, MK particles loosely clump together, leading to the presence of many large pores. Sponge-like gel products were formed progressively as the hydration continued, and these gels were deposited on the surface of the collected particles and this activity spread outwards. So, gaps are completely filled. In the next step, MK particles were surrounded with a thick gel layer, tightening the microstructure of the geopolymer paste.

Sum et al. (2004) and Zhang et al. (2005) investigated the MK based geopolymer activated by potassium solution. They stated that MK particles clumped loosely together at an early stage, causing the presence of several large pores. As before hydration, gel products progressively deposited on the surface of particles and so, these voids were completely filled with these products. In the next step, the MK particles were covered with a thick gel layer and geopolymer paste microstructure turned into much denser.

Granizo et al. (2004) activated MK and MK + $Ca(OH)_2$ mixtures cured at 45 °C with 5 and 12 M NaOH solutions at a ratio of 1:1. They reported that the CSH gel was easily generated in the existence of $Ca(OH)_2$ with a low NaOH concentration. With both calcium hydroxide and without calcium hydroxide, the formed basic product had the identical network structure as the generalized formula $Si_2Al_2Na_2H_4O_{10}$. The alkali material production rate was so slow when $Ca(OH)_2$ was utilized in medium where that of alkalinity was higher.

2.2.1.2. Blast Furnace Slag

Slag is one of the waste products of the manufacturing of different metal types. The components of slag are alumina, silicates, calcium and magnesium (Awoyera & Adesina, 2019). Most of the slag used as a binder in concrete and as an alkali active material (AAM) is obtained from the steel and iron industry and such slags are called BFS (Bakharev et al., 1999). BFS are generated by immersing the molten slag in water and cooling it rapidly. Rapid cooling of molten slag transforms molten slag into particles smaller than 4 mm in size. Small-sized particles formed as a result of minimal crystallization during rapid cooling are mostly non-crystalline material (Tossavainen, 2007).

However, it should be mentioned that the composition of the slag varies based on used the raw materials by the metallurgical company to manufacture the metal. Such variations in raw materials may result in differences gepolymerization mechanism and final product (Wang et al., 1994; Puertas et al., 2018). So, it is very vital to ensure test mixtures before any large-scale application to analyze how the slag reacts during and after activation.

Alkali active slag (AAS) is the most well-known type of AAM because it consumes less energy when used instead of OPC as a binder (Jiang et al., 2014). In addition, 1 ton of slag production requires approximately 1300MJ of energy and causes only 0.07 tons of CO_2 (Awoyera & Adesina, 2019). Yet, same amount of OPC production require 5000MJ of energy and release 1-ton CO_2. In addition, AAS have been stated to enhance the mechanical and strength properties of concrete (Aydın & Baradan, 2014; Rashad, 2013). However, the main limiting factors in AAS use are high shrinkage (Puertas et al., 2018) and fast setting ability (Puertas et al., 2014).

Slag has been utilized in OPC concrete since 1983 to enhance its strength and durability (Miyazawa et al., 2014). However, it was also used as a binder for AAM by the Kiev Civil Engineering Institute, Ukraine, in the USSR in 1957 (Ko et al., 2013). And there are more than 100 patents and inventions certificates in the field of AAS (Bakharev et al., 1999), and the first patent was documented in 1908 (Provis, 2013). Today, research is still carried out in the field of AAS. In USA, scientist have studied since 1987 to develop alkaline activated slag cement consisting of a dry slag mix and an alkali activator (Roy, 1999; Angulo-Ramírez, 2017).

Common fresh characteristic difficulties of AAS are its low fluidity and fast setting, making it impossible to mix and place AAS in hot weather and tightly reinforced sections. Also, the high drying shrinkage of AAS compared to other alkaline active materials has played a major role in the rejection of AAS in the construction industry (Bakharev et al., 2001; Cartwright et al., 2015; Mastali et al., 2018).

2.2.1.3. Fly Ash

FA compose of clay, sand and organic material residues in the coal that come out of the furnace chimney during combustion. FA is a widely variable material that varies depending on not just the impurities exist in the fuel used in furnace before combustion, besides, the characteristics of the process of combustion and extinguishing has effects on FA. The most commonly used FAs in geopolymer production is poorer in Ca, i.e Class F FA with respect to ASTM C618.

Normally spherical FA particles can be hollow or contain fine spheres. However, particles are not uniform yet contain both glassy and crystalline phases. The distribution of the particle size includes a variety. In general, the equivalent diameter of 50% of the particles is below 30-40mm. The specific surface for FA is between 2500 and 5000 cm^2 / g and its density is between 2.2 and 2.8 g / cm^3. Having such a wide range of characteristics refer that special precaution have to be exercised while operating with FA to maintain a constant quality of the product obtained (Pacheco-Torgal et al., 2017).

FA quality varies according to coal type and incinerator. Variation in composition can differ both the nature and characteristic of the obtained alkali binders. In this context, Fernández-Jiménez and Palomo (2003) described the measures to be considered by FA for the production of high-quality binders as follows;

- Less than 5% unburned material
- Fe_2O_3 amount below 10%
- Slight CaO
- 40-50% reactive silica
- 80-90% of the particles are below 45 mm in size
- High glassy content.

2.2.1.4. Silica Fume

The SF is extremely pozzolanic and increases concrete resistance to extreme conditions (Gautefall, 1986; Kohno et al., 1989; Cheng et al., 2013). SF is being used in concrete to strengthen the characteristics of concrete such as compressive and bond strength and corrosion resistance, because of its high fineness and silica content (more than 90 percent) (Lee, 2016). It is also commonly used to improve concrete durability, since it reduces concrete permeability (Dutta et al., 2010; Khater, 2013) and provides resistance to corrosion (Khater, 2013). Previous studies have studied the impact of SFs on geopolymers. Especially Okoye et al. (2016) examined the influence of SF in various dosages on FA-based geopolymer concrete fired at 100°C by activating with NaOH and Na_2SiO_3. The outcomes stated that SF addition enhanced the compressive strength of geopolymer concretes. It was figure out that SF based geopolymer concretes are extremely resistant to exposure to 2% H_2SO_4, 5% Na_2SO_4 and 5% NaCl solutions. Thokchom et al. (2011) suggested that adding up to 5% SF to a geopolymer mortar considerably improves the mechanical properties of the geopolymer when subjected to a magnesium sulfate solution.

The appropriate SF amount in geopolymers was examined in a research in which the compressive strength of a MK-based geopolymer containing up to 7% SF substitution ratio increased due to a well-refined microstructure and a dense matrix. After 7% substitution, there was a decrease in strength (Khater, 2013). In another analysis due to compacted structure of microstructures with a well-bonded interlocking morphology, the compressive strength of geopolymer prepared with FA increased with up to a 2 % increase in nano-silica usage (Deb et al., 2015). Mercury intrusion porosimeter (MIP) results of a geopolymer mortar proved to have a lower pore volume in samples containing additional SF. Spaces between the sand particles were filled by fine SF particles and SF increased their mechanical properties by contributing to the reduction of porosity. The addition of SF as a partial replacement instead of FA to self-compacting geopolymer concrete prepared with FA resulted loss of workability (4.3%) (Bhavsar et al., 2014), however, compressive strength enhanced by 6.9% and bending strength by 11.5% (Memon et al., 2013) with usage of SF. The effects considering amount of SF on the geopolymer reaction were examined in a research, and the result showed that the higher silica presence lead in a large contribution of alumina to a geopolymer gel (Hajimohammadi et al., 2011). They explained that C-S-H gel formation is difficult with the pozzolanic reaction of $Ca(OH)_2$

and SF. Since geopolymers, composed of both FA and slag, contain a large number of gels with different properties (e.g., NASH, CASH) (Garcia-Lodeiro et al., 2011), the content, chemical composition and silicate structure of these gels have been deemed possible to be changed by introducing SF into the geopolymer.

2.2.2. Geopolymer Activators

The most major distinction between an alkali activated binder and a traditional Portland cement is that Portland cement strengthening is simply induced by mixing with water, while the addition of an aqueous alkali component is necessary for alkaline activation. Generally, aluminosilicate binder materials activated under high pH conditions with alkali hydroxides or silicates are classified as geopolymers. A chemical activator is required for this reaction to take place. Generally, these activators are divided into 2 groups. The first group of activators are grouped as alkali hydroxide sourced, the second group as alkali silicate sourced activators.

2.2.2.1 Alkaline Hydroxides

The sodium hydroxide is the hydroxide solution used most often as an alkaline activator. Although potassium hydroxide is used in advanced applications, there are few real-scale applications for lithium, rubidium and cesium hydroxides (Provis & Van Deverter, 2009). Alkali hydroxides are mostly derived electrolytically from chloride salts, indicating that the manufacturing process requires some energy use and related CO_2 emissions, but precise emission calculations around this process have also been made dependent on whether the chlorine produced during this process is a valuable goods or a by-product (Wiedema, 2008).

Hydroxide-activated FA mixtures frequently need heat curing, 60 C or higher according to FA reactivity (Criado et al., 2005), which is suitable in the manufacture of precast concrete but can cause problems in field operations. Both based on FA or BFS, hydroxide activated binders appear to show higher permeability and efflorescence patterns than their silicate activated counterparts (Shi, 1996). Since the rate of reaction achieved by the binder before strengthening is typically poor, resulting in an open microstructure with a mobile alkali-rich pore solution. Efflorescence and other apparent alkali mobility effects are obviously undesirable but can be resolved to some point by carefully monitoring curing conditions or introducing secondary sources of aluminum to ensure sufficient

reaction before the material is put into operation (Najafi et al., 2012). The very high degree of connectivity of silicate gels in these binders is due to this stability; the use of a silicate activator leads small silanol groups (partially depolymerized Si sites) losing water when heated, causing the characteristic expansion of unbound gels (Provis et al., 2009). Despite the drawbacks mentioned herein, there are instances where some aspects of technical performance can benefit from a hydroxide activator. An example of this is the extraordinary dimensional stability of the hydroxide-activated FA based geopolymer up to 1.000 °C (Provis et al., 2009). As the viscosity of alkali hydroxide is much significantly smaller than those of alkali silicate with equal concentration, hydroxide utilized matrix can frequently perform more favorable flowability than silicate used matrix.

The most important features of hydroxide solutions to be taken into account are viscosity and dissolution temperature. The alkaline hydroxide solution is the result of an exothermic reaction and releases a significant amount of heat. For example, assuming that dissociation of 10 moles of NaOH in one liter of water liberates 90% of the heat released as it passes to infinite dissolution, this would be about 400 kJ. As stated in the results of Simonson et al. (1989), when the average heat capacity of the NaOH solution is taken more or less equal to water, this amount of heat would be enough to increase the temperature of the water above 90 °C. It is obvious that if hydroxide solutions from solid precursors are to be prepared routinely in an industrial production environment, temperature rise should require to be evaluated and monitored so deliberatively.

In addition to all these, $Ca(OH)_2$ is also used in powder form in geopolymer systems. Although $Ca(OH)_2$ is an alkali hydroxide, it is not clear whether it is used as an activator or a source of extra "Ca" in the system. When $Ca(OH)_2$ is dissolved in the matrix, it can increase the pH of the environment to the 11-12.5 band, which is a desired behavior in the geopolymeric system to separate the aluminosilicate source into its components. But at the same time, it has been mentioned that it can be used as a "Ca" source in research since it is an extra "Ca" source when dissolved for geopolymerization. In this thesis, "$Ca(OH)_2$" was used as an alkaline activator. As given below, calcium hydroxide has broad range of positions in the geopolymerization reaction;

1. In order to generate amorphous or poorly arranged crystalline C-S-H or C-A-S-H, calcium hydroxide interacts with a sodium silicate solution, causing water

shortage in the alkaline mixture to maximize its alkalinity. The increased alkalinity of the substance contributes to higher dissociation and thus higher polycondensation-geopolymerization rates of existing aluminosilicates.

2. As a result of the charge balance, calcium hydroxide can be bound into a geopolymer gel by displacing cations in the geopolymer (Davidovits 1991; Guo et al., 2010).
3. To produce a C-S-H gel that creates additional nucleation sites for dissolved species formation and causes rapid hardening, calcium hydroxide can interact with silicate and aluminate species (Temujin et al. 2009; Guo et al. 2010).

After raising the $Ca(OH)_2$ addition to 10% in matrix containing MK, it reacts with the Na_2SiO_3 solution and precipitates CSH or Ca-Al-Si in amorphous or weak crystalline form, causing a lack of water in the alkaline medium. A rise in alkalinity would lead to greater rate of dissociation of the available aluminosilicate and a higher geopolymerization degree of polycondensation, resulting in a rigid structure with higher compressive strength. Higher substitution of $Ca(OH)_2$ results a decrease in strength, as the introduced $Ca(OH)_2$ needs additional Na_2SiO_3 for the development of C-S-H, and these C-S-Hs serve as nucleation sites in the generation of geopolymers. Moreover, the optimum geopolymer gel binder structure will be disturbed by extra lime and will inhibit the growth of strength. Nevertheless, this can be due to the local variation of the Si = Al binder ratio in the vicinity of the calcium silicate particles by Si and/or Al leaching, resulting in regions considered to be defects in the matrix under compressive strength testing with less than optimum microstructure (Khater, 2012).

2.2.2.2 Alkaline Silicates

Since Purdon's first work (1940), silicate utilization become the most widely utilized method of producing BFS-based AAM because of the versatility of the method and the ultimate excellent quality of the final product. Activator is typically added as a solution in a blend; but it can be used in a solid form or mixed with BFS in the system (Wang et al., 1994). It is well obvious that in alkali silicate utilized in BFS based geopolymer, the primary product of reaction is a weak crystalline C-A-S-H type gel (Wang and Scrivener, 1995; Puertas et al., 2011; Bernal et al., 2013) the structure of which is greatly affected by the content of the BFS and the structure of the activator (Ben Haha et al., 2011, 2012). The external product is formed rapidly with increasing formation with the presence of

high silica concentrations in the initially liquid filled regions (and thus a strong tendency towards oversaturation) (Brough & Atkinson, 2002; Gruskovnjak et al., 2006). Enhancing activator dosage mostly results to a well refined pore network (Melo Neto et al., 2008). Si and Al NMR (nuclear magnetic resonance) results showed that the utilization of silicate type activators induced the generation of a C-A-S-H gel (Provis & Van Deventer, 2014). The silicate solutions that attract the most attention in alkaline activation are those that contain sodium or potassium as alkali cation (Provis & Van Deventer, 2009).

The generic name for a sequence of compounds with the formula Na_2OnSiO_2 is sodium silicate. In practice, the n-rate can be any number. There are numerous properties of sodium silicates with distinct n that can have many diversified industrial applications. In 1640, Van Helmont first discovered sodium silicate by combining silica with excess alkali and entering a liquid matrix in moist places. During his experiments, Johann Nepomuk von Fuchs rediscovered it in 1818. In caustic soda potash, he dispersed silica, witnessed the solution's glass-like characteristics and named it glass water (Vail 1928).

2.3. Use of Construction and Demolition Wastes in Geopolymer Production

Construction demolition waste (CDW) is a rapidly increasing concern in many countries. Stokoe et al. (1999) notified that CDW occupied approximately 65% of Hong Kong's landfill at summit meeting in 1995. Formoso et al. (2002) stated that more than 50% of the waste in a landfill in the FA consists of construction waste. Craven et al. (1994) stated that construction action in Australian accounts for 20-30% of all waste accumulated in landfills. In the USA, CDW accounts for approximately one third of the material in landfills (Kibert, 2000). Serpell and Labra (2003) notified that only 10% of the 3.5 million tons of CDW produced in Chile is stored in allowed and regulated landfills. It is estimated that 0.5-1 tons of CDW is generated per capita annually in the European Union (Environmental Protection Agency, 1998). Environmental aspects of wastes from the construction industry have attracted great attention in recent years. For the construction industry this refers, among some other things, increased recycling. The recycling of building waste creates an opportunity to eliminate the need for energy and natural resources and can also lessen both the need for land for extraction of resources and the need for dump land. The advantages of recycling related to the materials and the way they are recycled (Thormark, 2001). In addition, the development and creation of new industrial goods from recycled materials has become increasingly important in recent

years. Geopolymer binders are count as such new industrial products. They have some improved engineering characteristic in comparison with Portland cement. The formation of geopolymers is associated with the activation of aluminum silicate substances with alkali metal hydroxide and alkali metal salt (Davidovits, 1999). Several investigations have been carried in recent years to discuss the feasibility of utilizing industrial waste materials as raw materials in the geopolymer binder production (Allahverdi & Najafi, 2009).

A geopolymer concrete was prepared by Yang et al. (2009a) containing a blend of recycled and natural aggregates. The geopolymeric binders was designed by waste concrete powder and MK (5-25%). NaOH/water glass mass ratio with a range 0.5-1.3 was used to activate gepolymer and after ambient curing for 28 days, the compressive strength of the geopolymer concrete was reached approximately 40 MPa.
Yang et al. (2009b, 2009c) examined the characteristic of geopolymers composed of concrete sludge. In study, the concrete slurry powder and silica sand were used with various amounts of MK (10-40%), and NaOH and water glass activator was used in matrix. To enhance mechanical performance, SF was introduced to matrix (0-10%) by replacing with concrete sludge. In these samples, SF presented active SiO_2, which is an advantage for geopolymerization, enhancing the mechanical performance of the mortars by making the structure denser.

Ahmari et al. (2012) investigated geopolymeric binder pastes by using ground concrete waste (GCW) dust used with FA. The findings showed the substitution of GCW enhances the compressive strength. In the study, the optimum GCW substitution for 5 and 10 M NaOH was 50% and the glass water / sodium hyroxide ratio was one and two. The maximum strength was achieved via utilizing a lower Ca / Si ratio (0.25). Expanding NaOH concentration led to an increase in strength, particularly for GCW amount less than 50%. The utilization of glass water has also enhanced the strength. Besides, SEM / EDX, XRD and FTIR analyzes have showed that Ca increases strength mainly because of the low calcium semi-crystalline CSH gel formation associated with the geopolymeric gel and the inclusion of Ca^{2+} in the geopolymer structure as charge balancing.

Alkali activated geopolymers which was consist of waste brick dust and concrete dust were investigated by Allahverdi and Kani (2009). In research, the final setting times of

the matrix prepared in various rate of these precursor vary between 100 and 250 minutes. Additionally, the obtained findings showed that the waste brick is more proper for geopolymerization reactions than waste concrete. In addition, in this study, mixtures reaching 10-40 MPa compressive strength were obtained.

Sun et al. (2013) investigated the waste ceramic based geopolymer activated by liquid sodium silicate, NaOH, and KOH solution. The first reaction mechanism and alkaline solutions have the greatest influence on the development of geopolymerization. With adequate heat treatment after calcination at 1000 °C, waste ceramic used geopolymers have shown enhancement in strength. Compressive strengths varying between 26-71 MPa were obtained.

RCB waste used geopolymer activated with sodium hyroxide (98% purity) and liquid sodium silicate has been investigated by Reig et al. (2013). NaOH and Na_2SiO_3 can both be utilized to activate the zeolithic RCB. They discovered that strengths could be enhanced by rearranging the ratios of SiO_2/Na_2O, water/binder and binder/sand. They obtained compressive strength varying between 4-50 MPa. In another study of Reig et al., RCB wastes were found to need higher moisture and lower NaOH than porcelain stoneware.

Rakhimova and Rakhimov (2015) investigated the geopolymer consisting of BFS and four various type RCB wastes activated by Na_2SiO_3 and Na_2CO_3 solution. They found that the alkali activator type, amount of RCB waste, grinding methods, curing conditions, and sources of RCB waste seemed to have an effect on the characteristic of the mixtures.

Rovnaník et al. (2016) investigated FA and brick utilized geopolymer activated with sodium hyroxide and sodium silicate. Equally usage of (in half shares) FA-brick powder showed proper compressive strength for geopolymers. Brick dust performed less dense structure than FA based geopolymer. Compressive strength varied between 5-65 MPa.

Zaharaki et al. (2016) investigated geopolymer consisting of electric arc furnace slag, tile, brick, CW and red mud activated by sodium hydroxide and sodium silicate. As a result, they published the following outputs; ratio of SiO_2 / Al_2O_3 and SiO_2 / CaO and NaOH molarity are effective for achieving the designed features of mixtures. And, it is a must

to have enough water in the system during the early activation steps. Their compressive strength varies between 2.5 and 76.1 MPa.

Robayo-Salazar et al. (2017) investigated the geopolymer consisting of RCB waste, CW and GW activated with NaOH and sodium silicate under various curing conditions. The use of RCB waste or CW has proved high compressive strength possible by regulating the formation of alkali activators at ambient.

Yıldırım et al. (2020) investigated alkali active binders produced using the complete use of mixed CDW based masonry elements as aluminosilicate binders. This study proved that waste/binders extracted from CDW-based wall elements could be utilized together in the development of alkali active binders. Roof tiles, blend/clay bricks, hollow bricks are used in the matrix. One of the important outcomes of this research is that these units can be obtained in a basic collocation of materials with different proportions, rather than using waste alone. Because selective demolition practices can be energy inefficient (requires individual separation and time consuming). However, a compressive strength of 80 MPa was reached with these mixtures.

Mahmoodi et al. (2020) focused on the production of 100% brick waste-based ambient cured geopolymer. An obvious connection was observed among the viscosity and setting times of the brick waste based geopolymers and the SiO_2 / Al_2O_3 and Na_2O / SiO_2 ratios. While the viscosity increased with the raising of SiO_2 / Al_2O_3 and Na_2O / SiO_2 ratios at the same liquid / solid ratio (0.3), setting times decreased with increasing Na_2O / SiO_2.

2.4. Rheology

Geopolymer matrix in the form of paste, in the desired shape in appropriate shaping methods could be given by applying forces that have direction, density and duration that will be created by elongation and shear deformations. It is very significant to consider the response of the system during the influence of forces in order to reach substance with the designed shape, using flawless and inexpensive techniques. Rheology has long played an important role in both the scientific and technological fields, due to its utility in understanding and controlling manufacturing processes. Rheology is a branch of science since it needs physics, mathematics, and materials science, and these properties of the material are directly due to rheological behavior.

Systems are split into solids and fluids in materials science. They absorb the energy by deforming it whenever the solid is subjected to external force. They return to their undeformed shape when the applied stress is eliminated. Fluids dissipates energy that produces an irreversible deformation, unlike solids. Which refer a fluid material does not revert to its initial condition when the external pressure is eliminated. Energy is spent in ways such as changing the shape and generating heat (Mezger, 2006). But, the real systems act as in a viscoelastic way, i.e. their deformation is partially reversible and partially irreversible. This causes the rheological method to be complicated and essential for the industrial process (Pacheco-Torgal et al., 2017).

Traditionally, rheology has been explained as "the study of deformations and the flow of matter" in the dictionary. This definition, however, is confusing. The description is similar to the concepts of continuity and does not identify specific rheological properties. The points below should be emphasized:

- Rheological researches are not related to "deformation and flow" yet related to the characteristic of matter that determine its behavior, that is, its response to deformation and flow.
- Rheology is the study of materials with properties defined by any relationship between force and deformation. The subject of rheology is not about all topics, but only those where nonlinear dependencies or deformation rates between forces and deformations are the main feature.
- Rheology is concerned with materials whose deformation causes a superposition of viscous and elastic effects.
- Rheology research substances under the impact of applied load with structural reforms.

Rheology is a science that investigate the mechanical performance of different solid-like, liquid-like and intermediate form materials. It achieves aims through models that represent the basic behavioral properties of materials. The behavior of the substance is a related with forces and shape changes. The rheological behavior of the material relevant to the time and environment scale of experiment (Malkin & Isayev, 2012).

2.4.1. Viscosity

The dynamic viscosity, in the Greek letter η, is one of the most common rheological term. It refers to the resistance of substance when deformed by an exterior load is irreversibly deformed. During deformation, this behavior can be attributed to inner friction in the substance. The more the viscosity of a substance means the lesser deformation during same exposed load per unit of time. A conventional viscosity description in rheology is explained by using the Two-Plate Model (Figure 2.5). The specimen is perfectly positioned, based on definition, between two perfectly parallel surfaces and at a distance of h from one to another. The sample is also presumed to have excellent adhesion to the two surfaces. To avoid pressure on the material, the F force is then applied parallel to the top surface.

Figure 2.5. Two-Plate Model for Viscosity

The shear stress σ (τ, also expressed as tau) is described as the force F applied per unit area A.

$$\sigma = \frac{\mathrm{F}}{\mathrm{A}}(Pa)$$

In this case, when the inner frictional force in the sample balance the applied external force, the motion of the accelerating upper surface can be evaluated in a starting stage until a constant Vmax speed is reached. If the system show a laminar motion, that is, when the movement of the fluid starts by sliding infinitely small layers on each other without any fluid mixture even on a microscopic scale, it is achievable to define the shear rate "$\dot{\gamma}$" (s-1) and the strain" γ". If the velocity of each fluid layer reduces linearly from a maximum to zero by contacting lower plate, the ratio between the speed Vmax (upper) of

the moving surface and the distance h between the parallel sheets is calculated as the velocity gradient.

$$\dot{\gamma} = \frac{\mathrm{Vmax}}{\mathrm{h}}$$

The shear rate is associated with the flow rate. The $\dot{\gamma}$ high values correspond to a high-speed flow. These two parameters are related by a third parameter known as dynamic viscosity which are explained as the ratio of shear stress σ (Pa) and shear rate $\dot{\gamma}$ (s^{-1}). The dynamic viscosity unit of measure in the SI system is Pascal.second (Pa.s).

$$\eta = \frac{\sigma}{\dot{\gamma}} (Pa.s)$$

Viscosity is not certainly a steady characteristic for a material and is actually quite rare since in most case scenarios, viscosity changes due to the influence of various variables. The simple and prevalent material classification split materials into "Newtonian" and "non-Newtonian" fluids. Newtonian manner covers materials that of viscosity does not vary with different shear rate and assumes parameters that may influence the matrix is steady. It should be kept in mind that since change in temperature, precipitation of solid phase, evaporation of liquid phase and ongoing reaction in materials, etc. can vary the condition of matrix. Non-Newtonian fluids have only a difference in viscosity based on changes in the shear rate in matrix where other parameters remain constant. Mechanisms of non-Newtonian behavior are categorized as given,

- Shear thinning refers the matrix where decrement in viscosity observed with growing shear rate.
- Shear thickening refers the matrix where increment in viscosity observed with growing shear rate.

Because of the viscosity of such materials is not steady, viscosity of material is defined as "apparent viscosity" for such materials. Commonly, systems consisting of solid powder dissolved in a medium to high concentration liquid state exhibit non-Newtonian attitudes. The change in viscosity with shear rate is referred to the rearrangement of the dispersed

phase in the continuous phase that promotes or prevents flow. The phenomenon of viscosity change in the existence of shallowly charged solid particles is due to the rupture of electrostatic interactions among particles (Pacheco-Torgal et al., 2017).

2.4.2. Yield Stress

For useful application, it is essential to establish the yield stress σ_0 described as the lowest shear stress that needs to start the flow of the system. In the profession of rheology, after a comprehensive examination, it is stated that there is clearly no such constraint and that its manifestation is merely a problem with the system's stress response time, but the utilization of the idea of yield stress in the field of application continues to be useful for practical purposes.

Several common behaviors in rheology are visualized in Figure 2.6 as a general overview. The first is Newtonian fluids, evidenced by a steady viscosity displayed by a straight line with fixed slope. The second is the shear thinning fluids without yield stress (also called pseudoplastic); the third is shear thinning by yield stress (also called plastic), which varies from the preceding one in terms of yield point. With increased shear rate, both the 2nd and 3rd behaviors demonstrate a less linear relation on shear stress, which appears to mean a decrement in viscosity with an increment in $\dot{\gamma}$. The fourth represent the dilatant behavior demonstrated by a higher than linear increment in shear stress, related to an increment in viscosity with shear rate. The fifth is similar to Newtonian-type behavior but is Bingham fluid with a yield stress (Pacheco-Torgal et al., 2017).

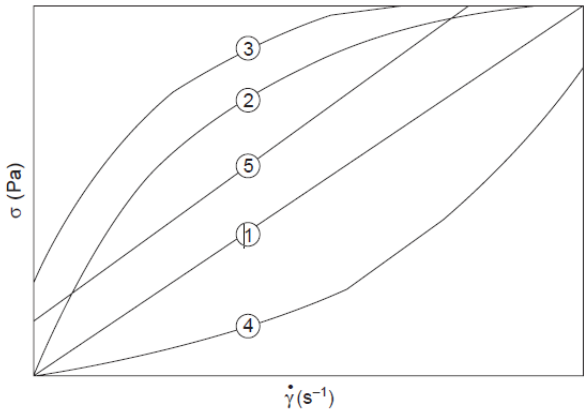

Figure 2.6. Typical Rheological Behaviors Representation: (1) Newtonian Flow, (2) Plastic in appearance (shear thinning), (3) Plastic, (4) Dilatant-Expanding fluid, (5) Bingham Flow

2.4.3. Time Dependence

Most systems show behavior called "time dependent" that expresses itself as a differentiation in viscosity in a progress of time at steady shear rate or shear stress. There are opposite behaviors as "antitixotropy" (also called reopexy) and "thixotropy". Both behaviors are specific time dependent. The term "time dependency" could be understand by examining the Figure 2.7.

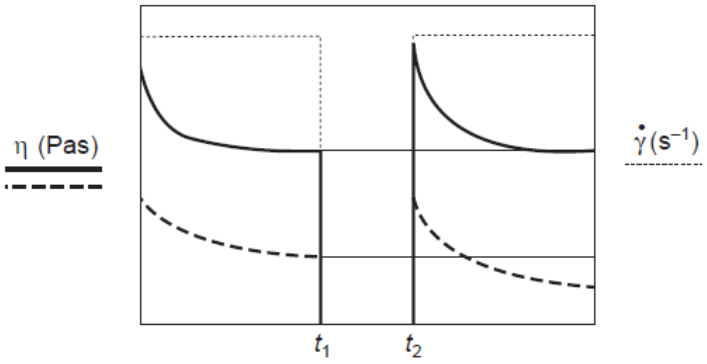

Figure 2.7. Switching procedure, shear rate versus viscosity

If materials are exposed to shear rate long enough to allow a steady viscosity value to be obtained, they can demonstrate the given viscosity trends: (i) the sample demonstrated by the straight line is time dependent and is particularly thixotropic, (ii) dashed line is referred simply time dependent.

A geopolymeric system does not exhibit very similar behaviors to thixotropic or anti-thixotropic because of its reactivity and the creation of precipitation and evaporation events. The geopolymer rheological action can more generally be identified depending on time (Pacheco-Torgal et al., 2017). To clarify meanings of term, thixotropy could be described as the progressive decrement in viscosity value over time for a steady applied shear stress, pursued by a graded recovery anytime the stress is eliminated (Cullen P.J., 2012).

2.4.4. Viscoelasticity

Viscoelastic systems have intermediate properties between the two limiting states of the ideal solid and ideal fluid. As understanding from the name, “visco” means materials that acts as fluid and “elastic” means materials that acts as solid materials, therefore, viscoelastic materials show both characteristic properties of fluid and solid under the stress. Generally, polymers show this viscoelastic behavior since they are comprised of

different fibers and structure in it. Viscous, elastic and viscoelastic behavior of materials are represented in Figure 2.8. Both during molding and in the early phases of consolidation, such behavior patterns could have some significance. It is obvious that the elastic component should enhance in comparison to the viscous one during the consolidation process. In such situations, the techniques of rheological assessment are quite critical to detection of alteration in materials at the microstructural dimension, particularly in the early steps (Pacheco-Torgal et al., 2017).

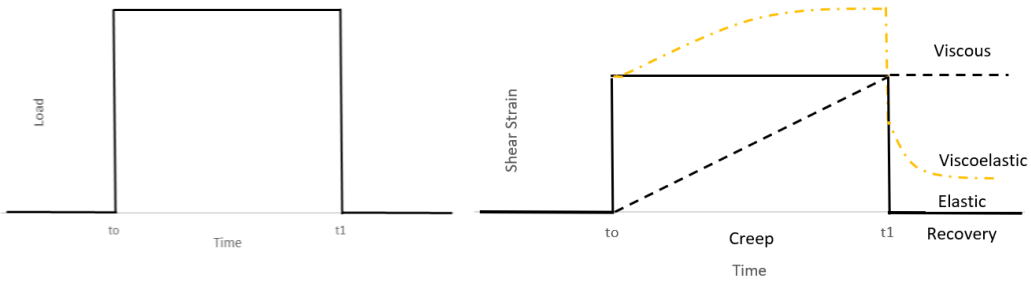

Figure 2.8. Deformation behavior of materials

2.4.5. Rheological Measurement Methods

Rheological testing methods proposed for cohesive cement-based compositions (Srinivasan et al., 1999; Li et al., 1999a, 1999b; Toutou et al., 2002; Lombois-Burger, 2003) over the last decade were originally advanced for conventional materials (plastics, rubbers, soils and metals), meaning that when executing rheological studies, consideration must be given to the sophistication of cement science. The method of rheological testing could be classified into two classifications;

a) Direct test methods dedicated to providing knowledge, which are very helpful from chemical and physical perspectives such as yield value, torque.
b) Analytical methods that enable rheological flow curves to be calculated with classical parameters (shear stress, viscosity).

Although, parallel plate plastometer, direct cutting box (or Casagrande direct cutting box),instrument kneader (torque rheometer) were used to identify rheological features of materials (Alfani & Guerrini, 2005), rotational rheometer was more common method to analyze to reach required knowledge about rheology in recent years.

According to the Searle theory, most rotational viscometers/rheometers work. A motor manipulates a coil in a stationary container. The coil rotation velocity is preinstalled and

generated the motor torque required to spin the metering coil. This torque is designed to exceed the friction force of the material being tested and is thus a measurement of its viscosity. The dynamic viscosity (η) of a sample is measured by a rotational viscometer. Dynamic viscosity is described by Newton's Law as ratio of shear stress over shear rate (Mezger, 2011). When viscosity is measured in a rotational viscometer, a specific shear stress or a specific shear rate is implemented to the sample, respectively. Speed and torque could be transformed into rheological variables if the experiment is carried out conforming a standard measurement geometry regarding ISO 3219. Using a correction factors, the speed of the viscometer is transformed to shear rate and torque is also transformed to shear stress by a conversion factor.

The shear rate is predefined in a standard rotational test. It implies that the selected shear rate of the viscometer converts it into velocity and measures the torque obtained and then converts to shear stress (Mezger, 2011). Such a measurement is called the flow curve, in which the shear rate increases, and the resulting shear stress is measured.

2.4.6. Flow Curve

Standard rotation methods are viscosity operations that related with shear rate, shear stress, several condition. On the one hand, the outcomes of a rotational test could be shown as a flow curve diagram demonstrating the resulting values of shear stress and corresponding viscosity. An assessment of the rotary rheometer in which the shear rate is progressively augmented, and the corresponding shear stress is measured for corresponded shear rate is termed as the flow curve. At low shear rate, the viscosity of the specimen at rest is recorded, and at high shear rate, the viscosity of the specimen in motion is tested. A flow curve could be obtained on the rotational rheometer through predefined settings. The shear rate increases progressively with the period of the specified measuring point for each point. The flow curve exhibits shear stress and corresponding shear rate in a graph. Typically, each specific measuring points are combined with lines to draw the flow curve (Anton Paar Wiki).

2.4.6.1 Calculation of Yield Point with Flow Curve

Materials with yield stress begin to move out once behaving external load is higher than one’s inner structural strength. Underneath the yield stress, the material is "solid-like". For instance, if no external force acts, the toothpaste does not move out of the nozzle.

Over the yield stress, the specimen passes out of the tube and starts behaving as a liquid. The yield point is not fixed value of the substance and yet varies according to method of measurement and analysis. There are a variety of different techniques available to find out yield point of material. In rotary rheometers, the yield point is generally reached from the flow curves. The yield point could not be directly observed, but which is measured utilizing the model (e.g. Bingham, Casson or Herschel-Bulkley). In models, the yield point value τ_0 is calculated by extrapolating the flow curve towards into a low shear rate. Each various model provides a particular yield point since these measurement models are working in different principle.

The Bingham regression model assesses the yield point of materials by using constant slope approach (see Figure 2.9) (Bingham, 1916 and 1922). Recent decades, it was a simple method of determining the point of yield before the computer was used. Bingham equation for yield point is as follows;

$$\tau = \tau_B + \eta_B \cdot \dot{\gamma}$$

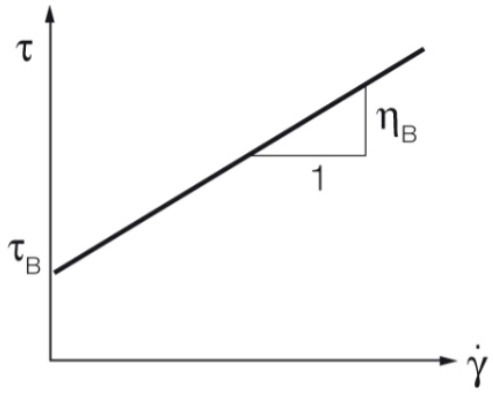

Figure 2.9. Bingham Regression Model

For the measurement of the Casson yield point, the curve fitting application is executed by using Square Root function (see Figure 2.10) (Casson, 1959). This takes into account the bending of the curve and is therefore more suitable than the Bingham calculation for shear thinning and shear thickening materials. Casson equation for yield point is as follows;

$$\sqrt{\tau} = \sqrt{\tau c} + \sqrt{\eta c \cdot \dot{\gamma}}$$

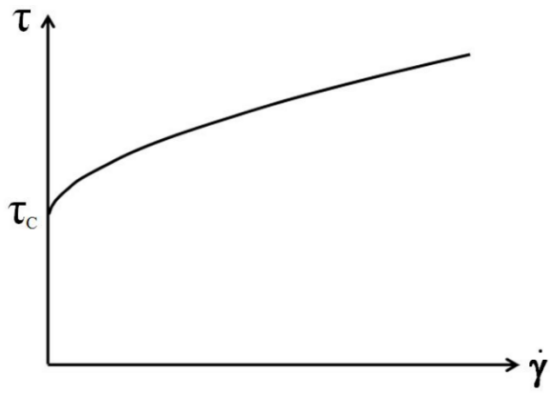

Figure 2.10. Casson Regression Model

Herschel-Bulkley regression identify a material's flow curve with yield stress and shear-thinning or shear-thickening behavior at stresses upon the yield stress (see Figure 2.11) (Herschel, 1926). The Herschel-Bulkley equation for the pour point is as follows;

$$\tau = \tau_{HB} + c \cdot \dot{\gamma}^{p}$$

τ_{HB} defines the pour point of the material. c is called the "flow coefficient" or "consistency index", which represent the viscosity at a given shear rate. The P (known as the "Herschel-Bulkley index") define the flow action of the material;

p <1: shear thinning

p> 1: shear thickening

p = 1: Bingham flow behavior

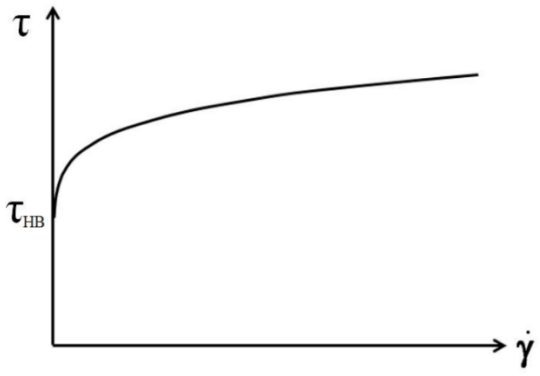

Figure 2.11. Herschel-Bulkley Regression Model

2.5. Rheology and Workability of Geopolymer

2.5.1. Conventional Geopolymer

There are various studies on the rheology of conventional geopolymers in the literature. Although most of these are on setting time and workability, in recent studies, a detailed rheology study of geopolymers using rheometers has become widespread. Vance et al. (2014) researched the effects of activator type and molarity on the rheological features of FA based AAM. It has been shown that the viscosity of the activator and the volume solution / solid ratio excessively affect the plastic viscosity of matrix. It has been found that the rheological features of NaOH or KOH activated FA based geopolymer are mainly affected by variation in the viscosity of the solution and the surface load of the FA grains. It has been observed that the yield stress and plastic viscosity of the suspensions tend to be zero at low activator Ms (silica modulus) and increase with Ms.

Carlos et al. (2012) worked on the rheological behavior of FA-based geopolymer paste prepared under various mixture design formulations using a rheometer. In this context, the influence of superplasticizers on the viscosity of geopolymers was investigated and the following outputs were obtained: geopolymer act like a Bingham fluid and shows thixotropy. The molarity of hydroxide has an influence by increasing the viscosity of the matrix, and the ratio of silicate to hydroxide does not show a considerable effect. The rheology was importantly influenced when the superplasticizer was used. While the polycarboxylate superplasticizers managed to slightly lower the viscosity of the paste, the naphthalene sulphonate superplasticizer not only enhanced the viscosity but also caused rapid setting.

Yasser Rifaai et al. (2019) investigated the flow and viscoelastic features of FA-based geopolymers activated via various NaOH molarity with a coaxial cylinder rheometer. Although the geopolymers studied exhibit a shear thinning behavior, rheological features are highly influenced by NaOH molarity. Augmenting the NaOH molarity to 7 mol / L lead an increment in yield stress, storage modulus and rigidity. In addition, using higher molarity lead in lower yield stress, storage modulus and setting rate because of the predominance of repulsive forces between the particles, thus avoiding network formation. Marta Palacios et al. (2008) researched the setting and rheological features of alkali active slag paste and mortars. The rheology of alkali active slag pastes and mortars are mostly associated with the alkali activator used. When the activator solution is glass water, it fits

the Herschel-Bulkley model with significant structural distortion, whereas when NaOH is activator, these pastes and mortars behave like Bingham fluids. On the other hand, enlarging the mixing time can significantly delay the hardening of the glass water activated slag pastes, with initial and final setting times of about 3 and 10 hours respectively, now a possibility. This provides a practical and convenient way of controlling the undesirable rapid setting of these materials, that has the opportunity to facilitate a broad range of technological implementations easier.

Aboulayt et al. (2014) investigated the rheological behavior of a fresh MK-based geopolymer and the effect of adding calcium carbonate. Tests show that two models characterize these formulations: the Bingham model and the Herschel-Bukley model. While the addition of calcium carbonates does not appear to have any effect on the development of viscosity, it does offer remarkable sensitivity to geopolymerization temperature.

Poulesquen et al. (2011) investigated the rheological characteristics of alkali-activated MK during geopolymerization using dynamic rheometer. Rheological parameters of G ', G" and tan δ were obtained by the strain amplitude test. When the geopolymer is activated by KOH the nature of silica has few effects on the viscous and elastic modulus, and the setting time is rapid with NaOH and at higher temperatures, independent of the geopolymer. NaOH expedite the geopolymer curing kinetics regarding to KOH and makes the flat parts of the viscoelastic module shorter. Also, tan (δ) over time indicates that the elastic component (G') changes faster than the viscous component (G") in the case of KOH.

Serag (2020) et al. conducted a study on BFS-based geopolymers. The findings demonstrated that the elevated alkaline solution / FA ratio improved the workability and gave an expanded setting time, however, the inferior alkaline solution / FA ratio gained remarkable compressive strength.

Chindaprasirt et al. (2007) worked on the workability and strength of geopolymer mortar compose of coarse lignite FA with high calcium. The findings showed that the workability of geopolymer was related to the ratio of Na_2SiO_3 to NaOH and the NaOH molarity. The

reached compressive strength is between 10-65 MPa and it has been observed that increment in NaOH and sodium silicate molarity decrease the flowability.

The particle size of bottom ash, alkali / ash ratio, Na_2SiO_3 / NaOH ratio and NaOH molarity were investigated by Sathonsawaphak et al. (2009). The effects of water, NaOH and naphthalene-based superplasticizer additions on the workability and strength of geopolymer were discussed. The inclusion of water enhanced the flowability of the geopolymer better than the utilization of naphthalene-based superplasticizers with a same light decrement in strength. The introduction of the NaOH solution relatively increased the flowability of the mixture while preserving the strength of the geopolymer.

2.5.2. Construction Demolition Waste-based Geopolymer

Rheological properties such as shear stress, yield stress, viscosity, etc. of CDW-based geopolymers have not been excessively investigated since CDW materials started to be used in geopolymer matrix as binder in recent years. Rovnaník et al. (2018) and Keppert et al. (2018) two researchers studied the rheological features of geopolymers composed of RCB and ceramic powders. Rovnaník et al. (2018) stated that introducing brick precursor to MK-based geopolymers reduced the thixotropic behavior and plastic viscosity. In addition, it was found that the more brick dust, the greater the retardation in the development of yield stress.

Keppert et al. (2018) studied the influence of CaO substitution on the rheological features of ceramic precursor. The findings demonstrated that the yield point of waste ceramics based geopolymer is quite low, but high calcium ceramic powder results higher yield stress than lower calcium ceramic powder used paste.

In Allahverdi and Najafi Kani (2009) and Rakhimova and Rakhimov (2015) studies, the setting time of geopolymer was evaluated. According to the results of Allahverdi and Najafi Kani (2009), there is a connection among the Na_2O molarity and the final setting of the CDW-based geopolymer (waste brick and concrete waste). All geopolymer binders result longer setting with lower Na_2O content (6%). The final setting time of geopolymer can be compared to ordinary cement-based matrix. Besides, the authors stated that all geopolymer binders had an initial pseudo-setting because of the high thixotropic features of the fresh matrix. It was reported that increment in Na_2O concentration with a fixed

Na_2O / SiO_2 ratio leads to an acceleration of geopolymerization yet might lower the final setting time.

Rakhimova and Rakhimov (2015) studied the influence of the specific surface area of brick waste and BFS and 2 various activators (Na_2SiO_3 and Na_2CO_3) on setting time of geopolymer. Findings proved that by increasing the specific surface area of the binder from 300 m^2 / kg to 900 m^2 / kg, setting times reduced. In addition, Na_2CO_3 increased setting time regarding to Na_2SiO_3 with a same specific surface area.

Rheological properties such as, shear stress, yield stress and viscosity have rarely been analyzed in the researches in details, making these topics attractive for further researches (Dadsetan et al., 2019). With the increment in usage of CDW based geopolymer in order to make world green again by using waste materials as raw materials in concrete technology, knowledge about rheology of geopolymer will be become more essential for different advanced construction application such as self-leveling, shotcrete, 3D additive manufacturing. Therefore, to apply geopolymer in a work area as wide as concrete, rheology of geopolymer must be known down to the last detail. By enlarging application area of CDW based geopolymer by means of enhancing its properties with the knowledge of its rheology and mechanic properties in details, requirement for new landfill area, contamination of earth and groundwater resource, CO_2 emission, hazardous dust and greenhouse gasses will be reduced. In addition, there is not much information about rheologic performance of CDW-based geopolymer in literature. Therefore, in that thesis, workability and rheological properties of CDW-based geopolymer systems together with mechanical properties are investigated. In that context, empirical and advanced test equipment were used to clarify how rheological and mechanical properties of CDW-based geopolymer with usage of various activator type, dosage and combination, changes. Although, the main objective of this thesis study is to understand how activator type, rate and dosage effects the geopolymer's rheologic and mechanical properties.

3. MATERIALS AND METHODOLOGYY

Under this title, physical and chemical properties of each materials used in mixtures during the studies are explained. In addition, the test methods used to investigate the fresh and hardened engineering characteristic of the CDW-based mixtures are explained in detail.

3.1. Materials

During the thesis studies, CDW-based materials which are hollow brick, red clay brick, roof tile, glass waste and concrete waste and besides that various industrial waste, BFS, SF and FA, were used as binders. To activate binder for geopolymerization, sodium hydroxide (NaOH), calcium hydroxide ($Ca(OH)_2$) and sodium silicate (Na_2SiO_3) were used as an activators. Mortar phase mixtures were prepared with recycled aggregates obtained from CDW.

3.1.1. CDW Based Binders

The waste materials used in the thesis studies were procured from the demolished buildings within the Ankara province and were categorized into five groups as HB, RCB, RT, GW and CW. Clay-based materials, HB, RCB and RT, were obtained from the roof and wall sections of construction during the demolition of the buildings that was at the end of service life. Glass waste was used among the CDW based binders due to its high silica content and amorphous structure, and in the thesis comprehensive waste management was targeted. Concrete waste also was used as binder and was obtained from the structural elements of the building. Obtained materials from the demolition were subjected several processes to reach proper particle size distribution. To do that, each of the waste materials obtained from the urban transformation areas in the Ankara province as a result of the selective demolition process was crushed in a jaw crusher to reach approximately 0.5 cm in size and subjected to grinding process in a ball mill until it reached approximately cement fineness. The initial, crushed and ground states of the materials are presented in Figure 3.1 and the SEM images of these materials are shown in Figure 3.2. The chemical contents of the CDW-based binder materials are shown in Table 3.1, and X-ray diffraction (XRD) phase diagrams are shown in Figure 3.3.

(a)

(b)

(c)

(d)

(e)

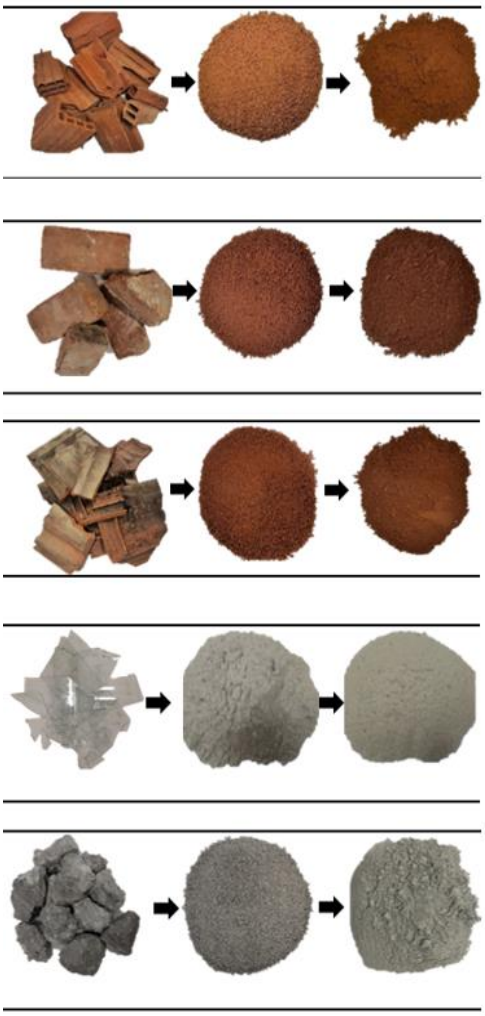

Figure 3.1. a) HB, b) RCB, c) RT, d) GW and e) CW materials, respectively, the initial state, crushed state, ground state

Table 3.1. Chemical contents of binder materials

%	Hollow Brick (HB)	Red Clay Brick (RCB)	Roof Tile (RT)	Glass Waste (GW)	Concrete Waste (CW)
SiO_2	39.7	41.7	42.6	66.5	31.6
Al_2O_3	13.8	17.3	15.0	0.9	4.8
Fe_2O_3	11.8	11.3	11.6	0.3	3.5
CaO	11.6	7.7	10.7	10.0	31.3
Na_2O	1.5	1.2	1.6	13.6	5.1
MgO	6.5	6.5	6.3	3.9	0.9
SO_3	3.4	1.4	0.7	0.2	0.5
K_2O	1.6	2.7	1.6	0.2	0.7
TiO_2	1.7	1.6	1.8	0.1	0.2

P_2O_5	0.3	0.3	0.3	0.0	0.1
Cr_2O_3	0.1	0.1	0.1	0.0	0.1
Mn_2O_3	0.2	0.2	0.2	0.0	0.1

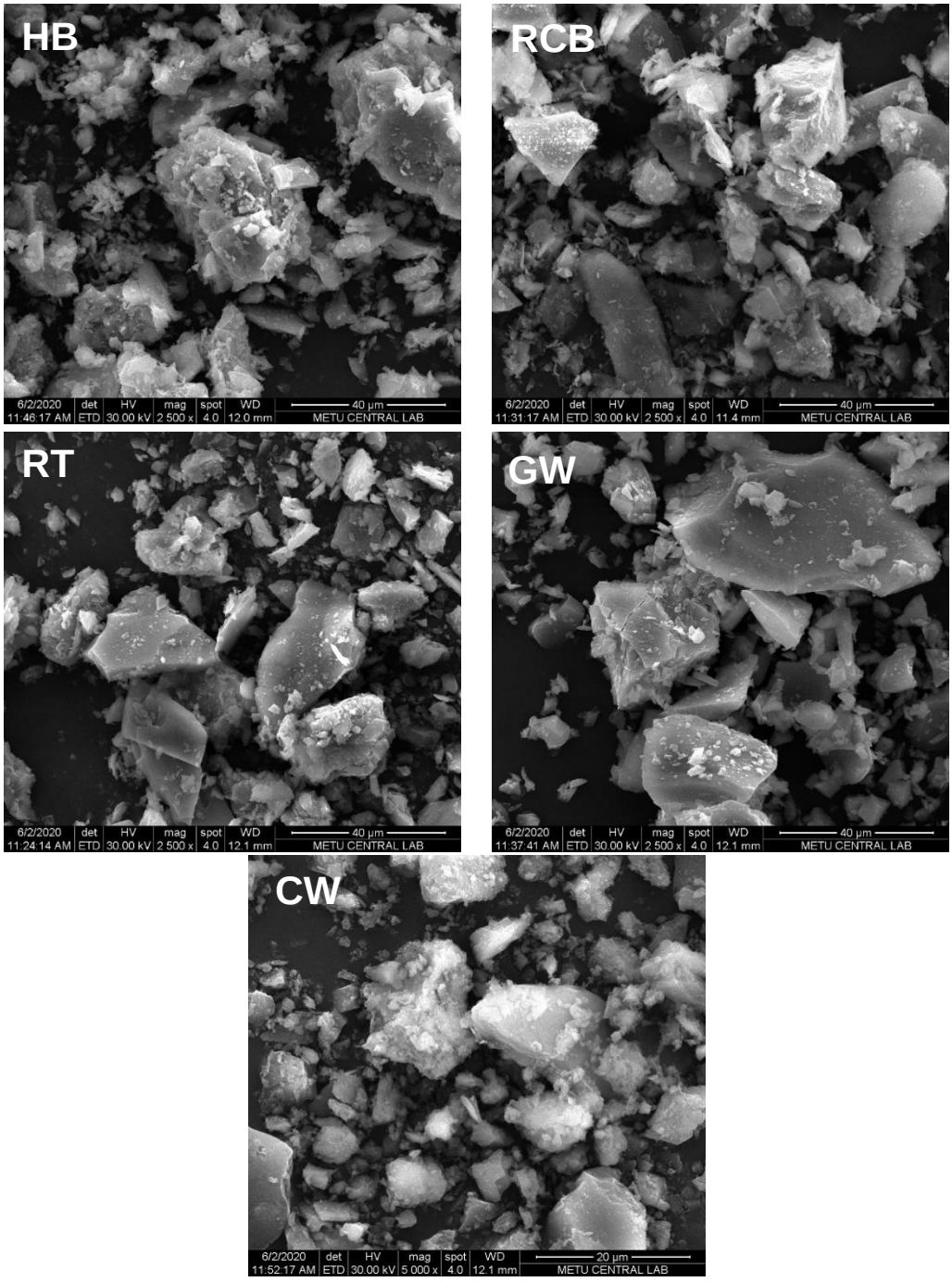

Figure 3.2. SEM images of a) HB, b) RCB, c) RT, d) GW and e) CW

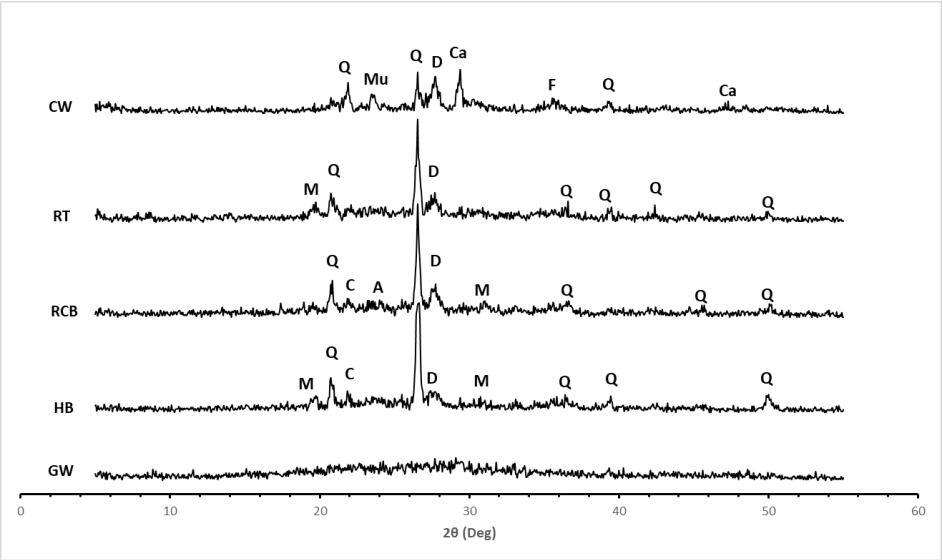

Figure 3.3. XRD phase diagrams of powder materials

Table 3.2. Chemical formulations and PDF numbers of crystalline phases.

Crystalline Phase	Symbol	PDF Number	Chemical Formula
Quartz	Q	96-101-1160	SiO_2
Crystobalite	C	96-900-8230	SiO_2
Diopside	D	96-900-5280	$Al_{0.6}CaMg_{0.7}O_6Si_{1.7}$
Mullite	M	96-900-5502	Al_2O_5Si
Akermanite	A	96-900-6115	$AlCa_2Mg_{0.4}O_7Si_{1.5}$
Calcite	Ca	96-900-9668	$CaCO_3$
Muscovitte	Mu	96-101-1050	$Al_3H_2KO_{12}Si_3$
Foshagite	F	96-901-1044	$Ca_4H_2O_{11}Si_3$

As expected, the Quartz phase was the major crystalline peak with the highest intensity for RCB, RT, and HB. The other major peaks were determined as Diopside for each masonry units. However, for the CW, major peaks were observed at Quartz, Diopside and Calcite mainly. The minor crystalline phases detected for CDW-based precursors are given in Table 3.2. Besides the brick-based portion of CDW, the GW had an amorphous with a widen peak centered around approximately at 2θ values of 28°.

Within the scope of the thesis, mortar mixtures have been prepared with HB, RCB, RT, GW, and CW as a binder and recycled aggregate having 2 mm maximum aggregate size were utilized. Particle size distributions of CDW-based binder materials in powder form, which were grinded and used in mortar mixtures are given in Figure 3.4.

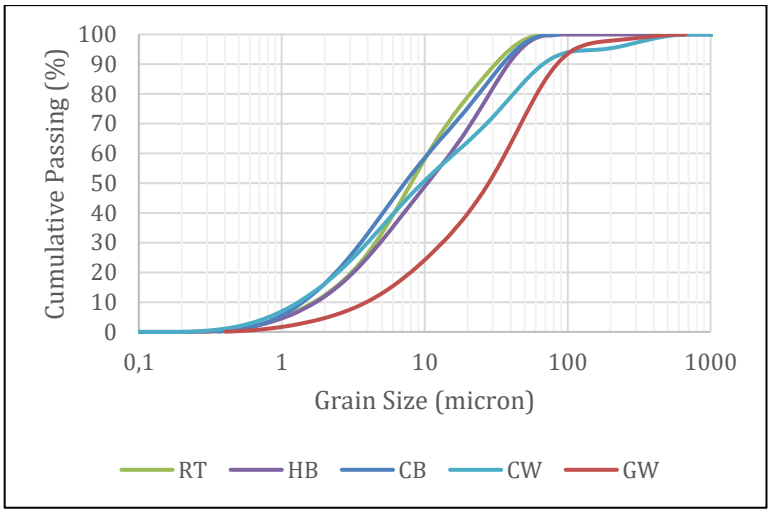

Figure 3.4. Particle size distribution of powder materials used in Mortar Phase

As can be seen from the Figure 3.4, 50% of the HB, RCB, RT and CW materials are below 10 microns, while this rate is 30 microns for GW. When the particle size of less than 40 micron was examined, it was observed that while HB, CB and RT similarly had a fineness of 90% in this range, this was observed in the range of 80-90% for CW and 60% for GW.

3.1.2. Mineral Additives

The use of some mineral additives in order to improve the performance of CDW-based binders when deemed necessary within the scope of the project was also considered, and as a result of the literature review, it was decided to use mineral additives such as BFS, SF and FA when needed. It is predicted that the high calcium and silicon contents of BFS, FA and SF will contribute to improving the mechanical and rheological properties of the mixtures containing 100% CDW-based materials. By using them in the geopolymeric system, these mineral additives were recovered with the status of by-product from waste status, in line with the purpose of the project. Chemical contents of mineral additives are presented in Table 3.3.

Table 3.3. Chemical contents of mineral additives

%	Blast Furnace Slag	Fly Ash	Silica Fume
SiO_2	32.10%	60.07%	85.0%
Al_2O_3	11.20%	21.35%	0.0%

Fe_2O_3	0.62%	7.41%	0.0%
CaO	36.10%	0.99%	1.0%
Na_2O	0.31%	0.99%	0.0%
MgO	5.64%	1.82%	0.0%
SO_3	1.21%	0.22%	2.0%
K_2O	0.83%	2.91%	0.0%
TiO_2	1.07%	0.94%	0.0%
P_2O_5	0.01%	0.15%	0.0%
Cr_2O_3	0.00%	0.03%	0.0%
Mn_2O_3	1.48%	0.08%	0.0%

3.1.3. Alkaline Activators

Within the scope of the thesis, three types of alkali activators, NaOH, $Ca(OH)_2$ and Na_2SiO_3, were preferred to be used as a result of the preliminary studies carried out in different projects and extensive literature review.

3.1.3.1. Sodium Hydroxide (NaOH)

NaOH, caustic soda, is a substance that is frequently used in the chemical industry, yet also has wide usage areas in different sub-branches of the industry. NaOH, which occurs as a result of the electrolysis of water and sodium chloride, can be obtained in various phases and forms. NaOH can be solid and liquid form, and it can be in the form of flakes, beads and sticks with the same chemical content when it is solid. When sodium hydroxide contact with water, it dissociates into sodium (Na +) and hydroxide (OH-) ions in a medium and releasing a large amount of heat since this reaction is exothermic. Released OH- ions increase the alkaline level of the environment and increase the pH of the system. The rising alkalinity also increases the dissolution degree of Al and Si minerals in the structure of binder materials. NaOH is the most widely used activator in alkali activation studies due to its easy availability and affordable price. Even though the heat generated during the preparation of the solution varies according to the molarity of solution (especially after 5 molar), in each case it threatens occupational health and safety. So, NaOH solutions should be prepared with necessary precaution.

In literature, there is no ideal determined NaOH concentration for geopolymeric systems since required alkalinity to break Al and Si bond can vary according the aluminosilicate sources and its structure. There are studies that yield good results from mixtures with both

high and relatively low concentrations. NaOH used within the scope of the thesis, has been produced by Protecting Klor Alkali San. ve Tic. A.Ş in the form of flakes. Detailed information about used NaOH is given in Table 3.4.

Table 3.4. Properties of sodium hydroxide (NaOH)

Properties	Condition	Unit	Result
Appearance	-	-	White flake
Sodium hydroxide	min. 98	%	98.27
Sodium chlorite	max. 0.10	%	0.02
Sodium carbonate	max. 0.40	%	0.35
Iron (Fe)	max. 15	ppm	13.17

3.1.3.2 Calcium Hydroxide ($Ca(OH)_2$)

Calcium hydroxide, known as slaked lime, is chemically represented as $Ca(OH)_2$, and obtained following the interaction of quicklime with water. $Ca(OH)_2$, which increases the alkalinity of the system due to its chemical form when dissolved in medium, is used activator in literature due to its contributions in the geopolymerization process. It can also contribute to the acceleration of the reaction since it provides an extra source of "Ca" in the system. In that way, calcium hydroxide contributes to the generation of C-S-H and C-A-S-H structures in the system which provide a denser matrix formation. Therefore, it is predicted that the introducing of $Ca(OH)_2$ will enhance to the mechanical properties of the matrix as a result of denser structure with formation of extra C-S-H and C-A-S-H structure. Calcium Hydroxide can be introduced to the system both directly as powder or mixed with water to activate the geopolymer systems. The $Ca(OH)_2$ used in the thesis studies was supplied from “Tekkim Kimya” in powder form in 5 kilogram boxes. Properties of $Ca(OH)_2$ are demonstrated in Table 3.5.

Table 3.5. Properties of calcium hydroxide ($Ca(OH)_2$)

Properties	Value
Molecular Weight	74.09 g/mol
Melting Points	550 °C
Purity (%)	min. 87
MgO (%)	max. 1
Acid-insoluble (%)	max. 1
Loss on ignition (%)	max. 3
Grain Size (<90 mm) (%)	min. 90

3.1.3.3. Sodium Silicate

Sodium silicate, water glass, has chemical formula of Na_2SiO_3. Sodium silicate has a liquid and colorless form, and it is used for different application in various industrial branches. Sodium silicate is one of the major used alkali activators in geopolymer matrix after NaOH. Sodium silicate can seriously affect the mechanical and rheological properties of the systems. Sodium silicate, more stable in high pH environments, increases the silica content in the matrix together with the soluble silicate content. Therefore, its dual use with NaOH, which increases the alkalinity and dissolution degree of the environment, is widely seen in the literature in geopolymer matrix. However, sodium silicate can shorten the setting time and have a negative effect on the workability time in systems including sodium silicate. The sodium silicate used in this thesis study was supplied by "Emir Kimya". Characteristics of the product are shown in Table 3.6.

Table 3.6. Properties of sodium silicate (Na_2SiO_3)

Parameter	**Value**
SiO_2 (%)	23
Na_2O (%)	11
Module (SiO_2/Na_2O)	1.9
Baume (20 °C, Be[1])	40
Density (20°C, gr/cm^3)	1.4
H_2O (%)	66

3.1.4. Recycled Aggregate

Among the total construction and demolition waste, the share of reinforced concrete structural elements is quite high when it is compared to other elements such as walls, roof etc. The study conducted by Oikonomou (2005) stated that this share reached almost 40% and the share mainly composed of concrete waste. Considering the high amount of concrete waste generated as a result of demolition, it is obvious that produced recycled aggregate should be reused in geopolymer other than powder form in order to benefit from the concrete waste in the most efficient way. When literature is examined, recycled aggregate obtained from waste concrete is most common method to recover waste concrete all over the world in both concrete and geopolymer system since waste concrete in general contains natural aggregate up to 70%. To use waste concrete as recycled aggregate, first, the concrete wastes obtained in the form of rubble were divided into smaller pieces with hammer drills and these pieces were broken in jaw crushers to reach

appropriate smaller pieces. In the scope of thesis, the aggregate used in mortar phase has a fineness of less than 2 mm and were obtained by sieving all of the broken concrete wastes as a result of given processes. Although usage of recycled aggregate in matrix is beneficial in terms of environment, it was predicted that the mortar residues on the surfaces of the recycled aggregates will increase the water absorption requirement of the recycled aggregates compared to natural aggregates and it can cause compressive stress reduction due to residues which weaken the interface transition zone. In literature, several treatments were applied to recycled aggregate to improve its weakness. However, these processes also cause CO_2 emission, water and energy consumption that were tried to lower in the scope of study. In the thesis, recycled aggregate was directly used in matrix without any treatment.

3.2. Methodology

In this part of the thesis, the mixture design, preparation and experiments, that has been used during thesis study, are explained in detail.

3.2.1. Preparation Procedure of Mixtures

First, flake shaped NaOH particles were added to the water with an arranged ratio to prepare adjusted solution for activation of precursor. Since the NaOH dissolution reaction is an exothermic, the prepared solution temperature started increase suddenly in a very short time just after the reaction start. For the occupational health and safety, the prepared solutions were kept under room temperature to lower its temperature. During this stage, to prevent evaporation of water since whenever water evaporate solution molarity changes and water/binder ratio of system as well, solution was stored in closed bottle. The rate and amount of binder materials, activators and aggregates used in the mixtures were arranged according to preliminary studies carried out in past and ongoing projects of thesis advisor and the literature. In the first stage of mix, all of the powder formed materials including $Ca(OH)_2$ were introduced to the container and mixed together in the Hobart branded mixer (see Figure 3.5) at low speed for 1 minute to ensure homogeneous distribution of powder form materials. After homogeneous distribution of powder form materials, the prepared sodium hydroxide solution was gradually added to the mixer while mixer was working at still low speed. The mixture was mixed for one more minute at lower speed to obtain homogeneous distribution of the sodium hydroxide to each powder form materials. After this step, according to the prescription of mixture in terms of having

sodium silicate or not, the mixture procedure continued differently. For the sodium silicate containing mixture, sodium silicate was added to the mixer just after the uniformly dispersion of sodium hydroxide (1 minute after addition of NaOH) and mixed 90 seconds at low speed and 60 seconds at medium speed. For the mixtures not containing sodium silicate, after the uniformly dispersion of sodium hydroxide, the mixture was continued to mix for 60 seconds but at medium speed and the mixing process was ended.

Figure 3.5. The mixer used in thesis studies

Some part of the prepared mixtures was used to determine rheological properties of fresh form of mixtures and some part of it was filled into 50* 50 * 50 mm cubic molds (Figure 3.6) to check the compressive strength on the 7^{th}, 14^{th} and 28^{th} days.

Figure 3.6. 19. 50 * 50 * 50 mm molds

3.2.2. Curing Conditions

In previous similar studies, it has been observed that the increase in temperature accelerates the geopolymerization reactions and provides the samples with higher mechanical properties. However, in all the works carried out so far within the scope of the thesis, only the curing process was carried out under ambient conditions (Figure 3.7).

Figure 3.7. Samples cured under ambient conditions

3.2.3. Test Methods

Consistency is a measure of the flowability of the prepared mortar or paste. The water amount and the flowability of the mixture are directly proportional. However, the increment in water content causes a decrease in mechanical properties as a result of extra pore formation after mixture harden. Geopolymer mixtures exhibit plasticity behavior and shapeable character for a while. In a time, mixture loose its plasticity and get harden as result of geopolymer reaction. The time from the beginning of geopolymer reactions until hardens by losing plasticity is called the setting time.

The w/b ratio of 0.33 was chosen for each mixture at the beginning of thesis study. However, after the behavior of activator with various combinations were tested, the w / b ratios of 0.36 and 0.39 were also tested to see how w/b ratio effects rheology and mechanical performance of geopolymer. For the analysis of the material, empirical tests such as flow table, buildability, vane shearing test were performed on fresh mixtures.

3.2.3.1. Flow Table

The flow table test conforming in the ASTM C1437-15 standard provides information about the flowability of the material. In the flow table test, the material is filled in two stages into a truncated cone which has a base inner diameter of 100 mm, inner diameter of the ceiling 70 mm and a height of 60 mm and positioned on the table. Then the filled material is leveled with the help of spatula. Then, the cone is removed vertically, and the flow table is dropped from a height of 12.7 mm for 25 times in 15 seconds. The amount of spreading of the material in two perpendicular directions are measured with ruler and recorded (Figure 3.8). Using the data obtained from test, the deformability index (Γ) was calculated using the formula given below. In this equation, d_0 represents the base diameter of the mold (100 mm), d_1 and d_2 represents a recorded spreading value perpendicular to each other.

$$\Gamma = \frac{d_1 d_2 - d_0^2}{d_0^2}$$

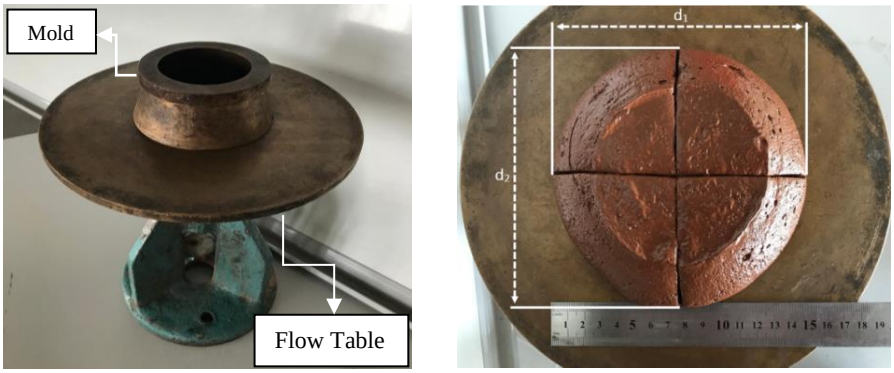

Figure 3.8. Flow table test representation

3.2.3.2. Vane Shear Test

The main objective of this thesis study is to understand how activator type, rate and concentration affects the geopolymer's rheological and mechanical properties. In this context, shear test was conducted to evaluate the flowability properties of fresh mortar. Although this method has been suggested for land use especially in determining soil properties, it has also been successfully applied in measuring the thixotropy and flow properties of fresh paste (Khayat et al., 2008; Metwally et al., 2012). Within the scope of the study, this test was carried out using a pocket-type Vane shear tool, and the rheological features of the mortar mixtures were examined by determining the resistance of the material against shear force (Figure 3.9).

Figure 3.9. Indication of the vane shear device and application of the test

This method can give different values as yield stress depending on the rotator or blade of the test device although the test device is adjusted. Therefore, the results are used to find the relative yield stress between samples, even though they do not give real values as numerical values. Since the test apparatus is simple and is used for initial and easy observation, this method has been used for comparative analysis of samples rather than specific yield stress values. Before the test operation, vane shear apparatus was located into the mixture till blades fully immersed into mixtures (Figure 3.10). Later, by applying gradually increasing force toward clockwise direction, the apparatus tried to be rotated until blades started to turn freely. After freely rotation of apparatus, shear yield stress value of mixture was read from indicator on apparatus.

In addition, open-time behavior of the material was observed with this apparatus. As it is known, the materials lose their consistency by setting over time and this loss of consistency affects the pumpability of the material and its quality after pumping (pore, crack, froth, etc.). This test method was applied to the samples at the 30th, 60th and 120th minutes in addition to the measurement immediately after the preparation of the mixture in order to see the change in behavior of the materials over time. In this way, information about the setting times and open time performance of the mixtures was also provided.

Figure 3.10. Example of Vane shear tests performed at 0, 30, 60 and 120 minutes

3.2.3.3. Buildability

Buildability of mixture is related with the viscosity and yield stress performance and directly proportional with it, means higher the yield stress or viscosity, the better the buildability performance. Yet, after a threshold value in terms of buildability performance of mixture depending on content, mixture starts to lose its flowability performance because of much dense microstructure with higher viscosity or yield stress. The buildability test is a test method inspired by the ASTM C1437 standard but does not have its own standard. In the literature, it is seen that different test procedures are applied, but in this study, the test method used by Nematollahi et al. (2018) were used. In the flow table method, the material was compressed into the mold in the form of truncated cone in the same way and the material was kept in the mold for one minute after the compression process. Immediately afterwards, the mold was removed and a glass plate placed in order to distribute the load on the material homogeneously, together with the glass plate on it, loads were placed with a total weight of 600g. The material was subjected to load for a minute, then the load was removed, and the final height value of the material was read from two perpendicular directions and the collapse degree was analyzed (Figure 3.11).

Figure 3.11. Buildability Test Application

3.2.3.4. Compressive Strength Test

The compressive strength test applied in thesis was carried out in accordance with ASTM C109 standard by using 50 x 50 x 50 mm molds. Samples were taken out from the mold after 24 hours casting and left for curing in ambient conditions having 25 ±2 temperature and %50 ± 5 relative humidity. By using uniaxial load enforcer test equipment with the rate of 0.9 kN/s, specimens were tested at 7^{th}, 14^{th} and 28^{th} days (Figure 3.12). The obtained results represent the mechanical performance of the samples.

Figure 3.12. Compressive Strength Test Instrument

3.2.3.5. Rheometer

The mortar mixtures prepared to obtain the rheological characteristics of the material more effectively and efficiently, were tested with Anton Paar brand rheometer device (Figure 3.13). This is a rotational rheometer type and the maximum torque value it can measure is 200 mN.m. Since the device is very sensitive and is not widely used to test such construction materials, experiments were carried out with various corrections in order to measure the features of the produced geopolymer.

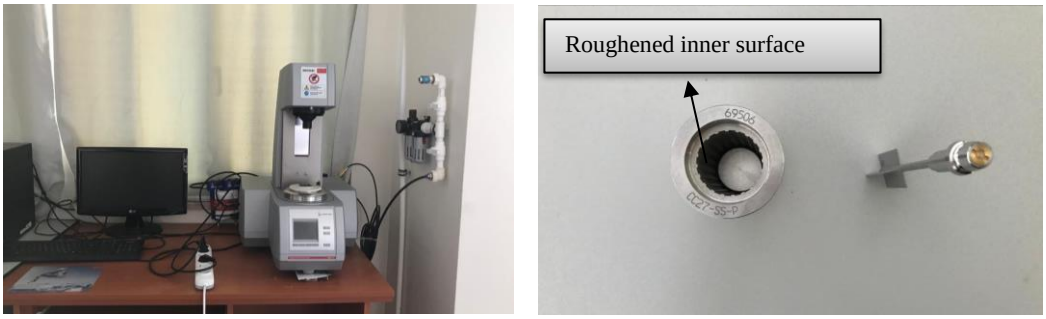

(a) (b)

Figure 3.13. (a) Rheometer to be used within the scope of the study, (b) Material loading chamber and stirrer of the rheometer

In order to determine the rheological properties of each produced mortar mixture by rheometer, it is planned to use a 4 different method, which is determined to be better in determining the rheologic and thixotropic property of the material. The rheometer device measures two parameters, namely "Speed" and "Torque", and converts these parameters to desired rheological values (shear rate and shear stress) by using a certain conversion coefficient. These values obtained are used to determine various rheological property indicators such as viscosity and yield stress by using appropriate methods / formulations. Since the rheometer device used within the scope of the thesis is very sensitive, the maximum particle size of the material to be tested in the device should generally not exceed 2-3 mm, although it depends on the size of the measuring vessel and mixer used. And the rheometer device can read a maximum torque value of 200mN.m. First of all, considering these limits of the device, it has been tried to determine the appropriate consistency range in order to perform the test successfully. In this context, as a result of empirical experiments, a recipe that is considered more viscous in terms of consistency than other mixtures has been tried to achieve a more fluid consistency in which the device can work comfortably by increasing the w/b ratio by 0.03 up to 0.39 ratio, starting with the w/b ratio of 0.33. Samples prepared with these three different w / b ratios were subjected to preliminary tests in four different test methods, and the mixture properties in accordance with the operating limits of the device were tried to be determined. Information about the test methods planned to be used for the rheometer are given below.

3.2.3.5.1. Up and Down Curve Method

The first experiment tested within the scope of the tests performed using the rheometer was the Up-Down test method. For this test method, the fresh mixture was first subjected shear rate from lower rate to higher rate in order to break the bonds formed in the inner structure and corresponding shear stress were recorded (Up Curve). Then, mixture was subjected to shear started from higher rate to lower rate and shear stresses corresponding to each shear rate were recorded (Down Curve). By fitting a linear trend line (Bingham model - Hershel-Bulkley model etc.) to the points in the rheograms obtained in this way, the point where this line intersects the shear stress axis was determined as yield stress and the slope of the line was determined as plastic viscosity. During this experiment, the shear rate was started from 0.01 s^{-1} and increased to 100 s^{-1}, and then it was reduced from 100 s^{-1} shear rate to 0.01 s^{-1} shear rate. In this process, the torque resistance of the sample to the mixer is converted to shear stress. And as a result of these processes, shear stress

versus shear rate plot has been obtained. When regression models suitable for the slope and behavior of this graph were applied, the yield stress value has been reached. At the same time, the ratio of shear stress to shear rate obtained as a result of this experiment gave the viscosity value. To investigate flow behavior, this test method was used by different researches for a long time on various type of materials (Chen et al., 1992; Papo, A. & Piani, L., 2004; Labanda, J. & Llorens J., 2005; Iotti et al., 2011; Divoux et al., 2011b, 2013).

For this test, firstly, a mixture consisting of 100% CDW based materials with 0.33 w / b ratio, activated with 6.25 Molar NaOH and 10% $Ca(OH)_2$ was selected. This recipe is one of the most dense / viscous paste mixes obtained in empirical experiments in the preliminary study performed to understand the behavior of the material at the beginning stage of the CDW-related studies. In order not to encounter a possible excessive strain due to aggregates and to prevent excessive strain on the device, the appropriate consistency range was determined initially by using paste mixes.

While the sample prepared with a ratio of 0.33 w / b was testing, the device indicated 199 mN.m at the first reading at the beginning of the test. The test was stopped because the limit value of the device was approached. Afterwards, the test was started again using the mixture prepared by increasing the w / b ratio to 0.36. At the end of the test, the rheometer read a maximum torque of 85 mN.m for a ratio of 0.36 w / b. When the experiment was tested in a mixture of 0.39 w / b, a torque value of 47 mN.m was recorded. As a result, it was concluded that the device can measure mixtures rheologic properties at 0.36 and 0.39 w / b ratios. One thing to note here is that the increment in the density of the consistency augments the possibility of encountering wall slip situation that generally occurred in solder paste materials and cause slippage while testing materials which results lower viscosity then the bulk viscosity of mixtures (Barnes, 1995; Kalyon, 2005;Durairaj et al., 2010). This was seen as a negative situation in terms of the accuracy of the results and keeping the w / b ratio high has taken its place among the measures to be taken to prevent this situation. Also, the used chamber was roughed to increase adhesion between material and chamber surface, to decrease possibility of wall-slip condition (Kolli et al., 1997, Iotti et al., 2011). When Bingham model was applied to the results obtained from the flow curve, the sample with a ratio of 0.36 w / b showed a yield stress of 5501.2 Pa, while the sample with a 0.39 w / b ratio showed a yield stress performance of 2886 Pa. Figure 3.14

shows Up-Down curves drawn by using the results obtained from the rheometer as a result of the test performed on samples with 0.36 and 0.39 w / b ratios.

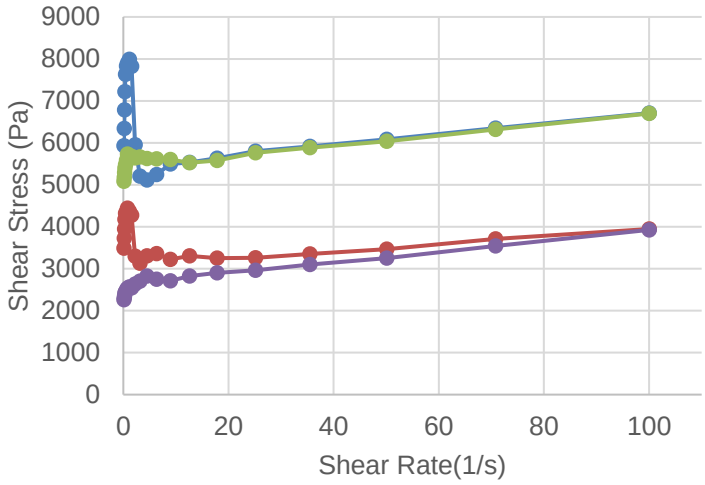

Figure 3.14. Up-Down Curve of samples with 0.36 and 0.39 w / b ratios

When the graphs in Figure 3.14 were examined, it was understood that another point to be considered here was a dramatic increase in the shear stress value observed shortly after the test was started. In the first stage, the value first peaked with a sudden increase and then decreased in the same way. Afterwards, it continued to test by showing a steady increase. The reason for this behavior was interpreted as the Wall-slip situation or pseudo setting properties of geopolymer could be occurring. In order to prevent this situation and erase the loading history (Divoux et al., 2011a, 2011b), the samples were subjected to pre-shear force in later experiments. No sudden increase or decrease was encountered in the Up-Down curve obtained after this preloading process. In order to get a reliable and accuracy result, it was decided to apply the regression models applied to interpret the results to the Down curve instead of the Up curve. Since, the sample have been subjected to both a preload and a shear force along the up curve means materials in chamber became more homogenous. As a result, the following standards were determined for this test;

Initially, samples were subjected to pre-shear to prevent possible Wall-Slip and pseudo-setting. In order to perform this preloading process, the samples in the measurement chamber was exposed to shear force from 0.01 to 100 s^{-1} shear rate. After this preload, the sample was rested for 1 minute and then the Up-Down test method was applied to the sample. The rheological properties of the mixture were determined by applying the appropriate regression model to the plotted rotation curve according to the result. Since

the preload / shear force was applied initially and the test needs about 10-12 minutes, it was decided to do this experiment every 20 minutes to test open time performance of mixtures. Preliminary studies have already shown that the rheological properties of the mixtures did not change much in a short time. The time-dependent rheological behavior of the waiting material was investigated by this method as by the vane shear tool (empirical experiment). Finally, for the following reasons, it was decided to use the 0.39 w / b ratio within the scope of this test.

- First, it has been observed that the device will not be facing so difficult in terms of torque value at this w / b ratio.
- Secondly, it has been deemed more appropriate to choose 0.39 instead of 0.36 in order to avoid any problem due to the thickening in the mortar.
- This value was deemed appropriate as it may be difficult to study the effect of activators at very high w / b ratios (e.g. 0.42, 0.45).

3.2.3.5.2. Constant Shear Rate Method

Secondarily, samples were tested by subjecting them to a constant shear rate of 0.03 s^{-1}. This constant shear rate method was also utilized in several researches to find out rheologic properties of different kind of materials especially, static and dynamic yield stress and thixotropic performance of materials (Barnes, H.A., 1997; Chhabra,R.P., 2010; Yang et al., 2014; Jeong, S., 2019; Zhang et al., 2019b). Samples were initially subjected to 15 minutes of shear rate to find out the optimum w / b ratio, and after the test standards were determined, the mortar mixes were exposed to a shear rate of 0.03 s^{-1} for 20 minutes. In this experimental method, the graph of the change of torque with time was drawn. The paste showed a linear elastic behavior until a certain threshold torque value was reached, after this value, the bonds were broken, and the material started to flow. This threshold value has been converted to the stress value and expressed as "yield stress at rest". The yield stress at rest is also called static stress. This value depends on the rest period and could be used in the interpretation of thixotropy. As the material was subjected to shear force, a decrease in shear stress has been observed after this value, and after a while, a constant stress value has been obtained. This value is called "dynamic shear stress". Torque-time and shear stress-time graphs of samples prepared with 0.33, 0.36 and 0.39 s / b ratios and having the same mixture and activator ratios as in the previous test are given below (Figure 3.15). As can be seen from the graph, the sample prepared at a rate of 0.33

w/ b forced the torque values of the device. No problems were observed with torque values for 0.36 and 0.39. However, since the mixes tested were paste samples (some torque value increase was expected when transitioning to the mortar form for the same mixture) and in order to stay on the safe side and also to work at the same w/b ratio with other tests, the w/b ratio was also selected as 0.39 in this test method.

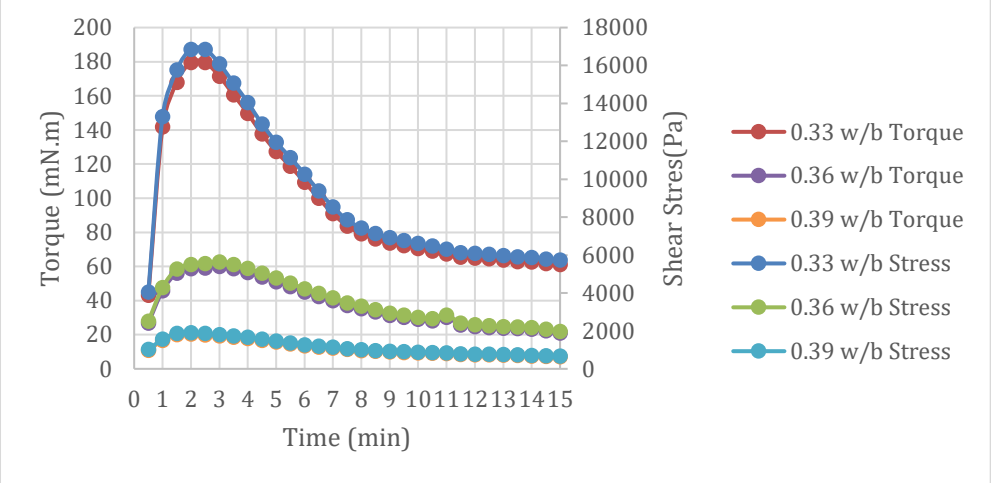

Figure 3.15. Torque and Shear Stress variation at constant shear rate over time of samples prepared with 0.33, 0.36 and 0.39 water / binder.

The following points were taken into account when interpreting the results obtained from this test:

- The material begins to flow once the static yield stress has been surpassed and the dynamic yield stress has been sustained. For pumping or injecting applications, therefore a lower dynamic yield stress is feasible, which not only brings too little strain on the motor drive and also reduces the potential of separating water from the blend.
- A higher static yield stress could result the mortar to be stiffer when stationary state, which could lead to need higher energy to flow but this case result better buildability for formless application such as additive manufacturing areas. Therefore, the optimum equilibrium between high static and low dynamic yield stress is critical for construction applications since having high static viscosity could increase energy needs, or lower dynamic stress could lower the resistance of materials to stands out exposed load.

Björn et al. (2012) define thixotropic fluids as dispersions that increase the viscosity of the fluid material at rest and form an intermolecular force system, flocculation. To able of material to move out, exterior load is needed to break down bonding forces, that reduce viscosity which called as the flocculation stage. In rheology, the exposed stress equal to or greater than the static yield stress of a material would cause clumping to dissolve. At this stage, while the structures are breaking, if the material is stirred continuously, the least potential viscosity is achieved to sustain a steady shear rate. This is related to the dynamic yield stress of a material. The significant observation of thixotropic materials is that materials clump again as shortly as the existing load is eliminated and the blending process removed. So, a thixotropic material in short time return initial hardness as consequences of an increment in viscosity after agitation is stopped (Kruger et al.2019).

3.2.3.5.3. Various Constant Shear Rate Method

As in the previous test method, samples were exposed to a constant shear rate for a while in this test method. But this time, both higher and different shear rate values were tested on the sample within the same test scope. This test method, first, utilized by Lapasin et al., (1983), yet later it was developed/modified by Erdem et al. (2009). In that thesis study, modified method was utilized, however, arranged shear rates during tests were rearranged as given below.

The fresh sample placed in the test container was subjected to a shear force for 2 minutes at a constant shear rate of 0.2 s^{-1} at the end of a 5-minute rest period. Then, the same sample, which was left to rest for 2 minutes, was exposed to a shear rate of 0.3 s^{-1} for 2 minutes, this time at a slightly higher rate. The same procedures were repeated for 0.4 and 0.5 s^{-1} shear rate. By observing the varying of shear stress with time at each rate, the initial stress and equilibrium stress for each rate were determined. Obtained results were collected in the stress-rate graph and the area between the curve obtained for the initial stresses (τ_b) and the curve obtained for the equilibrium stresses (τ_d) is calculated and named as "structural breakdown area" and this area has been used to interpret thixotropy (Erdem et al., 2009). This experiment was first tested on samples prepared with a ratio of 0.39 w / b and at the end of the test, the device recorded a maximum torque value of 52 mN.m. This value is considered to represent an ideal consistency for testing on the instrument as in other test methods. Therefore, this test method has not been tried on

samples prepared with 0.33 and 0.36 w / b ratio. As a result, this test was conducted on mortar samples with a ratio of 0.39 w / b after preliminary work.

3.2.3.5.4. Three Interval Thixotropy Test Method - 3ITT

The test method was very useful in determining the thixotropy of materials (Toker, et al., 2015). It was generally used in 3D additive manufacturing researches since the processes represent steps of application regarding additive manufacturing (Panda et al.,2018a, 2018b, 2020). In the 3ITT method, which is a fairly short and simple test method, specimen was first exposed to a low shear rate (0.1 s^{-1}) for 1 minute, then suddenly exposed the sample to a fast shear rate of 10 s^{-1} for 10 seconds and finally, the sample was again subjected to the initial low shear rate for 50 seconds. The purpose of doing all these were to be able to observe how the viscosity of the material changes when the material was exposed to a high shear rate / force and when the load on mixture was removed. Briefly, it was examined how much of its consistency can recover when the load was removed from the material. If the material can be restored to its original state, it can be said that it is very suitable for additive manufacturing as having high thixotropic behavior. Because this test simulates the 3D manufacturing stages very well. The sample prepared first was placed in the mortar chamber of the 3D printer pump, which can be expressed as resting state, and this can be understood as the state of the material under low shear force in this test method. The prepared mixture then encounters a high shear force as it moves through the pump and inside the pipe, which can be compared to the second step in the test, in which mixture was exposed to a high shear rate. When the last mixture leaves the tip of the nozzle, there was no load left on it and in this case it represents the last step of the method. After this point, the prepared mixture must return to its original form / consistency in order to carry the next layer on top of it without deformation. The return in this consistency can be defined as thixotropy and evaluated with this test method. In this test method, a ratio of 0.39 w / b was used.

4. RESULTS AND DISCUSSIONS

4.1. Development of Geopolymer Mortar Mixtures

In the process of designing the mortar mixtures within the scope of the thesis, the gains obtained from the preliminary studies tests performed while understanding the behavior of the material on the paste mixtures and information from literature were taken into consideration and accordingly, a series of geopolymer mortars were produced in order to test various characteristics in fresh and hardened condition. Flow table, buildability and vane shear tests were conducted in order to test effects of activator type, rate and combination on fresh properties of CDW based geopolymer. In addition, to find mechanical properties, compressive strength tests were conducted at the 7^{th}, 14^{th} and 28^{th} day on 50 x 50 x 50 mm cubic samples conforming with the ASTM C109 standard. Within the scope of the thesis, CDW-based recycled aggregates with maximum aggregate size of 2 mm have been used with a s/b ratio of 0.35.

4.1.1. Mortar mixes produced with CDW using solely NaOH or binary combination of $Ca(OH)_2$ and NaOH (1st Series)

In the process of designing mortar mixtures, a production series (1^{st} Series) was created in which only CDW-based materials (HB, RCB, RT, GW and CW) were used as binder material, and in these mixtures, 10% by weight of the total binder was made of glass waste and 10% was concrete waste. The remaining 80% was HB, RCB and RT in equal weight. In the mixtures, w/b ratio of 0.33 was initially chosen and solely NaOH or binary usage of $Ca(OH)_2$ and NaOH were utilized as alkali activators. The reason for this was that Na_2SiO_3, which was also observed in preliminary studies on paste mixes, had negative effects on shortening the setting time and consistency. While the NaOH solution was added to the system in four different concentrations, 7.5, 10, 12.5 and 15M, $Ca(OH)_2$ activator was added in four different proportions as 0%, 4% 8% and 12% by weight of the binder. For mortar mixtures, it was aimed to see how excess $Ca(OH)_2$ addition will effect rheology and mechanical performance that's why upper limit of addition was arranged as 12%. The test results of these mortar samples (1^{st} Series) produced using 100% CDW in the first stage are presented in Table 4.1. The results are also given in graphics in Figure 4.1 and 4.2 for better understanding.

Table 4.1. Experimental results of mixtures of mortar produced with 100% CDW activated with NaOH or $Ca(OH)_2$ and NaOH together (Series 1)

Sample	NaOH (M)	$Ca(OH)_2$ (%)	Si/Al	Na/Si	Ca/Si	Γ (Flow ability Index)	Build ability (Final Mortar height) (cm)	Shear Yield Stress (N/cm^2)				Compressive Strength (MPa)		
								Initial	30 Min	60 Min	120 Min	7 Day	14 Day	28 Day
A1	7.5	0	5.66	0.17	0.30	1.16	4.4	0.8	2.1	5.7	-	7.8	9.0	10.4
A2		4	5.66	0.17	0.35	0.90	4.4	1.5	3.8	7.8	-	9.4	11.9	15.2
A3		8	5.66	0.17	0.40	0.72	4.5	2.3	4.7	8.2	-	8.8	13.1	15.0
A4		12	5.66	0.17	0.45	0.58	4.6	4.2	6.6	9.0	-	9.6	11.7	14.4
A5	10	0	5.66	0.21	0.30	1.37	4.2	0.4	2.7	3.2	6.8	8.4	9.8	11.1
A6		4	5.66	0.21	0.35	1.15	4.2	1.0	3.1	4.2	7.6	9.0	12.0	15.1
A7		8	5.66	0.21	0.40	0.85	4.3	2.5	4.0	5.0	8.5	9.7	12.0	15.5
A8		12	5.66	0.21	0.45	0.55	4.5	4.3	5.2	6.5	9.2	9.3	12.2	15.8
A9	12.5	0	5.66	0.24	0.30	1.02	4.2	0.4	3.3	4.5	7.8	8.6	9.8	11.6
A10		4	5.66	0.24	0.35	0.80	4.3	1.7	4.3	7.5	-	9.1	11.8	12.0
A11		8	5.66	0.24	0.40	0.61	4.5	2.5	5.2	8.3	-	9.0	12.6	14.4
A12		12	5.66	0.24	0.45	0.49	4.7	4.7	7.5	9.3	-	7.9	12.1	15.8
A13	15	0	5.66	0.28	0.30	1.09	4.3	1.1	3.9	9.0	-	9.0	10.2	10.8
A14		4	5.66	0.28	0.35	0.95	4.4	2.2	5.6	-	-	10.2	12.6	15.0
A15		8	5.66	0.28	0.40	0.65	4.6	3.0	7.5	-	-	11.2	13.1	16.5
A16		12	5.66	0.28	0.45	0.56	4.6	4.3	8.2	-	-	11.2	11.9	17.9

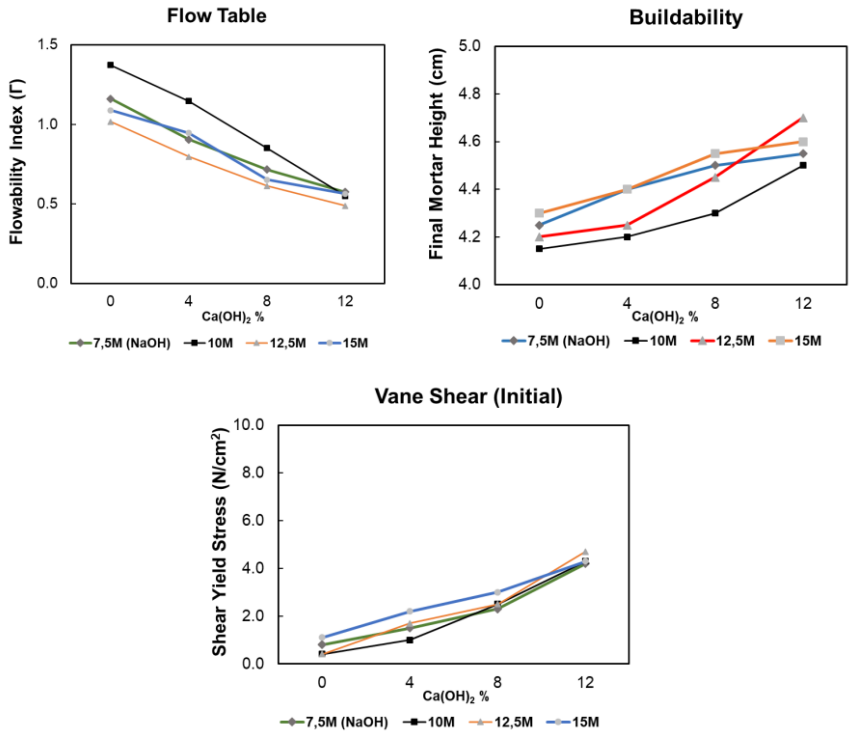

Figure 4.1. The flow table, buildability and vane shear test results of the mortar mixes produced with 100% CDW materials by using NaOH or $Ca(OH)_2$ and NaOH together (Series 1)

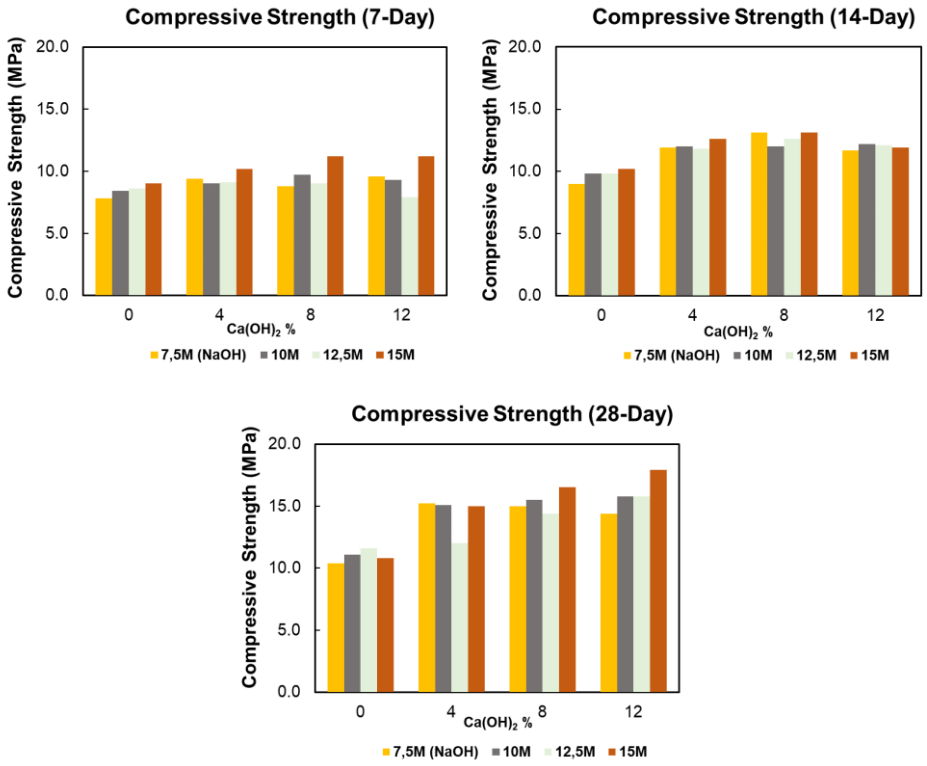

Figure 4.2. Compressive strength test results at different ages of the mortar mixtures produced by using 100% CDW materials and activated with NaOH or $Ca(OH)_2$ and NaOH together (Series 1)

When examining the results of the flow table experiment from Table 4.1 and Figure 4.1 (flow index (Γ) values), in almost all mixtures with the same $Ca(OH)_2$ content (except mixtures containing 12% $Ca(OH)_2$), the flowability values increased as the NaOH content augmented from 7.5 M to 10 M. Therefore, more workable / fluid mixtures were obtained in terms of consistency. However, every increase in NaOH content after 10M has a negative effect on fluidity. When the buildability results were examined, similar trends to those obtained from the flow table were observed. Likewise, in almost all mixtures containing the same amount of $Ca(OH)_2$ content (except mixtures containing 12% $Ca(OH)_2$), as the NaOH content increased from 7.5M to 10M, more settlement was observed, so mixtures that were more fluid in terms of consistency and less preserving shape stability compared to others were obtained. However, as NaOH content increased after 10M value, decreases were observed in the amount of settlement which means buildability performance increased. Although there are studies stating that when the molarity of NaOH increases, the mixtures become more viscous (Memon et al., 2013b; Varaprasad et al., 2010; Li et al., 2013), this situation was not fully observed in this study. After a certain concentration value, the tendency of the material to behave is reversed. Therefore, based on the reactivity of the dust particles obtained from waste materials and their bonding properties in alkaline environments, it can be said that there is a certain NaOH molar threshold or an ideal molar value / range for the used CDW-based binder mixture (Reig et al., 2013; Kourti et al., 2010). In terms of flow table test results, in mixtures with equal NaOH content, the increase in $Ca(OH)_2$ content caused a negative effect in terms of workability / fluidity, causing the mixtures to spread less. Similarly, in the buildability test values, the increment in the amount of $Ca(OH)_2$ in the mixtures with equal NaOH content caused less settlement as a result of 600 gr weight located top of sample as explained in Methodology section. Similar to conventional concrete, considering that the workability performance of geopolymer mixtures is greatly affected by the water content (Hardjito et al., 2008; Wattimena et al., 2017), one reason for this situation is that increment in $Ca(OH)_2$ increases the powder content in the mixture (resulting decrease in w/b ratio). On the other hand, another reason for this situation can be attributed to the fact that the increment in $Ca(OH)_2$ and the increase in Ca^{2+} ions exhibit stronger electrostatic attraction and charge neutralization and accelerate the geopolymerization process (Zhang et al., 2019).

As explained before, it is understood that the flow table has a dynamic test process when it is taken into consideration that the flow table is fell from a height of 12.7 mm 25 times in 15 seconds. This situation creates a shear stress effect on the material and reduces the viscosity, thus enabling the material to spread more easily. However, this is not the case for the buildability test performed by applying a static load of 600 g, and the high settlement in this test means that the viscosity and yield stress of the material is relatively low.

Open-Time performance of mixtures are significant in various application since if materials lose its consistency in short period, it could not be transported or allow proper time for casting etc. Considering this situation, when the results of the vane shear test applied at various ages (0, 30, 60 and 120 min) starting from the moment the mixtures were prepared, almost all of the mixtures containing high NaOH (for 12.5M and 15M NaOH) within the next 60 minutes it hardened (reaching a yield stress above the limit values of the vane shear tool) that could not be measured.

As can be relatively predicted from the results of other tests on fresh mortar mixes, shear stress values obtained from mixtures with 10M NaOH concentration are lower at almost all ages (especially in older ages). While almost all other mixtures hardened by completely losing their flowability within 120 minutes, mixtures containing 10M NaOH were able to maintain their fluidity to a certain extent even at the end of 120 minutes. The relatively rapid processability of mixtures with a NaOH concentration of less than 10M may be attributed to the insufficient alkali activator content to dissolve the binding materials and thus relatively less geopolymeric reactions occur. The increase in NaOH concentration (after 10M) may have accelerated the geopolymerization process by increasing the pH of the mixtures, resulting in a higher dissolution rate (Görhan and Kürklü, 2014). In addition, the high solution alkalinity obtained with the increasing NaOH concentration caused a high release of Si^{4+}, Al^{3+} and Ca^{2+} from the binding materials during the "leaching" reaction, which could accelerate the activation process and accelerate the setting process by enabling the rapid formation of geopolymerization products around the unreacted particles (Zhang et al., 2019). On the other hand, it has been seen that the increase in $Ca(OH)_2$ increases the shear stress in mixtures with equal NaOH content at all ages, where the consistency of the mixtures allows measurement. There are studies in this direction in the literature (Fan et al., 1999; Huseien et al., 2016),

this hardening mechanism probably depends on the formation of $CaCO_3$ (Davidovits, 2015; Leong et al., 2016). Besides, similar to the influence of the increase in NaOH concentration, the increase in OH^- concentration here also caused the formation of a large number of active groups by rapidly breaking the glassy silica-alumina chains, and in this case, it could accelerate the activation process, allowing the rapid formation of geopolymerization products and shortening the setting time (Fan et al., 1999).

When the data of the compressive strength are examined, it is seen that the strength values of the mixtures containing high concentrations of NaOH (15M NaOH), especially of the early age (7 Days) samples, are higher than the mixtures containing lower concentration of NaOH. Among all the results, although it was observed that the increment in NaOH molarity had a favorable influence on compressive strength, contrary to this situation, it was observed in behaviors. While low NaOH concentrations (the concentration to hydrolyze the proper amount silicon and aluminum in precursor are not high enough) do not ensure enough molarity in the matrix, high molarity can cause residual alkali molarity that results existence of unreacted solution and weakens strength (Komnitsas et al., 2015). In addition to this, the shortening of the setting time depending on the activator content may reduce the dissociation of the precursor and cause more unreacted particles in the matrix and thus decrease the strength capacity (Pacheco-Torgal et al., 2008). Based on this, the compressive strengths of the mixtures prepared with the CDW based binder have a certain molar threshold of NaOH or an ideal molar value / range depending on the content, as is the case with fresh properties. As a matter of fact, this is valid for other activators as it can be seen from Table 4.1, the increase in $Ca(OH)_2$ content in the samples has a positive influence on the compressive strength in places (especially in the transition from 0% $Ca(OH)_2$ addition to 4% $Ca(OH)_2$) and in some cases $Ca(OH)_2$ addition has also had a negative effect. The difference between the compressive strength values of the samples containing 0% $Ca(OH)_2$ and samples with 4% $Ca(OH)_2$ content became more pronounced at older age. In addition, as stated, although the increase in $Ca(OH)_2$ content sometimes had some negative effects on the mechanical characteristics, the strength values of all samples using $Ca(OH)_2$ were higher than those without $Ca(OH)_2$. This strength increase could be attached to the addition of $Ca(OH)_2$ to the system, leading the formation of extra C-(A)-S-H and N-A-S-H gels by releasing heat as a consequences of the exothermic reaction of calcium with alkaline solutions (Provis et al., 2009b; Temuujin et al., 2009; Phoo-ngernkham et al., 2014; Garcia-Lodeiro et al., 2013; Dombrowski et

al., 2007).On the other hand, while there is not much difference between the early (7 days) and the final age (28 days) compressive strength results in samples with low $Ca(OH)_2$ content, it was determined that the increase in $Ca(OH)_2$ content continued the geopolymeric reactions after 7 days due to the high alkaline environment and increased the strength. In terms of fresh properties, mixtures with relatively suitable flowability and long workability time could reach 15-16 MPa values as 28-day compressive strength.

Effects of water/binder ratio on geopolymer mixtures was investigated in terms of both mechanical and rheological aspects. Mixtures of A6, A15 and A16 were selected by considering the rheological and mechanical properties of the material from the samples produced within the scope of Series 1. While selecting mixtures, high buildability performance (>4), low vane shear results (<3-4), proper flowability index (>1) and high mechanical performance were considered. The selected mixtures were prepared according to 0.36 and 0.39 w/b ratios to observe the influence of w/b ratio on the rheological and mechanical performance of the material by changing only the water contents. The results of the mixtures are presented in Table 4.2. In addition, all results are presented in graphs for easy comparison (Figure 4.3 and 4.4).

Table 4.2. Experiment results of mortar mixes produced using different w / b ratios with 100% CDW materials and activated with NaOH or $Ca(OH)_2$ and NaOH together.

Sample	Flow Table		Flow ability Index (Γ)	Buildability (Final Mortar Height) (cm)	Shear Yield Stress (N/cm^2)				Compressive Strength (MPa)		
	X Direct. (cm)	Y Direct. (cm)			Initial	30 min	60 min	120 min	7 day	14 day	28 day
A6 (0.33)	14.7	14.6	1.15	4.20	1.0	3.1	4.2	7.6	9.0	12.0	15.1
A6 (0.36)	17.1	17.1	1.92	4.05	0.5	1.4	2.0	3.3	8.3	9.5	13.3
A6 (0.39)	18.1	17.7	2.20	3.50	0.0	0.8	1.0	2.5	7.5	10.2	12.6
A15 (0.33)	12.8	12.9	0.65	4.55	3.0	7.5	-	-	11.2	13.1	16.5
A15 (0.36)	14.6	14.6	1.13	4.50	1.6	4.3	-	-	8.4	9.1	11.6
A15 (0.39)	14.7	14.9	1.19	4.10	2.0	4.8	7.5	-	7.3	10.2	11.3
A16 (0.33)	12.5	12.5	0.56	4.60	4.3	8.2	-	-	11.2	11.9	17.9
A16 (0.36)	13.2	13.4	0.77	4.65	3.3	7.2	-	-	9.8	11.5	12.8
A16 (0.39)	13.0	13.2	0.72	4.50	3.2	7.4	-	-	8.0	11.3	11.3

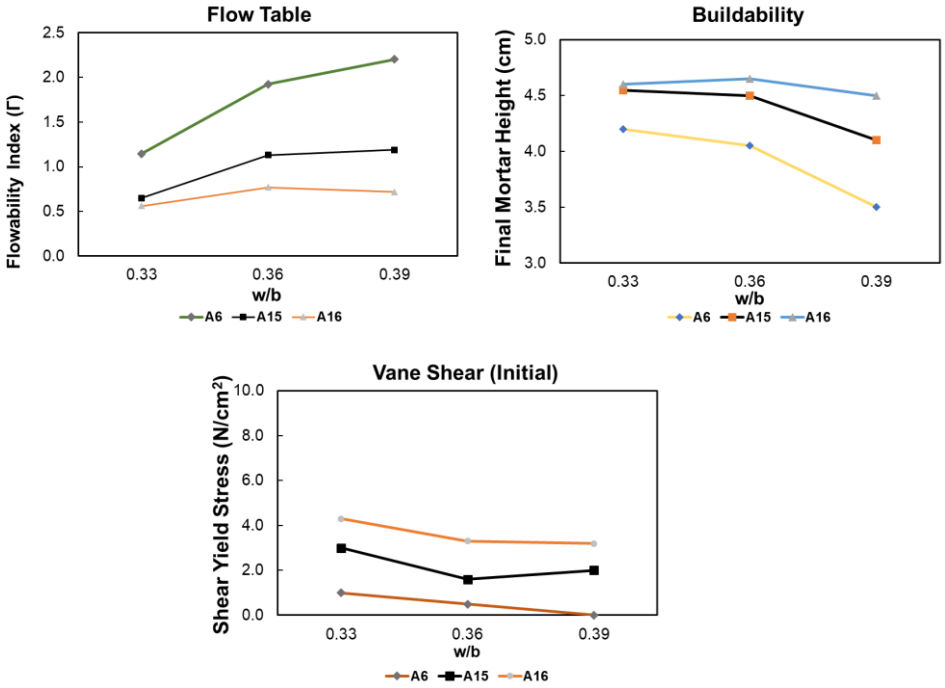

Figure 4.3. Flow table, Buildability and Vane Shear test results of mortar mixes produced by using different w/b ratios with CDW materials activated with solely NaOH or combination of $Ca(OH)_2$ and NaOH

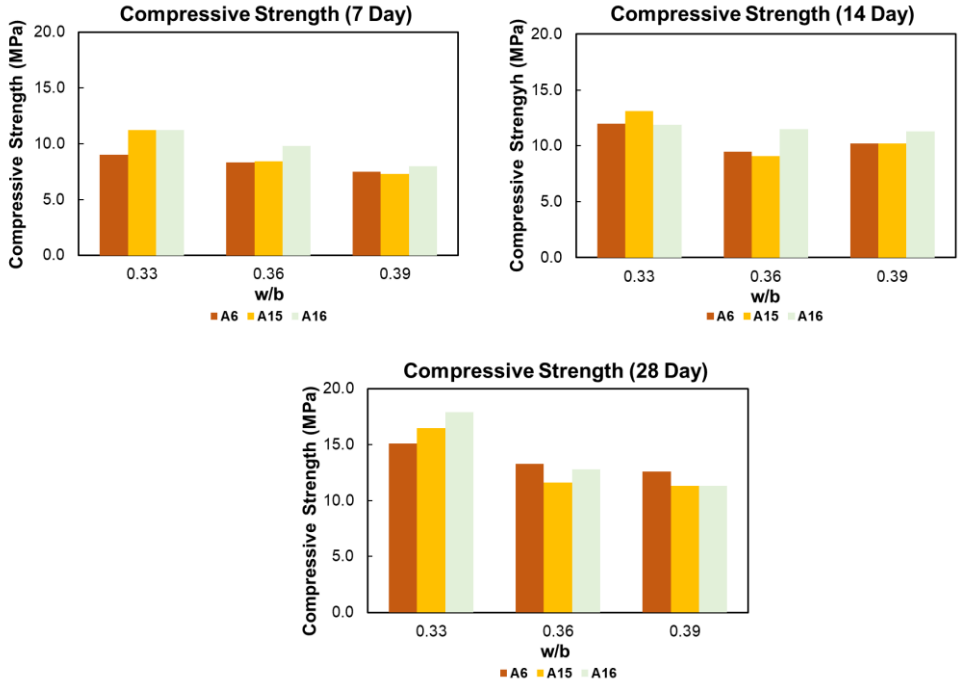

Figure 4.4. Compressive strength test results of different ages of mortar mixes produced by using different w / b ratios with CDW materials activated with solely NaOH or combination of $Ca(OH)_2$ and NaOH

Water content is a crucial matter in geopolymerization and participates in the dissolution of aluminosilicate and polymerization of geopolymers (Hajimohammadi et al., 2010). And workability performance of geopolymer mixtures is greatly affected by the water content (Hardjito et al., 2008; Wattimena et al., 2017). As expected, the increment in the w/b ratio increased the flowability of the mixture and adversely affected the buildability performance since the water in free form that does not participate chemical reaction in medium was increased (Aliabdo et al., 2016). In addition, as the w / b ratio increased, the long-term workability performance of the mixtures improved. The lower w/b ratio could not be sufficient to prepare a medium for dissolution of aluminosilicate sources resulting in the rapid setting (Siyal et al., 2016). In addition, the results demonstrated that the compressive strength decreased as water content was increased, this implies that geopolymer concrete's compressive strength is inversely correlated to the w/b ratio as in cementitious concrete (Patankar et al., 2013; Adam, 2019). Because a higher w/b increases the geopolymer pore volume, resulting in a reduction in compressive strength (Cui and Wang 2019). When the results were examined in detail, the changes in performance in terms of both rheology and mechanical, from 0.33 to 0.36 w/b was more pronounced compared to the transition from 0.36 to 0.39 w/b. Overall, although increment in w/b ratio changes the performance of materials, trends of materials relative to each other in terms of rheological and mechanical performance were not changed considerably.

4.1.2. Mortar mixes produced with CDW materials using $Ca(OH)_2$, NaOH and Na_2SiO_3 activators in various combinations (2nd Series)

Since compressive results from the 1st series were not high enough, a new production series (2nd Series) was created within the scope of the development of suitable geopolymeric mortars. In this production series, 100% CDW mixture with the same content and usage rates as the previous series was used as the binding material. As the alkaline activator, in addition to the $Ca(OH)_2$ and NaOH activators used in the previous series, Na_2SiO_3 activator was also included in the system to analyze effects of it on rheological properties and the compressive strength. For this series, again, the ratio of 0.33 was used as w / b, and water content in the Na_2SiO_3 activator was taken into consideration while preparing the mixtures. In line with the results obtained from the first series, two different $Ca(OH)_2$ ratios, 4% and 8%, were used at this stage with three different NaOH concentrations, 10-12.5-15M. For the Na_2SiO_3 activator, two different usage ratios were chosen such that 1 or 2 times the amount of NaOH by weight. However,

since NaOH solutions produced in all cases except 10M NaOH concentration crystallized and turned into solid form after being allowed to cool (NaOH saturated solution limit is exceeded) when Na_2SiO_3 / NaOH ratio of 2 was tried to used, tests could not be performed on these mixtures. The experimental results of the mortar samples (Series 2) produced by using $Ca(OH)_2$, NaOH and Na_2SiO_3 activators with 100% CDW based binder material are presented in Table 4.3. In addition to the raw data presented in Table 4.3, the results are also given in graphs in Figure 4.5 and 4.6.

Table 4.3. Experiment results of mortar mixes produced with %100 CDW activated with $Ca(OH)_2$, NaOH and Na_2SiO_3 activators (Series 2)

Sample	NaOH (M)	$Ca(OH)_2$ (%)	Na_2SiO_3/ NaOH	Si/Al	Na/Si	Ca/Si	Flowability Index (Γ)	Buildability (Final Mortar Height) (cm)	Shear Yield Stress (N/cm^2)		Compressive Strength (MPa)		
									Initial	30 min	7 Day	14. Day	28. Day
S1	10	4	1	6.04	0.22	0.33	2.90	2.0	0.0	-	16.1	18.3	26.3
S2		8	1	6.04	0.22	0.38	2.48	3.1	0.4	-	15.5	18	24.9
S3	12.5	4	1	6.14	0.26	0.33	2.44	1.1	0.4	-	18.6	23.1	34.0
S4		8	1	6.14	0.26	0.38	2.20	2.0	0.5	-	19.4	27.3	35.8
S5	15	4	1	6.23	0.30	0.32	2.80	2.0	0.5	-	15.1	22.4	24.7
S6		8	1	6.23	0.30	0.37	2.26	3.1	0.7	-	19.2	28.2	36.0
S7	10	4	2	6.42	0.24	0.31	2.03	2.0	0.5	-	16.5	21	25.1
S8		8	2	6.42	0.24	0.35	1.91	2.2	0.5	-	19.8	24	28.1

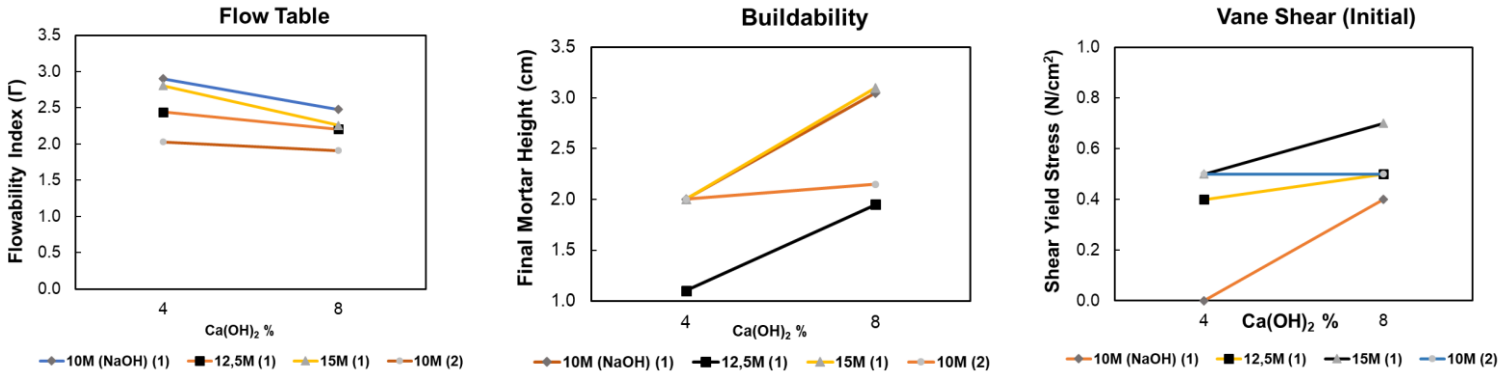

** Values in parentheses indicate the ratio of Na_2SiO_3 / NaOH.*

Figure 4.5. Flow table, buildability and vane shear test results of mortar mixes produced with 100% CDW activated with $Ca(OH)_2$, NaOH and Na_2SiO_3 activators (Series 2)

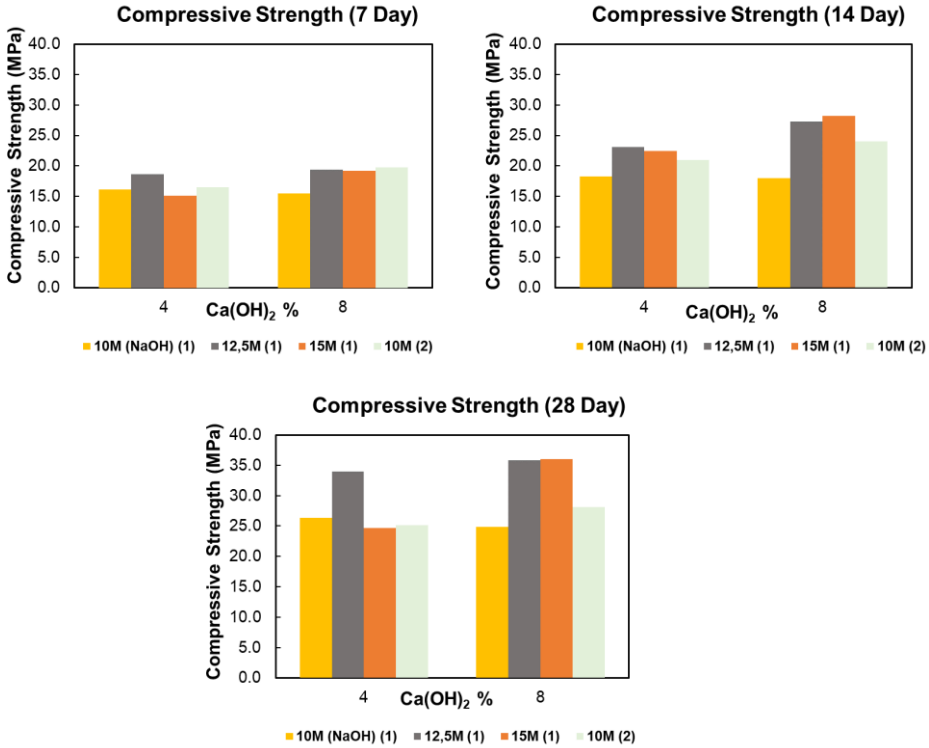

** Values in parentheses indicate the ratio of Na_2SiO_3 / NaOH.*

Figure 4.6. Compressive strength test results of different ages of mortar mixtures produced with 100% CDW activated with $Ca(OH)_2$, NaOH and Na_2SiO_3 activators (Series 2)

As seen in Table 4.3 and Figure 4.5, there is no linear relationship between the NaOH concentration used in mixtures with the same $Ca(OH)_2$ content and the flow table test results. As with the results from the 1st series, here too, mixtures with a concentration of 10M NaOH were spread more on the flow table than the others, and the lowest flowability values were obtained from mixtures with a NaOH concentration of 12.5M. Regarding the flow table test results, the increment in $Ca(OH)_2$ content in mixtures with equal NaOH content, similar to the trends seen in the 1st series, reduced the workability/flowability properties of the mixtures and caused less spread of mixtures. In the buildability tests, as in the 1st series, the increment in the $Ca(OH)_2$ amount of the mixtures had a positive effect in terms of maintaining the shape stability by causing less settlement. On the other hand, when the flow table and buildability test results of all the mixtures prepared in the 2nd series are compared with their equivalents in the 1st series, it is clearly seen that the addition of Na_2SiO_3 provides more fluid mixtures. This could be attributed to liquid/solid

ratio increment in medium since Na_2SiO_3 was added to mixture in liquid form(Hardjito et al., 2008; Sathonsaowaphak et al., 2009; Wattimena et al., 2017)

Augmenting the Na_2SiO_3 / NaOH ratio from 1 to 2 has caused the consistency of the mixture to be solidified and the results of the flow table to decrease. Because of the high viscosity of the Na_2SiO_3 solution, the increment in its content in the mixture (Na_2SiO_3 / NaOH) increased the mixture viscosity and decreased the flowability (Jumrat et. al., 2011; Sathonsaowaphak et al., 2009; Kotwal et al., 2015). On the other hand, the fact that the activator solution has a very high silica concentration with the increase of Na_2SiO_3 / NaOH ratio decreases the pH of the binder and enhances the viscosity of the solution, thus reducing the reaction degree of the powder material with the activator solution (Duxson et al., 2005b). This situation, which also affects the mechanical properties, is further detailed in the following sections.

When the vane shear test results are examined from Table 4.3 and Figure 4.5, it is seen that all mixtures harden by losing all their fluidity within the first 30 minutes. The addition of Na_2SiO_3 significantly shortened the setting time and negatively affected the long-term workability performance of the mixtures. The addition of Na_2SiO_3 to the mixture increases the geopolymerization reactions due to its soluble reactive silica content and shortens the setting times of the mixtures (Li et al., 2010; Kotwal et al., 2015; Goberis & Antonovich, 2004). When the results obtained from the measurement immediately after the preparation of the mixture were examined, it was understood that the effects of the changes in NaOH and $Ca(OH)_2$ content on the yield stress of the mixtures are in the similar trend as in the 1st series. At the same time, while augmenting the Na_2SiO_3 / NaOH ratio from 1 to 2 increased the yield stress of the mixtures, this increase was higher in mixtures with 4% $Ca(OH)_2$ content.

When the compressive strength results are compared with the first series samples that do not contain Na_2SiO_3 activator, it is seen that the Na_2SiO_3 activator significantly improves the compressive strength. This situation can be attributed to that the addition of Na_2SiO_3 activator to the system increases the Si / Al ratio of the final product of geopolymerization and provides the formation of a strong geopolymeric bond (Komljenović et al., 2010). Increasing the Si content increases the ratio of SiO_2 / Al_2O_3 and results in higher strength due to a denser structure by providing the generation of Si-O-Si bonds that are shorter

and stronger than Si-O-Al and Al-O-Al bonds (Jong, 1980; Bakri et al., 2009). The increment in Si content enhances and further encourages the geopolymerization reactions occurring in the mixtures (Al Bakri et al., 2012b; Phoo-ngernkham et al., 2015; Risdanareni et al., 2015). Augmenting the Na_2SiO_3/NaOH ratio from 1 to 2 did not positively affect the compressive strength of the mixtures as expected. Fundamentally, the increment in Na_2SiO_3 / NaOH ratio causes the increment in sodium amount in the matrix. Although sodium is essential for the generation of geopolymers because it behaves as charge balancing ions, excessive Na + content reacts with CO_2 in the atmosphere, causing the formation of sodium carbonate, interrupting the geopolymerization reactions and preventing the strength of the mixture (Barbosa et al., 2000). In addition, the excess Na_2SiO_3 content can negatively affect the compressive strength as it accelerates the evaporation of the mixing water and prevents the formation of a dense structure (Cheng & Chiu, 2003; Skvara et al., 2006). On the other hand, the effect of the changes in NaOH and $Ca(OH)_2$ amount on the compressive strength of the mixtures was similar to that in the 1st series. As a result, considering all the results, although better performance was obtained from the mixtures prepared within the scope of the 2nd series regarding mechanical properties, the results of the flow table, buildability and vane shear tests show that these mixtures are not suitable for application that needs long workable time (open time) and enough yield stress to carry load when it was fresh.

Effects of water/binder ratio on geopolymer mixtures was investigated in terms of both mechanical and rheological aspects in that series as well. Among the samples produced within the scope of Series 2, the S6 mixture selected by considering the rheological and mechanical features of the material was reproduced for 0.36 and 0.39 w / b ratios to observe the influence of w / b ratio on the rheological and mechanical features of the material by changing only the water content. However, it was observed that the setting time of the mixtures within these w / b ratios is rather short as in the series 2 and the flowability became so high. Therefore, they are not suitable for general application since it became more fluid and allow short time for workability. But, if the application is not required wide workable time (15-30 minutes) and consistency is not a problem, these mixtures could be used in these kinds of application.

4.1.3. Mortar mixes produced with CDW and BFS using solely NaOH or binary usage of $Ca(OH)_2$ and NaOH (3rd Series)

Although relatively high compressive strength values were obtained with the use of Na_2SiO_3 activator, it is aimed to provide improvements in terms of consistency and strength by adding mineral additives to the mixtures, since the mixtures with the desired properties (open time and adequate yield strength) cannot be obtained in terms of fresh properties. In this context, considering literature and geopolymerization reaction mechanism, a third production series was determined in which 20% of the binder powder material was BFS. Since, extra sources of Al, Si and Ca may include geopolymerization and result extra C-(A)-S-H and N-A-S-H which can give higher strength to matrix. In these mixtures, 10% of the total binder by weight consists of GW, 10% CW, 20% BFS and the remaining 60% equal weight HB, RCB and RT. As in the first two series, the w/b ratio of 0.33 and solely NaOH or combination usage of $Ca(OH)_2$ and NaOH were utilized as alkaline activators. The NaOH solution was added to the system at four different concentrations, 7.5-10-12.5-15M, as in the first series. $Ca(OH)_2$ was used in four different proportions as 0-% 4-% 8-12% by weight of the binder. The findings obtained from the tests performed on all these mixtures are presented in Table 4.4 and also in Figure 4.7 and 4.8.

Table 4.4. Experimental results of mortar mixes produced CDW and BFS activated with NaOH or $Ca(OH)_2$ and NaOH together (Series 3)

Sample	NaOH (M)	$Ca(OH)_2$ (%)	Si/Al	Na/Si	Ca/Si	Flowability Index (Γ)	Buildability (Final Mortar Height) (cm)	Shear Yield Stress (N/cm^2)				Compressive Strength (MPa)		
								Initial	30 min	60 min	120 min	7 Day	14 Day	28 Day
A17	7.5	0	5.79	0.17	0.45	1.76	4.1	0.6	2.3	4.6	-	16.5	20.1	23.9
A18		4	5.79	0.17	0.51	1.31	4.4	1.1	2.5	5.9	-	16.5	20.4	24.1
A19		8	5.79	0.17	0.56	1.07	4.4	1.9	3.7	7.3	-	15.3	17.6	22.1
A20		12	5.79	0.17	0.61	0.78	4.6	2.9	4.6	7.8	-	15.7	20.6	24.7
A21	10	0	5.79	0.21	0.45	1.84	4.0	0.5	2.0	3.0	4.5	15.6	17.7	23.1
A22		4	5.79	0.21	0.51	1.37	4.1	1.0	2.4	3.1	5.7	16.6	19.5	22.0
A23		8	5.79	0.21	0.56	1.16	4.2	1.9	3.3	4.0	6.5	16.2	20.7	25.8
A24		12	5.79	0.21	0.61	1.09	4.3	2.8	4.0	4.8	7.2	18.2	20.6	25.1
A25	12.5	0	5.79	0.25	0.45	1.74	4.1	0.9	3.0	3.7	6.1	15.7	18.6	23.7
A26		4	5.79	0.25	0.51	1.16	4.3	1.8	3.6	6.0	9.0	15.9	18.1	24.8
A27		8	5.79	0.25	0.56	1.02	4.4	2.5	4.2	7.4	9.5	17.7	20.8	24.6
A28		12	5.79	0.25	0.61	0.72	4.6	3.5	4.6	8.4	9.7	17.4	19.6	25.2
A29	15	0	5.79	0.29	0.45	1.37	4.2	1.0	3.0	8.5	-	14.9	18.5	22.4
A30		4	5.79	0.29	0.51	0.97	4.5	1.9	5.2	-	-	14.1	17.1	20.4
A31		8	5.79	0.29	0.56	0.84	4.5	3.0	7.0	-	-	15.3	17.6	20.2
A32		12	5.79	0.29	0.61	0.61	4.6	4.3	8.5	-	-	16.1	17.4	19.0

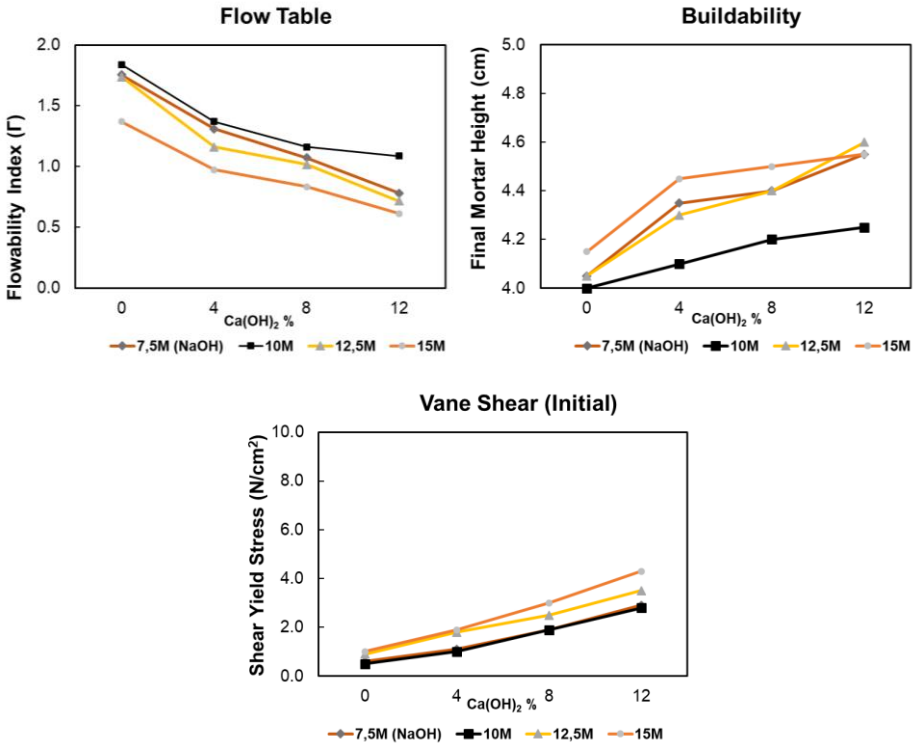

Figure 4.7. Flow table, buildability and vane shear test results of mortar mixes produced with CDW and BFS activated with NaOH or $Ca(OH)_2$ and NaOH together (Series 3)

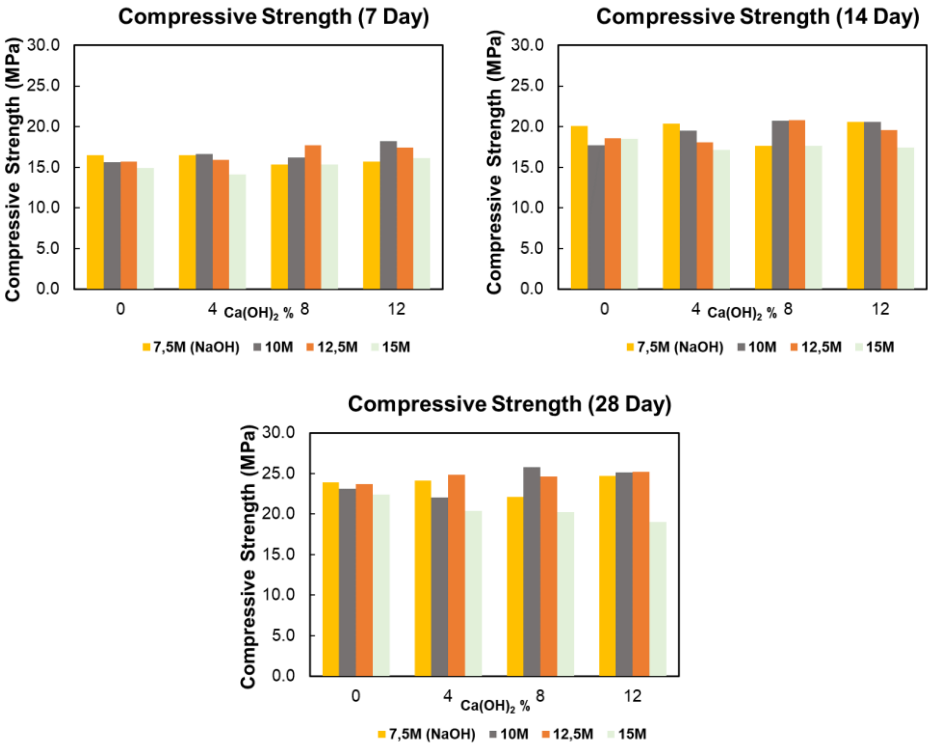

Figure 4.8. Compressive strength test results of different ages of mixtures of CDW and BFS activated with NaOH or Ca $(OH)_2$ and NaOH together (3rd Series)

The flow table test results (flow index (Γ) values) given in Table 4.4 and Figure 4.7 show that the increase of NaOH concentration from 7.5M to 10M in mixtures containing equal $Ca(OH)_2$, as in the 1st series, causes an increase in the flowability values. At 10M NaOH concentration, the flow values of the mixtures reached the peak value and the increase in the NaOH concentration after this point caused the flow values to decrease. Similarly, the results obtained from the buildability test show that a higher amount of settlement occurs in mixtures at 10M NaOH concentration compared to mixtures with other concentrations. In addition to this, the increase in $Ca(OH)_2$ content in mixtures with equal NaOH concentrations caused less spread of mixtures in the flow table test as in the 1st series. Likewise, in the buildability test, the increase in $Ca(OH)_2$ content caused the mixtures to collapse less by preserving the shape stability more under constant load which means that show higher buildability performance.

When the vane shear results of the mixtures were examined, almost all of the mixtures containing the highest concentration of NaOH (15M NaOH) completely set and hardened within 60 minutes after the preparation of the mixture. In addition, it was observed that mixtures containing the lowest concentration of NaOH (7.5M NaOH) completely hardened within 120 minutes and lost its consistency. In 10M and 12.5M NaOH concentrations, results were obtained even after 120 minutes by using vane shear test equipment. As with the results obtained from other series, the lowest shear stress values at all ages were obtained at 10M NaOH concentration in this series, it is understood from this that the 10M NaOH concentration provides a longer workability time compared to others. As in the previous series, it has been found that there was a certain NaOH molar threshold or an ideal molar value / range for fresh properties, depending on the binder content. $Ca(OH)_2$ increase in mixtures with equal NaOH content again caused increases in shear stresses as described above.

When the results of all these tests related to fresh features were evaluated in general terms, it was seen that the BFS substitution increases the spreading values in the flow table and the settlement values in the buildability test compared to the mixtures containing 100% CDW (Series 1), making the mixtures more fluid. In addition, BFS substitution positively affected the long workability performance of the mixtures. The increased workability with BFS substitution can be attributed to the dense structure of the BFS particles and the smooth and spherical surface properties, which absorb less water during mixing and

decrease the friction effect (ACI 233R-95, 1996; Laskar and Talukdar, 2008). This also reduced the yield stress of the mixtures by reducing the viscosity and also delayed the setting time. The influence of using BFS on the setting time of the material is parallel to the literature (Gesoğlu & Özbay, 2007; Boukendakdji et al., 2009; Boukendakdji et al., 2012; Johari et al., 2011; Brooks et al., 2000).

When the strength data were examined, it was observed that in the mixture groups with equal $Ca(OH)_2$ content, almost all mixtures containing high concentration of NaOH (15M NaOH) have lower compressive strength results compared to mixtures containing lower NaOH. This situation may be attributed to the fact that a homogeneous mixing process cannot be achieved due to the silica coagulation and rapid hardening resulting from the increased "Na^+" content, and therefore a weak and inhomogeneous geopolymerization process (Palomo et al., 1999). In addition, passing over an optimum NaOH solution molarity can lead to electrostatic protection, that reduces the activity of the ions, preventing the dissolution of the binders and leading a decrement in the compressive strength (Xiao et al., 2020). One of the primary solvent components conducting Si and Al activation in the matrix is Na^+, according to Ahmari et al (2012), and lesser strengths could be produced at greater Na^+ content attributed to the impact of other influences that reduced geopolymeric networks such as calcium.

Although high NaOH concentration causes relatively lower compressive strength, considering all the compressive strength results, a direct relationship could not be established between the changes in NaOH concentration of the mixtures and the compressive strength. Although there is an increment in the molarity of NaOH from place to place, there is an increment in the compressive strength, but there are cases where it causes a decrease. This situation is valid for $Ca(OH)_2$, and the effect of change in $Ca(OH)_2$ content of mixtures with equal NaOH concentration on compressive strength does not show a certain trend. However, when the compressive strength results of the 3rd series mixtures containing BFS and the 1st series mixtures prepared with 100% CDW were compared for the equal alkali activator content, it was seen that the BFS used as a mineral additive had a positive contribution to the compressive strength. There are also studies in the literature showing that mixtures with better physico-mechanical properties are obtained by adding BFS to clay-brick based geopolymers (Zawrah et al., 2016). It is known that adding more calcined source material improves the microstructure of the

geopolymer matrix, increasing its compressive strength (Van Jaarsveld et al., 2002; Deb et al., 2014; Serag Faried et al., 2020). As a result, $Ca(OH)_2$ was introduced to the system with the BFS substitution with a high rate of calcium compared to the CDW-based binders, and the calcium content of the mixtures prepared with these binder materials containing high silica and alumina was increased, and the samples produced gained higher strength (Bernal et al., 2011).

Effects of water/binder ratio on geopolymer mixtures was investigated in terms of both mechanical and rheological aspects in that series as well. A23, A26 and A28 mixtures selected from the samples produced within the scope of Series 3, considering the rheological and mechanical properties of the material, are only changed regarding the water content of 0.36 and 0.39 w / b ratios to observe the influence of w / b ratio on the rheological and mechanical features of the mixtures. The results of the mixtures are presented in Table 4.5. In addition, all results are presented in graphs for easy comparison (Figure 4.9 and 4.10).

Table 4.5. Experiment results of mortar mixes produced using different w / b ratios for CDW and BFS based mixtures activated with NaOH or $Ca(OH)_2$ and NaOH together

Sample	NaOH (M)	$Ca(OH)_2$ (%)	Flowability Index (Γ)	Buildability (Final Mortar Height) (cm)	Shear Yield Stress (N/cm^2)				Compressive Strength (MPa)		
					0 min	30 min	60 min	120 min	7 Day	14 Day	28 Day
A23 (0.33)	10	8	1.16	4.20	1.9	3.3	4.0	6.5	16.2	20.7	25.8
A23 (0.36)	10	8	1.61	4.15	0.4	1.4	2.5	3.3	13.8	18	18.8
A23 (0.39)	10	8	1.91	3.80	0	0.8	1.5	3.0	13.3	16.7	17.4
A26 (0.33)	12.5	4	1.16	4.30	1.8	3.6	6.0	9.0	15.9	18.1	24.8
A26 (0.36)	12.5	4	1.89	4.10	0.7	2.4	4.5	6.5	13.9	17.4	21.0
A26 (0.39)	12.5	4	2.03	3.85	0.5	2.0	2.9	7.0	13.9	16.5	18.5
A28 (0.33)	12.5	12	0.72	4.60	3.5	4.6	8.4	9.7	17.4	19.6	25.2
A28 (0.36)	12.5	12	0.99	4.50	2.0	5.0	8.0	-	16.2	19.8	22.1
A28 (0.39)	12.5	12	1.34	4.15	1.1	3.5	5.4	-	13.0	18.8	19.7

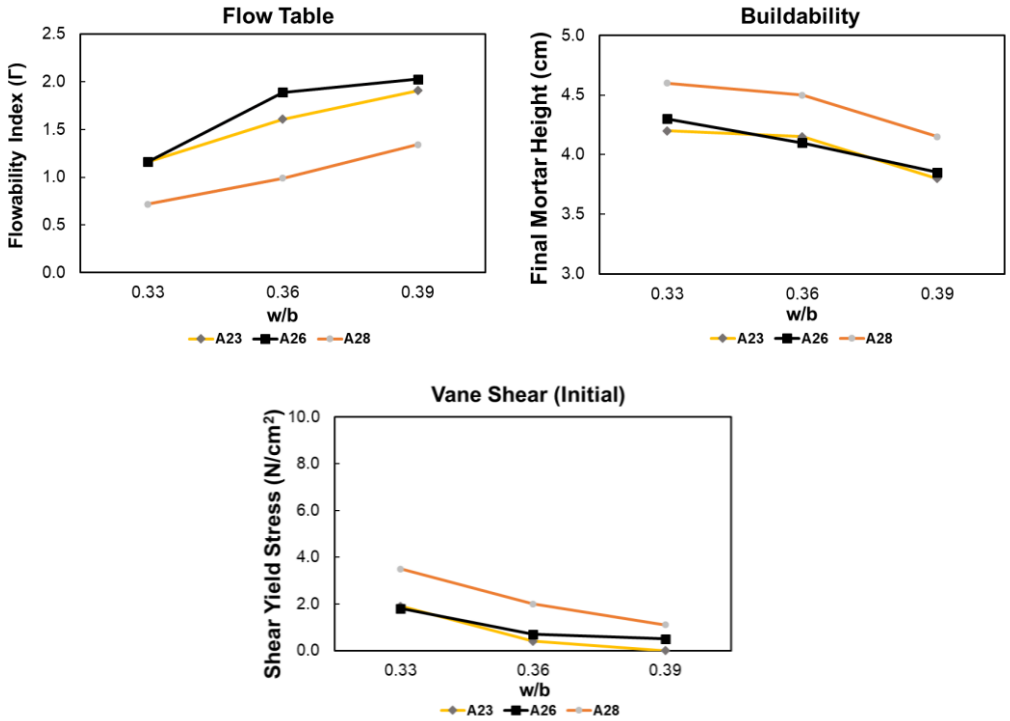

Figure 4.9. Flow table and buildability and vane shear test results of mortar mixes produced by using different w / b ratios for CDW and BFS based mixtures activated with NaOH or $Ca(OH)_2$ and NaOH together

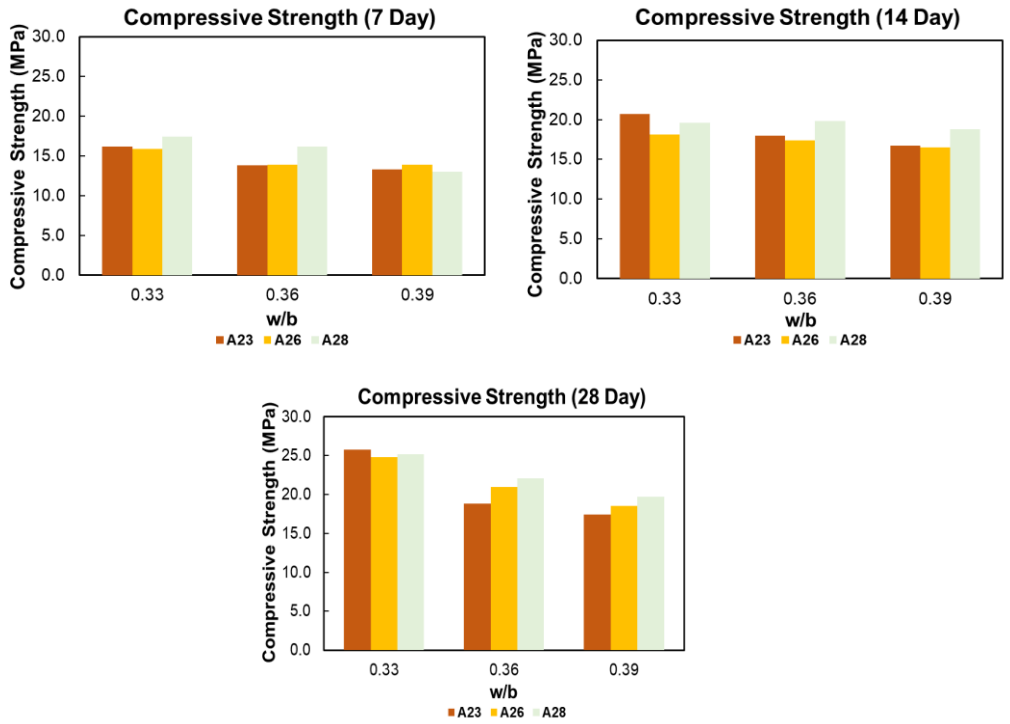

Figure 4.10. The compressive strength test results at different ages of mortar mixes produced using different w/b ratios for CDW and BFS based mixturesactivated with NaOH or $Ca(OH)_2$ and NaOH together

Water content is a crucial matter in geopolymerization and participates in the dissolution of aluminosilicate and polymerization of geopolymers (Hajimohammadi et al., 2010). And workability performance of geopolymer mixtures is greatly affected by the water content (Hardjito et al., 2008; Wattimena et al., 2017). As expected, the increment in the w / b ratio increased the flowability of the mixture and adversely affected the shape stability performance since the water in free form that does not participate chemical reaction in medium was increased. (Aliabdo et al., 2016). In addition, as the w / b ratio increased, the long-term workability performance of the mixtures improved. It ought to be considered that the lower w/b ratio could not be adequate to create a reaction circumstance for the dissolution of aluminosilicate sources leading to rapid setting (Siyal et al., 2016). In addition, the findings demonstrated that the compressive strength reduced as water in matrix was augmented, this implies that geopolymer concrete's compressive strength is inversely correlated to the w/b ratio as in cementitious concrete (Patankar et al., 2013; Adam, 2019). Because a higher w/b increases the geopolymer pore volume, resulting in a reduction in compressive strength (Cui and Wang 2019). When the results were examined in detail, the changes in performance in terms of both rheology and mechanic, from 0.33 to 0.36 w/b was more pronounced compared to the transition from 0.36 to 0.39 w / b. Overall, although increment in w/b ratio changes the performance of materials, trends of materials relative to each other in terms of rheological and mechanical performance were not changed considerably.

4.1.4. Mortar mixes produced with CDW and BFS using $Ca(OH)_2$, NaOH and Na_2SiO_3 activators in various combinations (4th Series)

Although improvements were achieved in compressive strength with BFS replacement, still results were also not satisfactory for general application as structural elements since it is below 30 Mpa. In this context, studies have been continued to obtain mixtures with suitable fresh properties and at the desired performance in compressive strength, another important parameter. As a result of the gains from the 2nd series, it was understood that the Na_2SiO_3 activator had a negative effect on the fresh properties, in order to establish a balance between rheological and mechanical properties, it was decided to test this activator in mixtures containing BFS. While determining the production series to be produced (Series 4), the results obtained from the previous mixture series were taken into account. In this context, 80% CDW + 20% BFS mixture with the same content and usage rates as the previous series was used as the binding material. $Ca(OH)_2$, NaOH and

Na_2SiO_3 activator were used together as alkali activator. For this series, the ratio of 0.33 was used as w/b, and the water content in the Na_2SiO_3 activator was taken into consideration while preparing the mixtures. As in Series 2, two different $Ca(OH)_2$ ratios, 4% and 8%, were used in this series, with three different NaOH concentrations, 10-12.5-15M. For the Na_2SiO_3 activator, two different usage ratios were chosen such that 1 or 2 times the amount of NaOH by weight. However, since NaOH solutions produced in all cases except 10M NaOH concentration crystallized and turned into solid form after being allowed to cool (NaOH saturated solution limit is exceeded) when Na_2SiO_3 / NaOH ratio of 2 was tried to be used, tests could not be performed on these mixtures. The test results of the mortar samples (Series 4) produced by using $Ca(OH)_2$, NaOH and Na_2SiO_3 activators together using CDW + BFS are given in Table 4.6 and are also presented in graphs in Figure 4.11 and 4.12 for better understanding.

Table 4.6. Experimental results of mortar mixes produced CDW and BFS activated with $Ca(OH)_2$, NaOH and Na_2SiO_3 activators (Series 4)

Sample	NaOH (M)	$Ca(OH)_2$ (%)	Na_2SiO_3/ NaOH	Si/Al	Na/Si	Ca/Si	Flowability Index (Γ)	Buildability (Final Mortar Height) (cm)	Shear Yield Stress (N/cm^2)		Compressive Strength (MPa)		
									Initial	30 min	7 Day	14 Day	28 Day
S9	10	4	1	6.20	0.23	0.47	3.00	3.3	0	-	29.4	31.7	37.9
S10		8	1	6.20	0.23	0.52	2.50	3.4	0.5	-	28.6	27.8	32.8
S11	12.5	4	1	6.30	0.27	0.46	3.18	1.2	0	-	26.4	28.9	34.9
S12		8	1	6.30	0.27	0.51	3.16	1.5	0	-	27.9	30.3	32.3
S13	15	4	1	6.40	0.31	0.46	2.90	1.5	0	-	30.6	30.6	41.8
S14		8	1	6.40	0.31	0.51	2.88	2.3	0	-	34.5	34.5	39.2
S15	10	4	2	6.61	0.24	0.44	3.31	1.0	0	-	31.3	37.7	42.8
S16		8	2	6.61	0.24	0.49	3.37	1.0	0	-	27.9	32.2	38.9

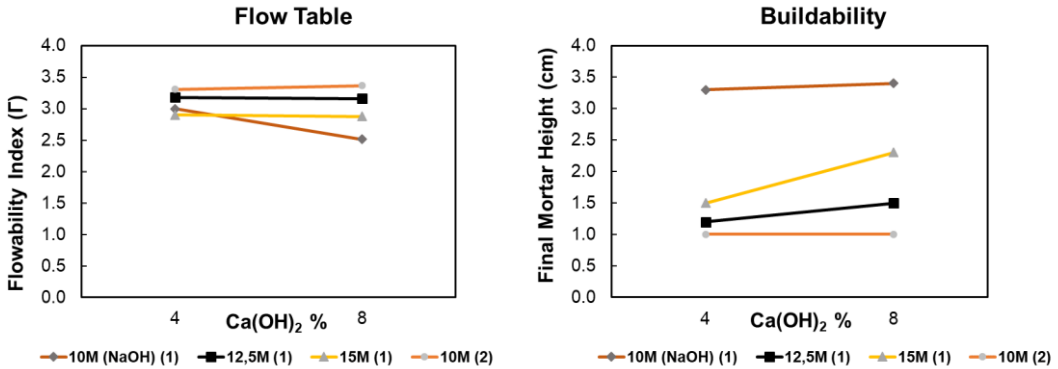

** Values in parentheses indicate the ratio of Na2SiO3 / NaOH.*

Figure 4.11. The Flow table and buildability test results of the mortar mixes produced with CDW and BFS activated with $Ca(OH)_2$, NaOH and Na_2SiO_3 activators (Series 4)

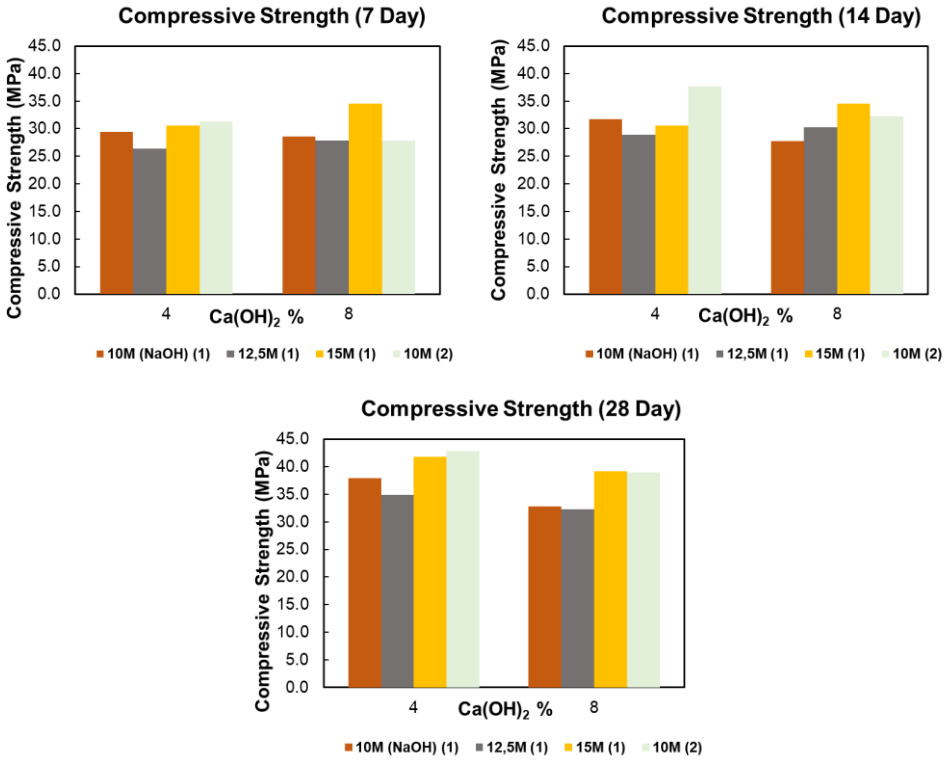

** Values in parentheses indicate the ratio of Na_2SiO_3 / NaOH.*

Figure 4.12. Compression strength test results of different ages of mortar mixes produced with CDW and BFS activated with $Ca(OH)_2$, NaOH and Na_2SiO_3 activators (Series 4)

According to the flow table results presented in Table 4.6, in mixtures with a Na_2SiO_3 / NaOH ratio of 1 and with the same $Ca(OH)_2$ content, unlike the previous mixture series, mixtures containing 12.5M NaOH concentration displayed a more fluid behavior and spread more. In the buildability tests, the mixtures with the same $Ca(OH)_2$ content and 10M NaOH concentration provided more shape stability and their final heights were higher (less settlement) after the static load effect. In this sense, in the flow table test of mixtures with 10M NaOH concentration, the spreading amount was close to the highest spread (containing 12.5M NaOH), while the shape stability was much better. In the flow table test, the increase in $Ca(OH)_2$ content in mixtures with 10M NaOH content caused the mixtures to spread less by reducing the workability / flowability properties of the mixtures. However, in mixtures containing 12.5M and 15M NaOH, the increment in $Ca(OH)_2$ content did not significantly affect the flow table test results. In terms of buildability test results, in mixtures containing equal NaOH, the increment in $Ca(OH)_2$ amount generally improved the buildability performance of the mixtures with little effect. On the other hand, augmenting the ratio of Na_2SiO_3 / NaOH from 1 to 2 increased the

flowability of the mixture, unlike the effect seen in the 2nd series, led an increment in the flow table results and the amount of settlement in the stability test. When the flow table and buildability test results of all the mixtures prepared in the 4th series were examined, it was clearly seen that more fluid materials were obtained compared to the 3rd series, and it was obvious that this situation was caused by the addition of Na_2SiO_3 as described in upper section.

When the results of the vane shear test were examined, it was seen that the mixtures had low viscosity and yield stress at a level that did not resist the vane shear tool from the measurements (initial case) after the preparation of the mixture. However, all these mixtures, which were quite fluid, lost all their fluidity in the first 30 minutes and hardened. The addition of Na_2SiO_3 accelerated the setting of the mixtures here, as in the 2nd series, and negatively affected the long-term workability performance (open time).

When the compressive strength results were compared with the 3rd series samples having the same binder content but not including Na_2SiO_3 activator, it was seen that the Na_2SiO_3 activator increased the compressive strength of the mixtures. There was no linear relationship between the increase or decrease in the NaOH concentration of the mixtures containing equal $Ca(OH)_2$ and the strength, and the highest strength was obtained at 15M NaOH after 28 days. In terms of 7 and 14 days compressive strength, the increment in $Ca(OH)_2$ content for the mixtures at 10M NaOH concentration decreased the compressive strength, while the other concentrations augmented. The increment in $Ca(OH)_2$ content in mixtures with equal NaOH concentration negatively affected the 28-day compressive strength results. Such decrease in strength may have occurred because of the increased Ca^{+2} ion amount due to both BFS and high $Ca(OH)_2$ content, which cuts geopolymeric networks (Ahmari et al., 2012). In addition, as the increasing Ca^{+2} ions react with the OH^- ions in the matrix dissolved from alumino-silicate materials in a high alkaline environment, the decrease in the pH of the matrix and the precipitation as $Ca(OH)_2$ may also partially cause the strength to decrease (Van Deventer et al. 2007; Komnitsas et al., 2015). Increasing the Na_2SiO_3/ NaOH ratio from 1 to 2 has had a positive effect on compressive strengths for almost all cases. Yet, this increase is not directly linear with usage amount. As a result, although much higher compressive strengths were obtained from the 4th series mixtures compared to the previous series, the negative effect of

Na_2SiO_3 addition on the fresh properties of the mixtures was also observed in these mixtures.

Effects of water/binder ratio on geopolymer mixtures was investigated in terms of both mechanical and rheological aspects. Among the samples produced within the scope of Series 4, the S9 mixture selected considering the rheological and mechanical features of the material was reproduced for 0.36 and 0.39 w / b ratios to observe the influence of w / b ratio on the rheological and mechanical features of the material by changing only the water content. However, it was observed that the setting time of the mixtures within these w / b ratios is rather short as in the series 2 and 4 and the flowability became so high. Therefore, they are not suitable for general application since it became more fluid and allow short time for workability. But, if the application is not required wide workable time (15-30 minutes) and consistency is not a problem, these mixtures could be used in these kinds of application.

4.1.5. Mortar mixes produced with CDW and different mineral additive mix combinations using binary usage of Ca(OH)2 and NaOH together (5th Series)

It was decided to try a new production series (series 5) in which different mineral additives are used together with BFS to provide the proper consistency for the mortar phase, to find out the effects of different mineral additives on the strength and consistency, and to reach adequate compressive strength values as well as suitable fresh properties. In the mixtures of this series, 80% of the binder material by weight is CDW materials (10% concrete waste, 10% glass waste, 60% equal weight perforated brick, blend brick and roof tile), the remaining part of 20% consists of mineral additives in different combinations and usage rates (four different combinations as 15% BFS + 5% SF, 10% BFS + 5% SF + 5% FA, 7.5% BFS + 7.5 % SF + %5 FA and 5% BFS + 10% SF + 5 % FA). In these mixtures, w / b ratio was 0.33 and as alkali activator, $Ca(OH)_2$ and NaOH were used. NaOH activator was used in 3 different concentrations as 10M-12.5M-15M solutions, and $Ca(OH)_2$ activator was used in two different ratios as 4% and 8% by weight of the binder. All tests performed on the previous series were also made on this series, and the test results of the mortar samples (5th series) in this production series are presented in Table 4.7.

Table 4.7. Experimental results of mortar mixes produced with CDW and various mineral admixture together activated with Ca (OH) 2 and NaOH (Series 5)

#	Sample	NaOH (M)	$Ca(OH)_2$ (%)	Mineral Addition	Si/Al	Na/Si	Ca/Si	Flow ability Index (Γ)	Build ability (Final Mortar Height) (cm)	Shear Yield Stress (N/cm^2)				Compressive Strength (MPa)		
										0 min	30 min	60 min	120 min	7 Day	14 Day	28 Day
Group 1	P1	10	4	%15BFS +%5SF	6.46	0.20	0.43	1.76	3.9	0.0	0.5	1.6	2.9	19.8	20.3	23.4
	P2		8		6.46	0.20	0.48	1.25	4.4	1.0	1.7	2.6	4.5	18.5	19.1	20.2
	P3	12.5	4		6.46	0.23	0.43	1.99	3.8	0.0	0.9	2.5	6.9	20.1	22.6	23.1
	P4		8		6.46	0.23	0.48	1.12	4.4	1.7	2.7	4.0	-	18.8	22.4	22.8
	P5	15	4		6.46	0.27	0.43	1.39	4.3	0.8	3.1	5.5	-	16.4	19.3	24.2
	P6		8		6.46	0.27	0.48	0.95	4.5	2.5	4.6	7.1	-	19.5	23.9	24.4
Group 2	P7	10	4	%10BFS +%5SF +%5FA	6.30	0.20	0.38	1.79	3.7	0.0	0.9	1.6	3.1	21.0	22.4	23.6
	P8		8		6.30	0.20	0.43	1.56	4.1	1.0	1.6	2.4	3.7	21.6	24.6	26.1
	P10	12.5	4		6.30	0.23	0.38	2.10	3.6	0.0	0.8	2.8	4.4	12.3	20.7	25.9
	P11		8		6.30	0.23	0.43	1.56	4.1	0.9	2.0	3.7	6.4	17.3	23.0	30.0
	P12	15	4		6.30	0.27	0.38	1.69	4.2	0.8	4.0	5.1	9.0	15.7	18.5	23.5
	P13		8		6.30	0.27	0.43	1.16	4.4	2.0	5.1	6.8	-	16.4	21.8	26.9
Group 3	P14	10	4	%7.5BFS +%7.5SF +%5FA	6.64	0.19	0.35	1.92	4.0	0.3	1.0	1.5	2.3	17.1	25.0	32.5
	P15		8		6.64	0.19	0.40	1.46	4.3	1.0	2.0	2.1	3.5	21.6	24.4	31.6
	P16	12.5	4		6.64	0.22	0.35	2.01	3.8	0.2	0.8	1.2	2.1	14.9	19.1	20.7
	P17		8		6.64	0.22	0.40	1.50	4.3	0.9	1.7	2.0	3.9	18.0	23.1	31.4
	P18	15	4		6.64	0.26	0.35	1.76	4.2	0.5	1.4	2.2	4.0	14.7	17.9	19.4
	P19		8		6.64	0.26	0.40	1.64	4.3	0.9	1.5	2.7	4.6	16.5	20.8	23.4
Group 4	P20	10	4	%5BFS +%10SF +%5FA	7.00	0.18	0.32	1.59	4.0	0.5	0.9	1.0	2.0	18.4	23.9	31.5
	P21		8		7.00	0.18	0.37	1.42	4.3	0.9	1.5	2.0	2.5	23.3	24.5	34.7
	P22	12.5	4		7.00	0.22	0.32	1.82	3.9	0.4	0.5	1.0	1.5	15.4	22.0	29.4
	P23		8		7.00	0.22	0.37	1.62	4.0	0.6	0.6	1.4	2.3	18.6	23.9	32.4
	P24	15	4		7.00	0.25	0.32	1.72	4.2	0.5	1.3	2.5	4.5	14.3	17.3	20.9
	P25		8		7.00	0.25	0.37	1.40	4.5	1.0	2.2	3.1	5.4	15.5	19.8	23.9

As can be seen from Table 4.7, there was no direct connection between the NaOH concentration and the flow table test results in mixture prepared with the same $Ca(OH)_2$ and mineral additive content. The highest flowability values for 4% $Ca(OH)_2$ content were obtained from mixtures with 12.5M NaOH concentration. For mixtures with 8% $Ca(OH)_2$ content, the effect of NaOH concentration varies for each batch of mixtures. In terms of flow table test results, in mixtures with equal NaOH content, the increment in the amount of $Ca(OH)_2$ caused the mixtures to spread less by reducing the workability / fluidity properties of the mixtures.

Considering the buildability test results, among the mixtures with 4% $Ca(OH)_2$ content, those with a concentration of 12.5M NaOH were less able to maintain their shape stability under constant load. Although there were very similar results in mixtures with 8% $Ca(OH)_2$ content, generally more settlement was observed in mixtures with 12.5M NaOH concentration. As in the previous series, the increment in the amount of $Ca(OH)_2$ in the mixtures with the same NaOH content in this series made the mixtures show better shape stability performance by reducing the amount of settling under constant load.

When the results in terms of mineral additive content were compared, the mixtures prepared using different combinations of BFS, SF and FA within the scope of the 5th Series, compared to mixtures where no mineral additive with the same alkali activator content was used (Series 1) or only BFS (series 3) used as mineral additive, it showed a more fluid / workable performance compared to that. It has been observed that it spreads more on the flow table and shows less shape stability/buildability performance and settle more under the buildability test (especially in mixtures containing 4% $Ca(OH)_2$). In this context, the use of SF and FA has significantly affected the fresh concrete properties of the mixes, resulting in a more fluid consistency. Based on the kind of materials, usage of them as a substitute material or as a mineral additive can have various influences on the features of concrete. The reason for this can be shown to be that they have different particle properties that determine their water requirements, packaging capabilities and reactivity when used as a binder for concrete, as well as their different chemical and mineralogical compositions. There are researches in the literature showing that the use of SF, FA and BFS has a positive effect on the fluidity of the mixtures. With the appropriate mixing ratio, fine powder additives densify the microstructures by filling the gaps and pores and can increase the fluidity of the mortars by showing a lubricating effect,

preventing the particles from sticking to each other. In this context, SF, known to have higher fineness and spherical shape, increases the fluidity of the material by reducing the water demand through the potential ball bearing effect, like to the FA case (spherical shape, smooth glassy texture and finer grain size) (Sellevold, 1987; Atiş, 1997; Joshi and Lohita, 1997; Erdoğan, 2003). When the mixtures produced within the scope of the 5th series were compared within themselves, Group 1 mixtures prepared using higher levels of BFS had relatively lower spreading values compared to other mixture groups (excluding some mixtures containing 10M and 12.5M NaOH with 4% $Ca(OH)_2$ content). They showed more shape stability (especially in mixtures containing 8% $Ca(OH)_2$) under the buildability test. When Group 1 and Group 2 results were analyzed comparatively, it was understood that FA substitution has a favorable influence on fluidity. Although the addition of SF affected the fluidity positively compared to the mixtures without SF, when all mixtures containing SF were compared within themselves, after a certain value / point, the SF increase had an adverse effect on the flowability / workability, it was found to cause a lower amount of spreading on the flow table and a lower amount of settling under the buildability test. Above the optimum amount, the high fineness of SF becomes more dominant (due to the potential ball bearing effect), causing in increased water demand and therefore lesser workability (Johari et al., 2011).

When the vane shear results of the mixtures were examined, the peak shear stress values were observed from the mixtures containing the highest concentration of NaOH (15M NaOH) in almost all cases. Except for some of the mixtures with high NaOH concentration in groups 1 and 2, measurements could be taken from all mixtures in the series even at 120 minutes. As with the results obtained from other series, the lowest shear stress values at all ages were generally obtained at 10M NaOH concentration in this series. On the other hand, in mixtures with equal NaOH content, the increment in $Ca(OH)_2$ led increases in the shear stress. When the results were evaluated in terms of mineral additive content, the 5th Series mixes prepared using BFS, SF and FA had less resistance to the vane shear device compared to their counterparts in the series where no mineral additive was used (1st Series) or only BFS (3rd series) was used as mineral additive.

When the mixtures in the 1st and 2nd groups were compared, no clear difference could be seen between the shear stresses, and it was deduced from this that the effect of SF and FA on shear stress was similar. Besides, the increase in SF content caused decreases in

shear stresses. As a result, the use of SF and FA as mineral additives has positively affected the long-term printability performance of the mixtures by extending the workable time.

In terms of compressive strength results, although there was no linear relationship between the change in NaOH concentration and compressive strength in mixtures with equal $Ca(OH)_2$ content, especially for mixtures containing FA, the compressive strength values decreased with the increment of NaOH. Although a high molarity of NaOH content (15M NaOH) often results in lower compressive strength results (especially for early age) compared to mixtures containing lower concentrations of NaOH, reverse was also observed. Likewise, the connection between the change in $Ca(OH)_2$ amount in mixtures with equal NaOH concentration and the compressive strength was mostly directly proportional, although there were contrary situations. When evaluated in terms of mineral additives, as expected, Series 5 mixtures with mineral additives had higher compressive strength for all ages than those without (1st Series). When the results of the 3rd series mixtures and the 1st group mixtures were compared, the influence of SF substitution on the compressive strength varied, and it had a favorable influence on the compressive strength at an early age and positively in some places in the advanced age. On the other hand, the increase in the SF content of the mixtures (from Group 2 to Group 4) provided significant improvements in compressive strength, especially for mixtures with 10M NaOH concentration, and decreased the compressive strength in mixtures with high NaOH content. In addition, although FA substitution negatively affected the 7-day compressive strength of mixtures with 12.5 and 15M NaOH concentrations compared to 1st Group mixtures without FA, this effect disappeared at the end of 28 days and caused higher compressive strengths.

Effects of water/binder ratio on geopolymer mixtures was investigated in terms of both mechanical and rheological aspects in that series as well. P6, P11, P15 and P21 mixtures selected from the samples produced within the scope of Series 5, taking into account the rheological and mechanical features of the material, only changed the water content to 0.36 and 0.39 w/b to examine the effects of the w/ b ratio on the rheological and mechanical features of the material. The results of the mixtures are presented in Table 4.8. In addition, all results are presented in graphs for easy comparison (Figure 4.13 and 4.14).

Table 4.8. Experimental results of mortar mixes produced using different w / b ratios with CDW and various mineral admixture together activated with Ca(OH)2 and NaOH together.

Sample	NaOH (M)	$Ca(OH)_2$ (%)	Flow ability Index (Γ)	Buildability (Final Mortar Height) (cm)	Shear Yield Stress (N/cm^2)				Compressive Strength (MPa)		
					Initial	30 min	60 min	120 min	7 Day	14 Day	28 Day
P6 (0.33)	15	8	0.95	4.50	2.5	4.6	7.1	-	19.5	23.9	24.4
P6 (0.36)	15	8	1.28	4.25	1.5	3.0	4.8	5.2	19.9	22.8	25.2
P6 (0.39)	15	8	1.50	4.05	0.6	1.2	2.0	4.7	15.8	17.9	20.5
P11 (0.33)	12.5	8	1.56	4.05	0.9	2.0	3.7	6.4	17.3	23.0	30.0
P11 (0.36)	12.5	8	1.64	4.15	0.9	2.5	3.8	4.1	16.7	19.0	23.6
P11 (0.39)	12.5	8	1.81	3.80	0.0	1.4	2.2	3.6	13.8	18.0	18.6
P15 (0.33)	10	8	1.46	4.25	1.0	2.0	2.1	3.5	21.6	24.4	31.6
P15 (0.36)	10	8	1.71	3.90	0.5	0.5	1.3	1.5	20.4	22.5	25.8
P15 (0.39)	10	8	2.50	2.80	0.0	0.2	0.5	0.6	17.0	23.0	23.5
P21 (0.33)	10	8	1.42	4.25	0.9	1.5	2.0	2.5	23.3	24.5	34.7
P21 (0.36)	10	8	1.51	4.10	0.3	0.5	1.4	2.7	19.2	27.0	28.6
P21 (0.39)	10	8	2.26	3.05	0.0	0.0	0.0	0.2	15.8	18.6	20.6

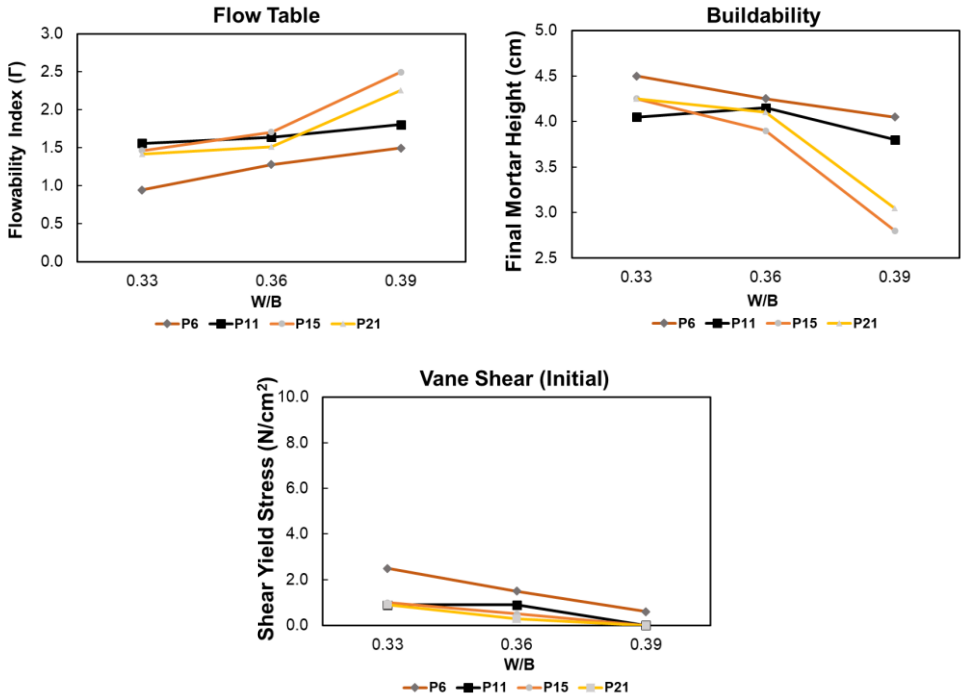

Figure 4.13. Flow table, buildability and vane shear test results of mortar mixtures produced using different w / b ratios with CDW and various mineral admixture together activated with $Ca(OH)_2$ and NaOH.

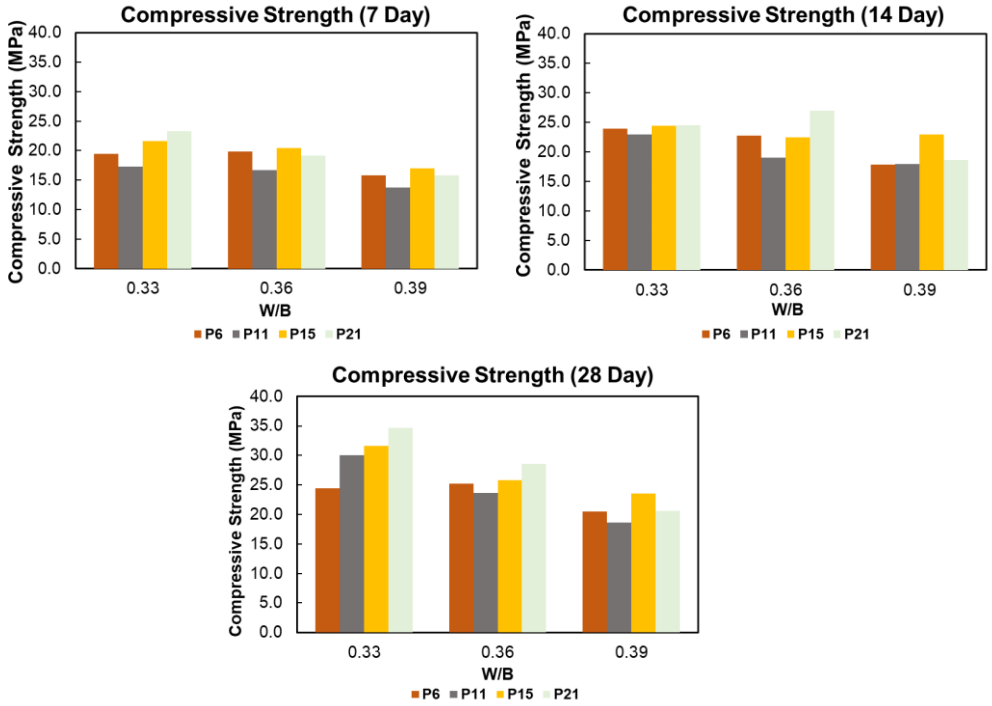

Figure 4.14. The compressive strength test results of different ages of mortar mixtures produced using different w/b ratios with CDW and various mineral admixture together activated with $Ca(OH)_2$ and NaOH

Water content is a crucial matter in geopolymerization and participates in the dissolution of aluminosilicate and polymerization of geopolymers (Hajimohammadi et al., 2010). And, workability performance of geopolymer mixtures is greatly affected by the water content (Hardjito et al., 2008; Wattimena et al., 2017). As expected, the increment in the w / b ratio increased the flowability of the mixture and adversely affected the buildability performance since the water in free form that does not participate chemical reaction in medium was increased (Aliabdo et al., 2016). In addition, as the w / b ratio increased, the long-term workability performance of the mixtures improved. It should be noted that the lower water-binder ratio could not be adequate to create a reaction circumstance for the dissolution of aluminosilicate sources leading to rapid setting (Siyal et al., 2016). In addition, the findings demonstrated that the compressive strength reduced as water amount was augmented, this implies that geopolymer concrete's compressive strength is inversely correlated to the water/binder ratio as in cementitious concrete (Patankar et al., 2013; Adam, 2019). Because a higher w/b increases the geopolymer pore volume, resulting in a reduction in compressive strength. (Cui and Wang 2019). When the results were examined in detail, the changes in performance in terms of both rheology and mechanic, from 0.33 to 0.36 w/b was more pronounced compared to the transition from 0.36 to 0.39 w/b.

4.2. Rheometer Measurement Results of 100% CDW based Geopolymer

0.39 w/b ratio was chosen in the experiments with the rheometer. Rheological experiments were carried out on samples prepared by using three different concentrations of NaOH solution as 10-12.5-15M and four different ratios of $Ca(OH)_2$ addition as 0-% 4%-8%-12% by weight of the binder. Mixtures containing Na_2SiO_3 were not tested with a rheometer, as they set gradually and quickly which deviate data continuously and give meaningless data. Since, the addition of Na_2SiO_3 to the mixture increases the geopolymerization reactions due to its soluble reactive silica content and shortens the setting times of the mixtures (Li et al., 2010; Kotwalet al., 2015; Goberis & Antonovich, 2004). When the samples containing silicate start to set quickly as a result of geopolymerization, an increase in torque and shear stress value was observed continuously and after a while the torque value approached the limits of the device and stop the test. And how Na_2SiO_3 effects the rheology of mixtures were interpreted with the data obtained from empirical test methods as in previous section. In general, the rheological and thixotropic properties of the materials were investigated by using the "Up

and Down Curve", "Constant Shear Rate (0.03 s^{-1})", "Various Constant Shear Rate", "Three Interval Thixotropy" test methods. The prescriptions and sample codes of the mortar mixtures used in the experiments to be made with the rheometer device are given in Table 4.9. In the dry mix of these mortar samples, 10% GW, 10% CW dust and equally 26.7% RCB, HB and RT were used as binders. As a filler material, recycled aggregate with maximum aggregate size of 2 mm, was used with 0.35 percent of the binder.

Table 4.9. Content of mixtures

Sample Code	**W/B**	**S/B**	**NaOH (Molarity)**	**$Ca(OH)_2$ (%)**
D1	0.39	0.35	10	0
D2				4
D3				8
D4				12
D5			12.5	0
D6				4
D7				8
D8				12
D9			15	0
D10				4
D11				8
D12				12

4.2.1. Up and Down Test Method

This test was applied to all samples in their first fresh state immediately after preparation of the mixtures and then repeated every 20 minutes for a total of 1 hour. Using this test method, the effect of the activators on the rheological characteristic of the material as well as how the yield points of the materials change with time were examined. Pre-shear force was applied to the samples in order to eliminate the inhomogeneous regions and air bubbles and to eliminate the possibility of Wall Slip condition. In addition, by applying pre-shear, pseudo setting was tried to prevent. After this application, Bingham, Casson and Hersch-Bulkley models were applied on the Down curve of the samples, and yield stress was calculated. Considering the concerns about the proper placement/distribution of the samples in the test container mentioned above, the yield points were calculated from the Down curve rather than the Up curve. During this test, the shear stress reached a peak in all samples while the pre-shear force was loaded and then decreased abruptly. This situation may be associated with the fact that the surface contacting with the air rapidly loses its moisture as a result of geopolymeric reactions and gets pseudo set. This

situation occurs only on the surface and when the shear stress value at the peak point is exceeded, the hardened area on the surface of the material breaks and the material becomes homogenous again. The situation could be understood more clearly in the graphic given below (Figure 4.15). As can be seen, the shear stress reached the peak value in preloading and then it fell to a certain level and stabilized. As a result of the preload applied to the material, the Up and Down curves were formed in a similar way.

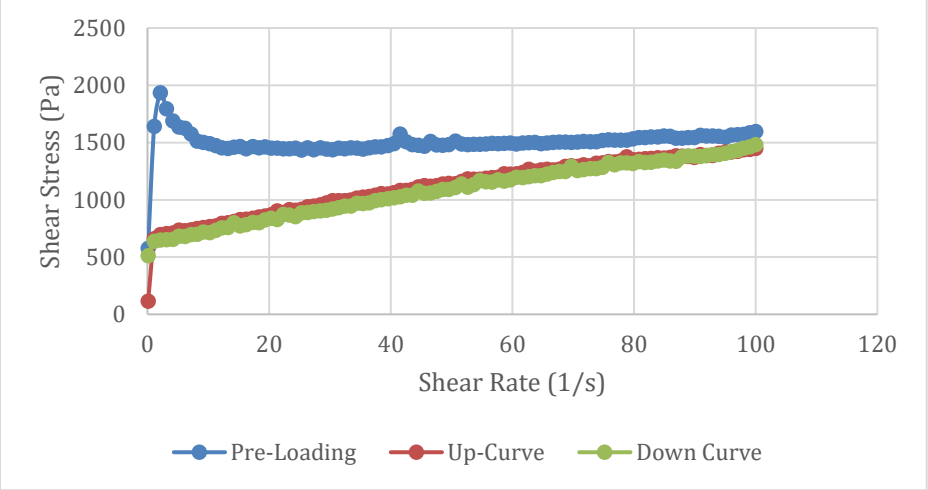

Figure 4.15. Up-Down Curve Graph Representation

4.2.1.1. The Effect of NaOH Molarity on Rheology

The mixtures were activated using NaOH solutions at 10 M, 12.5 M and 15 M concentrations using a single activator. The prepared mixtures were subjected to testing, and only Down curve graphs (Figure 4.16) and viscosity graphs (Figure 4.17) of the tested mixtures were given in order to reduce complexity and increase understandability. The yield stress points calculated by using Bingham, Casson and Herschel-Bulkley models and the highest shear stress values obtained in preloading are given in Table 4.10.

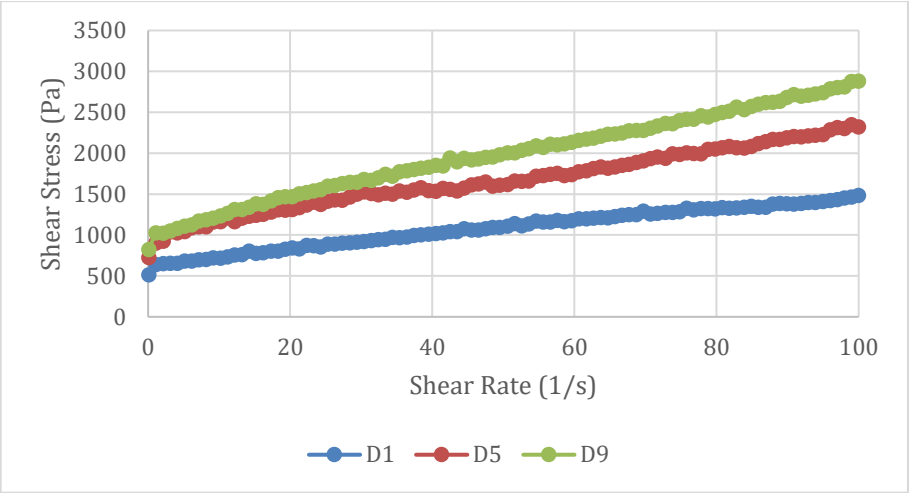

Figure 4.16. Down-Curve graph of D1, D5 and D9 coded mixtures

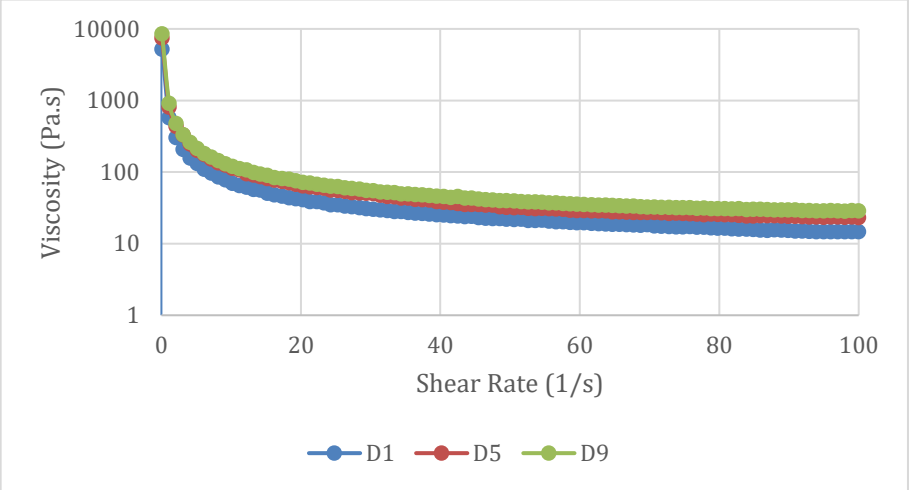

Figure 4.17. Viscosity-Shear rate graph of D1, D5 and D9 coded mixtures

Table 4.10. Maximum shear value of D1, D5 and D9 coded mixtures during preloading and yield stress values obtained from 3 different models

Sample Code	Pre-Loading Maximum Shear Stress (Pa)	Bingham Yield Stress (Pa)	Casson Yield Stress (Pa)	Herschel-Bulkley Yield Stess (Pa)
D1	1934.50	670.20	453.98	536.02
D5	2647.10	1017.40	692.31	1097.80
D9	4338.80	1123.60	711.92	1021.50

Examining the results, as the molarity increased, the preloading maximum shear required to move the material initially increased. In other words, the force required to break the hardened structure formed on the sample surface increased as the molarity increased. This situation can be attributed to the acceleration of geopolymerization reactions by

dissolving the materials faster due to the high alkalinity. Since NaOH concentration caused a high release of Si^{4+}, Al^{3+} and Ca^{2+} from the binding materials during the "leaching" reaction, which could accelerate the activation process and accelerate the setting process by enabling the rapid formation of geopolymerization products around the unreacted particles (Zhang et al., 2019). After preloading process, some regressions were made with the help of various models by using the yield stress graphs obtained as a result of the test performed with the Up-Down test method. According to the Bingham Model, the increase in molarity also increased the yield stress value, and while this increase was very significant in the transition from D1 to D5, it was recorded as much less at the transition from D5 to D9. Similarly, in Casson Model and Herschel-Bulkley Model, the yield stress value showed a significant increase in transition from D1 to D5, while the increase was less in transition from D5 to D9. When the flow values were evaluated quantitatively, Bingham model and Herschel-Bulkley model gave similar values, while Casson's results were slightly lower than others.

When the viscosity values were examined, the prepared geopolymeric mixtures exhibited the behavior of shear thinning (Pseudoplastic). Although the D9 sample had a slightly higher viscosity than D5 at high shear rates, the results were very close to each other at low shear rates. However, the D1 sample exhibited lower viscosity than the other two samples for both low and high shear rates due to as the concentration of NaOH increases, the mixtures become more viscous (Memon et al., 2013b; Varaprasad et al., 2010; Li et al., 2013). In the light of these data, the viscosity enhanced significantly while the NaOH molarity augmented from 10 M to 12,5 M, and the viscosity was not affected such amount when molarity changed from 12,5 M to 15 M.

4.2.1.2. The Effect of $Ca(OH)_2$ Addition Amount on Rheology

To clarify the influence of $Ca(OH)_2$ on yield stress and viscosity, test was carried out on samples prepared by using three different concentrations of NaOH solution as 10-12.5-15M and four different ratios of $Ca(OH)_2$ addition as 0%, 4%, 8% and 12% by weight of the binder. Firstly, the effect of $Ca(OH)_2$ was investigated on mixtures activated via 10M NaOH solution. The Down curve graphs (Figure 4.18) and viscosity graphs (Figure 4.19) of these samples are given below. The yield stress points of the samples and the highest shear stress values obtained in preloading phase are given in Table 4.11.

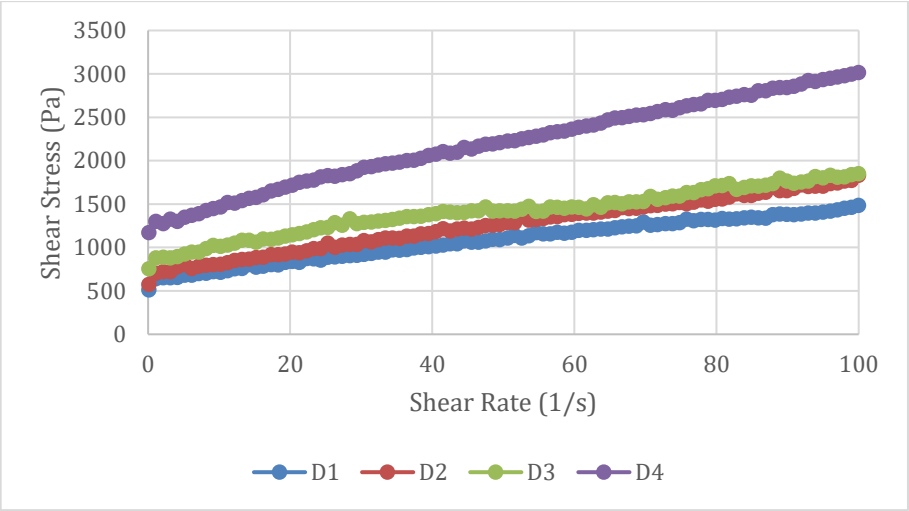

Figure 4.18. Down-Curve graph of D1, D2, D3 and D4 coded mixtures

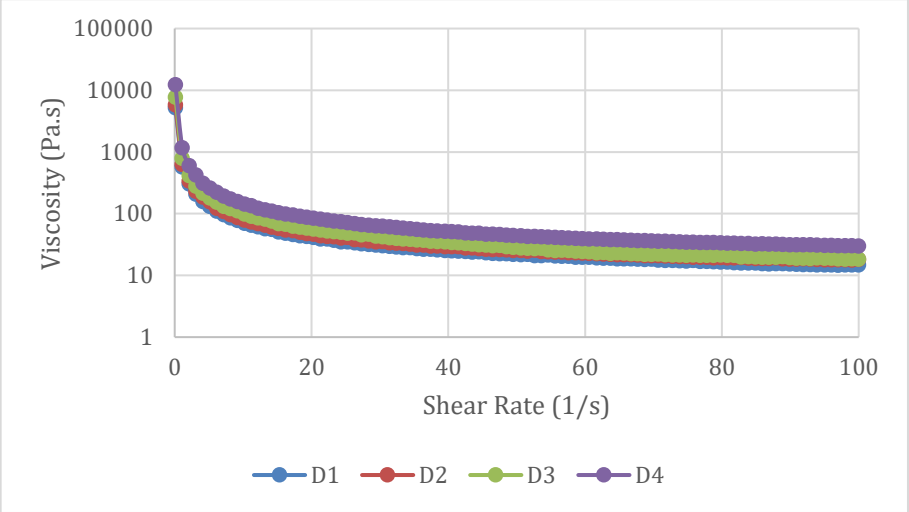

Figure 4.19. Viscosity-Shear rate graph of D1, D2, D3 and D4 coded mixtures

Table 4.11. Maximum shear value of D1, D2, D3 and D4 coded mixtures during preloading and yield stress values obtained from 3 different models

Sample Code	Pre-Loading Maximum Shear Stress (Pa)	Bingham Yield Stress (Pa)	Casson Yield Stress (Pa)	Herschel-Bulkley Yield Stess (Pa)
D1	1934.50	670.15	453.98	536.02
D2	2124.90	730.57	470.36	646.50
D3	4358.60	988.58	738.48	810.35
D4	8002.20	1366.40	927.68	1206.90

When the preloading values were examined, no significant increase was observed in the transition from D1 to D2, after this point the shear values in the preloading growingly increased and reached the value of 8002.2 Pa. The yield stress results obtained as a result of the regressions applied to the Down curve showed a continuous augmentation with the increment in $Ca(OH)_2$ usage rate since increment in $Ca(OH)_2$ increases the powder content in the mixture (water / binder ratio decrease) and increase in $Ca(OH)_2$ and the increment in Ca^{2+} ions exhibit stronger electrostatic attraction and charge neutralization and accelerate the geopolymerization process (Zhang et al., 2019). When the Bingham Model was examined, it was observed that the increase in $Ca(OH)_2$ usage rate from 0% to 4% provided a slight increase in the yield value, while the yield stress values increased more seriously and reached 1366.4 Pa value at the higher rates after this point. Similar behaviors were observed in the Casson and Herschel-Bulkley model. Although the yield values were different, the increase-decrease rates and the trends of the models were similar. When the viscosity values were examined at low shear rates, the increase in $Ca(OH)_2$ usage amount up to 8% caused a visible increase in viscosity values. This increase was much more noticeable in the transition from 8% to 12%. For high shear rates, a relatively small increase was seen when the usage rate of $Ca(OH)_2$ enhanced from 0% to 4%, whereas a considerable increase was not observed in the transition from 4% to 8%. In the transition from 8% to 12%, a very substantial increase was observed in viscosity values.

The Down curve graphs and viscosity graphs of the samples prepared using 12.5 Molar NaOH solution and determined $Ca(OH)_2$ are given in Figure 4.20 and 4.21 respectively. The yield stress points, and the highest shear stress values obtained in preloading of these samples are given in Table 4.12.

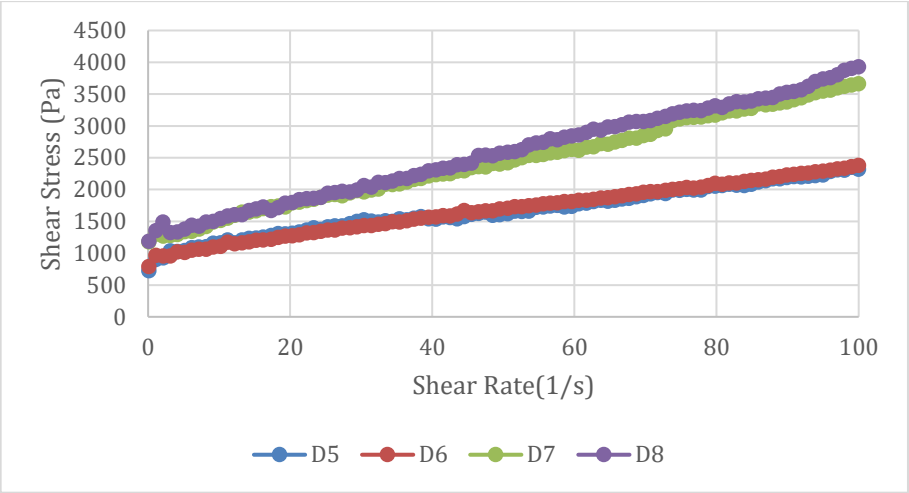

Figure 4.20. Down-Curve graph of D5, D6, D7 and D8 coded mixtures

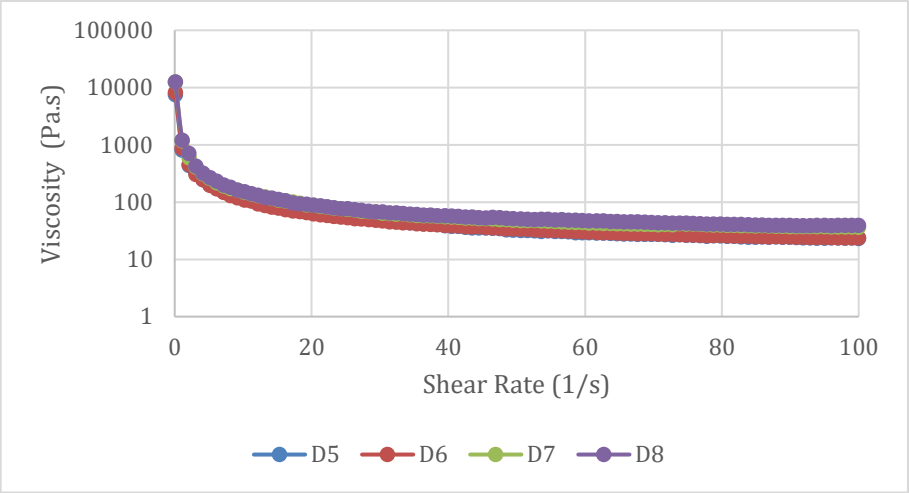

Figure 4.21. Viscosity-Shear rate graph of D5, D6, D7 and D8 coded mixtures

Table 4.12. Maximum shear value of D5, D6, D7 and D8 coded mixtures during preloading and yield stress values obtained from 3 different models

Sample Code	Pre-Loading Maximum Shear Stress (Pa)	Bingham Yield Stress (Pa)	Casson Yield Stress (Pa)	Herschel-Bulkley Yield Stess (Pa)
D5	2647.10	1017.40	692.31	1097.80
D6	2854.00	1004.10	661.43	937.90
D7	9970.00	1295.10	777.74	1395.90
D8	11763.00	1276.70	732.04	1276.60

When the preload values were examined, while D5 and D6 gave similar results, there was a very sharp increase in the transition from D6 to D7 and the shear stress value was reached 9970 Pa. While the amount of $Ca(OH)_2$ changed from 8% to 12%, the shear stress was increased significantly and reached 11763 Pa (Zhang et al., 2019). When the regression models for these samples were examined, Bingham model and Herschel-Bulkley model gave very similar results to each other and however, Casson Model recorded lower yield shear stress values in comparison to other models. Although the yield values were different here as well, the increase-decrease rates showed similar trends. While a slight decrease in the flow values was observed in all models during the transition from D5 to D6, the increase from D6 to D7 was observed more prominently in Bingham and Herschel-Bulkley models. A slight decrease was observed in the transition from D7 to D8, and this decrease was more pronounced in the Herschel-Bulkley model.

When the viscosity values were examined, while the use of 0% and 4% $Ca(OH)_2$ generally provided a similar viscosity, the samples at these two usage rates showed lower viscosity compared to the samples containing 8% and 12% $Ca(OH)_2$. Mixtures containing 8% and 12% $Ca(OH)_2$ also had similar viscosities. The difference in viscosity between mixtures containing low or high $Ca(OH)_2$ addition rate become more pronounced at high shear rates.

Finally, samples activated with 15M NaOH were tested. According to the test results, the Down curve graphs (Figure 4.22) and viscosity graphs (Figure 4.23) of these samples are given below. The yield stress points of the samples and the highest shear stress values obtained in preloading process are given in Table 4.13.

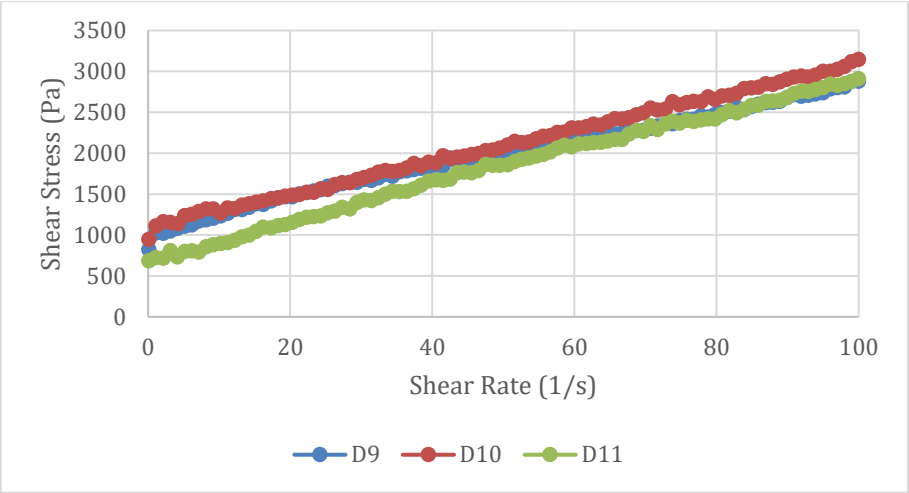

Figure 4.22. Down Curve graph of D9, D10 and D11 coded mixtures

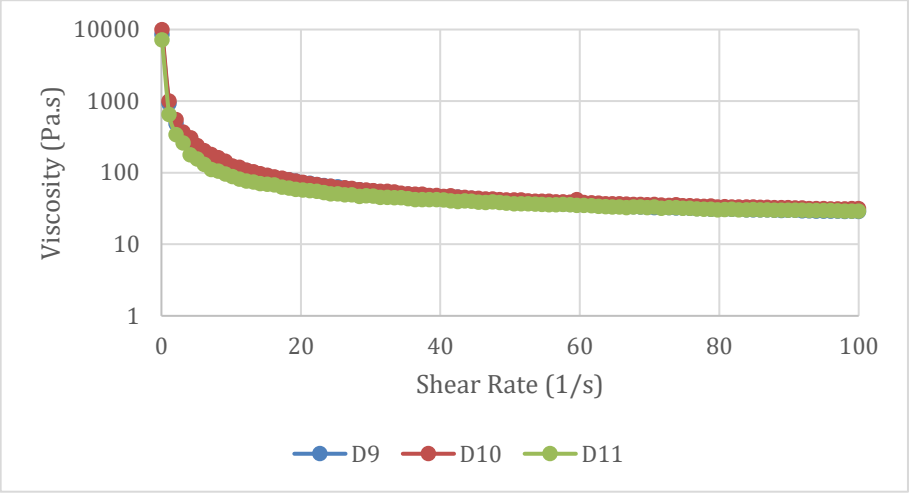

Figure 4.23. Viscosity-Shear rate graph of D9, D10 and D11 coded mixtures

Table 4.13. Maximum shear value of D9, D10, D11 and D12 coded mixtures during preloading and yield stress values obtained from 3 different models

Sample Code	Pre-Loading Maximum Shear Stress (Pa)	Bingham Yield Stress (Pa)	Casson Yield Stress (Pa)	Herschel-Bulkley Yield Stress (Pa)
D9	4338.80	1123.60	711.92	1021.50
D10	7171.10	1099.80	639.17	1083.30
D11	9858.70	704.98	332.04	521.56
D12	18770.00	-	-	-

When the preload values were examined, with the increasing $Ca(OH)_2$ content, the maximum shear stress value has increased continuously (Zhang et al., 2019). And the

torque capacity of the device has exceeded the value by increasing approximately twice during the transition from D11 to D12. For this reason, the test on the D12 sample has been terminated. According to the Bingham and Casson regression model, the yield stress values of the mixtures decreased with the augmenting content of $Ca(OH)_2$, and this decrease was more in the transition between high $Ca(OH)_2$ addition rates. In the Herschel-Bulkley model, while there was a very small increase in the transition from D9 to D10, a very serious decrease was observed afterwards. When the viscosity values were examined, significant differences were obtained at low shear rates. When the amount of $Ca(OH)_2$ augmented from 0% to 4%, the viscosity values increased slightly, whereas the viscosity decreased significantly when the amount of $Ca(OH)_2$ enhanced from 4% to 8%, a lower viscosity was obtained than the mixture without any $Ca(OH)_2$. However, at high shear rates, D9 and D11 perform similarly while D10 has a higher viscosity. This finding could be accredited to dissolution ability of $Ca(OH)_2$ in low and high alkalinity. Since, in higher alkalinity, solubility of $Ca(OH)_2$ is restricted due to charged ions (Granizo et al., 2004).

4.2.2. Open-Time performance of Up-Down Method

In addition to the tests performed on fresh samples immediately after the preparation of the mixtures, Up-Down curve tests were also performed on at 20, 40, and 60 minutes. The yield values obtained by the Herschel-Bulkley model sometimes decreased suddenly and distorted the results. In general, the results obtained with the Bingham model were found to be more consistent with the results obtained from the other two methods, and the data obtained at this stage were analyzed using the Bingham model.

4.2.2.1. Effect of NaOH Molarity on Rheometer over Time

Changes in rheological properties of mixtures prepared with 10M, 12.5M and 15M concentration NaOH as single activator were investigated. The yield stress points of these mixtures and the highest shear stress values obtained in preload are given in Table 4.14. When the maximum shear stress values during loading were examined, it was observed that the maximum shear stress values at 20, 40 and 60 minutes increased with increasing NaOH concentration since the increase in NaOH concentration may have accelerated the geopolymerization process by increasing the pH of the mixtures, resulting in a higher dissolution rate (Görhan and Kürklü, 2014). The preload value of the D9 sample increased more than D5 between 0-60 minutes, and that of the D5 sample more than D1. The

increase in molarity caused the material to set faster and thus the preload value increased. When the variation of yield stresses with time was examined, although a linear increase trend was not observed for 10 M, at the end of 60 minutes a yield value of 890.76 Pa has been reached with an increase of 32.9% regarding the initial state. The same manner was observed for the 12.5 M mixture. However, the increment in yield stress at the end of 60 minutes at 12.5 M compared to initial case (0 min) was very low. The reason for this can be that the material has not started to set and also in this range in which the device operation is very sensitive. These results show that this mixture does not lose consistency for 1 hour. When the 15M mixture was examined, although no linear increase was observed in the yield stress, at the end of 60 minutes, the yield stress showed a significant increase of 27.15% compared to the initial state and reached the value of 1428.7 Pa. Since NaOH concentration caused a high release of Si^{4+}, Al^{3+} and Ca^{2+} from the binding materials during the "leaching" reaction, which could accelerate the activation process and accelerate the setting process by enabling the rapid formation of geopolymerization products around the unreacted particles (Zhang et al., 2019).

Table 4.14. Maximum Shear Stress value of D1, D5 and D9 coded mixtures and yield stress values obtained from 3 different models at the end of 0, 20, 40 and 60 minutes

NaOH (Molarity)	Sample Code	Open Time (min)	Pre-Loading Maximum Shear Stress (Pa)	Bingham Yield Stress (Pa)	Casson Yield Stress (Pa)	Herschel-Bulkley Yield Stress (Pa)
10	D1	0	1934.5	670.15	453.98	536.02
		20	1994.3	852.78	598.38	554.08
		40	2069.0	775.08	508.87	781.87
		60	2178.0	890.76	607.57	916.08
12.5	D5	0	2647.1	1017.4	692.31	1097.80
		20	6104.8	970.88	642.51	260.83
		40	8603.9	966.55	631.32	863.63
		60	8125.1	1037.7	739.29	220.14
15	D9	0	4338.8	1123.6	711.92	1021.50
		20	10279.0	1238.0	900.20	751.66
		40	18870.0	1190.5	734.37	1113.80
		60	18870.0	1428.7	902.78	1256.90

4.2.2.2. The Effect of $Ca(OH)_2$ on Rheology over Time

To examine the impact of $Ca(OH)_2$ use on rheology over time, tests were carried out on all samples prepared using a 10-12.5-15M concentration of NaOH solution and four

different ratios of $Ca(OH)_2$. The results of test are represented in Table 4.15. First, mixtures prepared with 10M NaOH solution were examined. Between 0-60 minutes, the increase in the preload value was observed as 12.6%, 6.9%, 21.7%, 11.9%, respectively. In addition to that, the D2 sample showed a continuous increase and reached 1016.8 Pa yield stress after 60 minutes. The D3 sample also increased steadily until the 40th minute, but at the end of 60 minutes it decreased a little and reached a yield stress value of 1155.1 Pa. Although no regular increase was observed in the D4 sample, at the end of the 60th minute it reached 1567 Pa, which was 14.7% higher than the initial state. Increments in yield stress between 0-60 minutes were 32.8%, 39.2%, 16.8% and 14.7% for the D1, D2, D3 and D4 sample, respectively. It could be concluded that $Ca(OH)_2$ concentration after 4%, prevent the setting means geopolymerization. Since, excess amount of $Ca(OH)_2$ (Ca^+) would hinder the proper geopolymer gel structure and prevent strength development (Khater, 2012).

Table 4.15. Maximum shear stress value of D1, D2, D3 and D4 coded mixture and yield stress values obtained at the end of 0.20, 40 and 60 minutes according with 3 different models

$Ca(OH)_2$ Addition (%)	Sample Code	Open Time (min)	Pre-Loading Maximum Shear Stress (Pa)	Bingham Yield Stress (Pa)	Casson Yield Stress (Pa)	Herschel-Bulkley Yield Stress (Pa)
%0	D1	0	1934.5	670.15	453.98	536.02
		20	1994.3	852.78	598.38	554.08
		40	2069.0	775.08	508.87	781.87
		60	2178.0	890.76	607.57	916.08
%4	D2	0	2124.0	730.57	470.36	646.50
		20	2256.0	851.80	524.02	825.36
		40	2249.0	937.79	716.51	218.23
		60	2270.0	1016.80	750.34	738.94
%8	D3	0	4358.6	988.58	738.48	810.35
		20	4842.9	1109.70	885.68	536.10
		40	5628.4	1192.50	985.37	1183.90
		60	5303.8	1155.10	883.82	1140.10
%12	D4	0	8002.2	1366.40	927.68	1206.90
		20	7171.8	837.69	489.62	793.31
		40	8154.9	908.65	578.86	1021.30
		60	8955.4	1567.00	1113.60	1478.50

The results of the samples prepared with 12.5 M NaOH solution are given in Table 4.16. As the time passing, the maximum shear stress value during preloading increased in all $Ca(OH)_2$ ratios except for the 40th minute of D5. There was an increase of 206.9% and

253.5% for D5 and D6, respectively, between 0-60 minutes. For D7, these experiments could not be carried out after the 40th minute, whereas for the sample coded D8, the test could not be performed even at the 20th minute. According to the Bingham yield stress values, there was a decrement in the yield stress values in the first 20 minutes in the mixtures prepared with 12.5 M solution, even in the first 40 minutes for samples where the test could be performed. However, the material showed an increase in yield stress compared to the initial case at the end of 60 minutes, in the samples where the test could be carried out. At the end of 60 minutes, the yield stress values of D5 and D6 samples increased by 2% and 16.2%, respectively, compared to the original case. This showed that 4% $Ca(OH)_2$ addition increased viscosity since, the existence of $Ca(OH)_2$ beneficial the generation of several products that provide rigidity to the paste (Granizo, et al. 2004).

Table 4.16. Maximum shear stress value of D5, D6, D7 and D8 coded mixtures and yield stress values obtained at the end of 0.20, 40 and 60 minutes according with 3 different models

$Ca(OH)_2$ Addition (%)	Sample Code	Open Time (min)	Pre-Loading Maximum Shear Stress (Pa)	Bingham Yield Stress (Pa)	Casson Yield Stress (Pa)	Herschel-Bulkley Yield Stress (Pa)
%0	D5	0	2647.10	1017.40	692.31	1097.80
		20	6104.80	970.88	642.51	260.83
		40	8603.90	966.55	631.32	863.63
		60	8125.10	1037.70	739.29	220.14
%4	D6	0	2854.00	1004.10	661.43	937.90
		20	6013.80	925.81	598.20	946.50
		40	6979.20	883.88	589.06	745.07
		60	10089.00	1167.10	876.86	861.80
%8	D7	0	9970.00	1295.10	777.74	1395.90
		20	18870.00	1081.60	718.59	1228.30
		40	18870.00	-	-	-
		60	-	-	-	-
%12	D8	0	11763.00	1276.70	732.04	1276.60
		20	-	-	-	-
		40	-	-	-	-
		60	-	-	-	-

Finally, samples prepared with 15M NaOH concentration were tested in the Up-Down method to evaluate open-time performances at 0, 20, 40 and 60 minutes. The results obtained from the test are given in Table 4.17. When the maximum shear stress values obtained during the preload phase were examined, a continuous increase has been observed over time. This could be attributed that flowability of geopolymer mixtures was

significantly affected by water content (Hardjito et al., 2008; Wattimena et al., 2017) and increment in $Ca(OH)_2$ addition rate increased the powder content in the mixture, thus, water/solid ratio of mixtures was decreased and matrix become denser. While the test results of the D11 sample at the 40th and 60th minutes could not be obtained, the D12 sample could not be tested even in the initial state. When the yield stress data were examined, although the D9 sample did not show a linear increase, at the end of 1 hour it reached a yield stress value of 1428.7 Pa with an increase of 27.15% compared to the initial fresh state. When the D10 and D11 samples were examined, a sudden increase was observed compared to the measurement at the end of the first 20 minutes, and the rates of these increases were 55.32% and 270.18%, respectively. This could be explained in way that Ca(OH)2 may interact with suspended silicate and aluminate substance to develop a C-S-H gel that gives more nucleation core for formation of dissolved particles, resulting fast hardening (Temuujin et al. 2009; Guo et al. 2010). However, when the D10 sample was tested after 40 minutes, it slightly increased compared to the measurement value after 20 minutes. It could be attributed that the increase in OH^- concentration caused the formation of a large number of active groups by rapidly breaking the glassy silica-alumina chains (Fan et al., 1999), but, during geopolimerization, Ph values started to decrease as a result of reaction which means hardening process started to become slower.

Table 4.17. Maximum shear stress value of D9, D10, D11 and D12 coded mixtures and yield stress values obtained at the end of 0.20, 40 and 60 minutes according with 3 different models

$Ca(OH)_2$ Addition (%)	Sample Code	Open Time (min)	Pre-Loading Maximum Shear Stress (Pa)	Bingham Yield Stress (Pa)	Casson Yield Stress (Pa)	Herschel-Bulkley Yield Stress (Pa)
%0	D9	0	4338.8	1123.60	711.92	1021.50
		20	10279.0	1238.00	900.20	751.66
		40	18870.0	1190.50	734.37	1113.80
		60	18870.0	1428.70	902.78	1256.90
%4	D10	0	7171.1	1099.80	639.17	1083.30
		20	16339.0	1708.20	1116.70	1592.70
		40	18741.0	1757.70	1129.83	1494.50
		60	18870.0	-	-	-
%8	D11	0	9858.7	704.98	332.08	521.56
		20	18870.0	2609.70	1849.10	2583.50
		40	-	-	-	-
		60	-	-	-	-
%12	D12	0	18770.0	-	-	-
		20	-	-	-	-

		40	-	-	-	-
		60	-	-	-	-

4.2.3. Constant Shear Rate Test Method

The rheological and thixotropy behavior of mortar samples with different molarities of NaOH and addition rate of $Ca(OH)_2$ with 0.39 w/b ratio was investigated by using this test method. In this method, which has a very simple test procedure, the material was exposed to a steady shear rate for 20 minutes and a time-dependent graph of the torque was plotted. By using the results obtained from this experiment, the graphs were drawn biaxially to examine the change in shear stress with time. It was expected that the mortar materials would show a linear elastic behavior till a specific threshold torque value was over passed, and after this value, the bonds started to be broken and the material began to flow. This threshold value obtained from the experiments was converted to the stress value and expressed as "yield stress at rest". The yield stress at rest was also called static stress. As the material was subjected to shear rate continuously, a decrease in shear stress has been observed after this value, and after a while, a constant stress value has been obtained. This value was called dynamic shear stress and recorded as stress in the constant region within the scope of this test. By using differentiation between static and dynamic shear stress in terms of percentage was used to evaluate thixotropy behavior of mixtures as explained in upper section. In fact, the relationship between the material's stress value after being subjected to shear rate and its initial state gives a better information about thixotropy. Because thixotropy can be explained rather by the relationship between viscosity before and after exposure to shear force of the material.

4.2.3.1. The Effect of NaOH Molarity on Rheology and Thixotropy

To see the impacts of NaOH molarity on the rheological and thixotropic features of the material, samples activated with three different molarity values as 10M, 12.5 M and 15M were tested. The changes in the torque and shear stress values of the mixtures exposed to a constant shear rate of 0.03 s^{-1} are given in Figure 4.24.

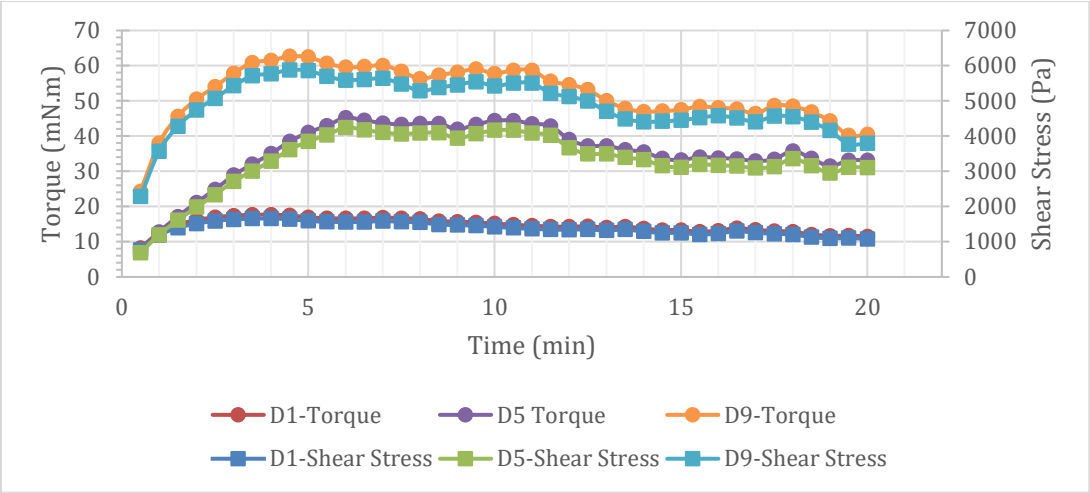

Figure 4.24. Shear stress values of D1, D5 and D9 coded samples exposed to constant shear rate.

When Figure 4.24 was examined, it was seen that as the molarity of NaOH increased, the torque and shear stress values at which the system peaks also increased. These peak values and the shear stress and torque values in the steady region are represented in Table 4.18.

Table 4.18. Torque and shear stress values at yield point and constant region of D1, D5 and D9 coded mixtures and percentage difference between yield and constant values in shear stress

Torque (mN.m)			Shear Stress (Pa)		Drop %
Sample Code	Yield Value (Static)	Constant Region (Dynamic)	Yield Value (Static)	Constant Region (Dynamic)	
D1	17.67	11.64	1658.10	1102.73	33.49
D5	45.22	32.57	4244.30	3082.23	27.38
D9	62.65	40.33	5879.90	3785.35	35.62

When the yield stress values at rest were examined, it was observed that this value increased as the molarity increased since as the concentration of NaOH increases, the mixtures become more viscous (Memon et al., 2013b; Varaprasad et al., 2010; Li et al., 2013). This increase was much more pronounced in the transition from D1 to D5. As stated before, although the yield stress at rest must be high enough for the mixture to carry the load on it better, its dynamic stress must be low enough to pass the nozzle through the pipes without forcing the pump and without water loss in an application where materials should be carried with the help of pump system. The differentiation between the static and dynamic stresses of the mixtures in terms of the results obtained within the scope of

the experiment was used to interpret thixotropy ability of materials, and also the high static tension of the material indicates that it will provide better performance in terms of buildability. D1 and D9 mortars showed a greater drop performance than D5 with rge values of 33.49% and 35.62%, respectively, during the transition from static to dynamic stress. Such result indicated that D1 and D9 had a better thixotropy performance than D5.

4.2.3.2. The Effect of $Ca(OH)_2$ Addition on Rheology and Thixotropy

$Ca(OH)_2$ was added to the samples initially activated with a 10 M NaOH solution in determined proportions. The data obtained as a result of the experiments made on these samples are presented in Figure 4.25. Static and dynamic yield value and percentage drops between two points are given in Table 4.19 for a better understanding of the results.

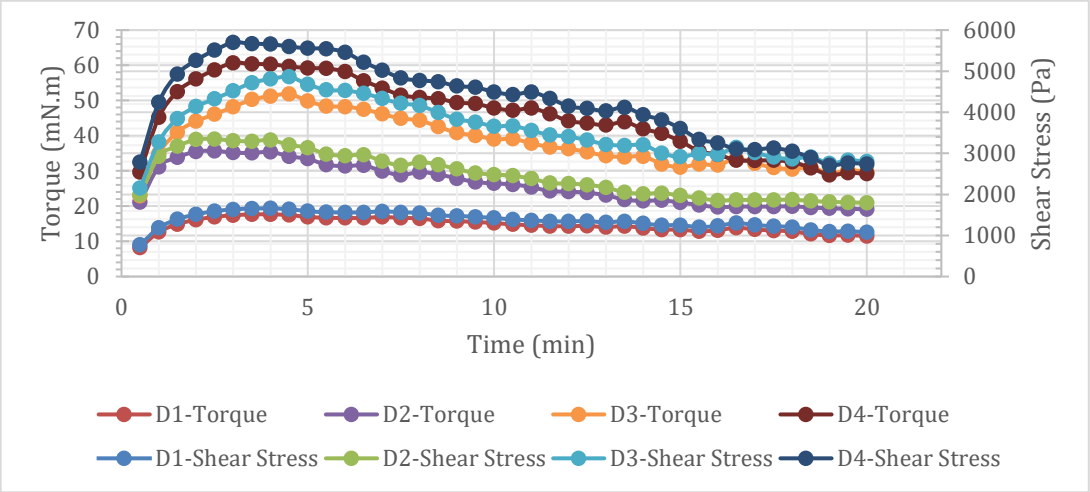

Figure 4.25. Shear stress and Torque values of D1, D2, D3 and D4 coded samples

Table 4.19. Torque and shear stress at yield point and constant region of D1, D2, D3 and D4 coded mixtures and percentage difference between yield and constant values in shear stress

Torque (mN.m)			Shear Stress (Pa)		Drop %
Sample Code	Yield Value (Static)	Constant Region (Dynamic)	Yield Value (Static)	Constant Region (Dynamic)	
D1	17.67	11.64	1658.10	1102.73	33.49
D2	35.68	19.25	3349.00	1815.15	45.80
D3	51.81	29.78	4862.60	2823.25	41.94
D4	60.69	29.16	5696.00	2776.50	51.26

As the content of $Ca(OH)_2$ augmented, the yield value of the material showed an increasing trend since increment in $Ca(OH)_2$ enhanced the powder content in the mixture

which decrease water content in matrix (Hardjito et al., 2008; Wattimena et al., 2017), and the amount of such increment was decreased as the content of $Ca(OH)_2$ increased since $Ca(OH)_2$ enhance the dissociation of aluminosilicate sources in the alkaline medium (Khater, H. M., 2012). When the dynamic stress values were examined, it has been observed that there was an increasing trend by increasing up to 8%, and then it has shown similar stress performance with 12% $Ca(OH)_2$ addition rate. When the drop in shear stress values was examined, mixtures containing 4% and 12% $Ca(OH)_2$ showed a more drop performance. This means that D2 and D4 show a higher thixotropic property.

The data obtained as a result of the experiment made on samples prepared with 12.5 Molar NaOH solution are presented in Figure 4.26. Static and dynamic yield value and percentage drop between two points are given in Table 4.20 for a better understanding of the results.

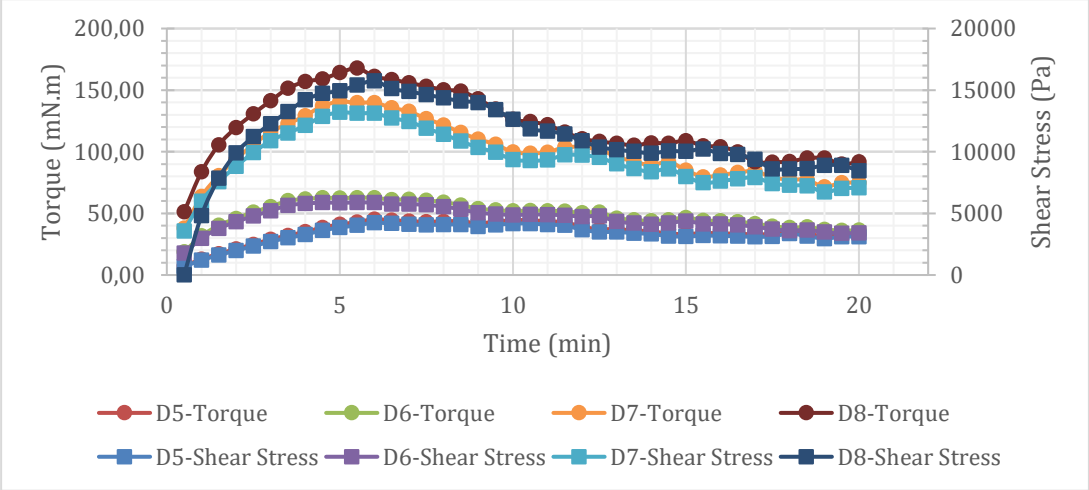

Figure 4.26. Shear stress values of D5, D6, D7 and D8 coded mixtures exposed to constant shear rate.

Table 4.20. Torque and shear stress at yield point and constant region of D5, D6, D7 and D8 coded mixtures and percentage difference between yield and constant values in shear stress

Torque (mN.m)			Shear Stress (Pa)		Drop %
Sample Code	Yield Value (Static)	Constant Region (Dynamic)	Yield Value (Static)	Constant Region (Dynamic)	
D5	45.22	32.57	4244.30	3082.23	27.38
D6	62.69	36.49	5883.20	3481.60	40.82

D7	140.69	76.78	13204.00	7213.70	45.37
D8	167.75	92.19	15743.00	8712.03	44.66

According to results, static stress value increased as the usage rate of $Ca(OH)_2$ increased, and this increase was more pronounced in the transition from 4% to 8%. The same was valid for the dynamic shear stress value. When the drop between static and dynamic shear stress were examined, the influence of $Ca(OH)_2$ addition on drop percentage was quite clear, but a linear trend could not be obtained with increasing $Ca(OH)_2$. In samples activated with 12.5M NaOH solution, it has been observed that the utilization of $Ca(OH)_2$ has a positive effect on thixotropy up to 8%. At the same time, the yield point of the shear stress increased continuously as the usage rate increased.

Finally, samples activated with 15 M NaOH were tested by this method to investigate their rheological and thixotropic properties. The data obtained as a result of the experiments made on these samples are presented in Figure 4.27 graphically. Static and dynamic yield value and percentage drop between these values are given in Table 4.21 for a better understanding of the results.

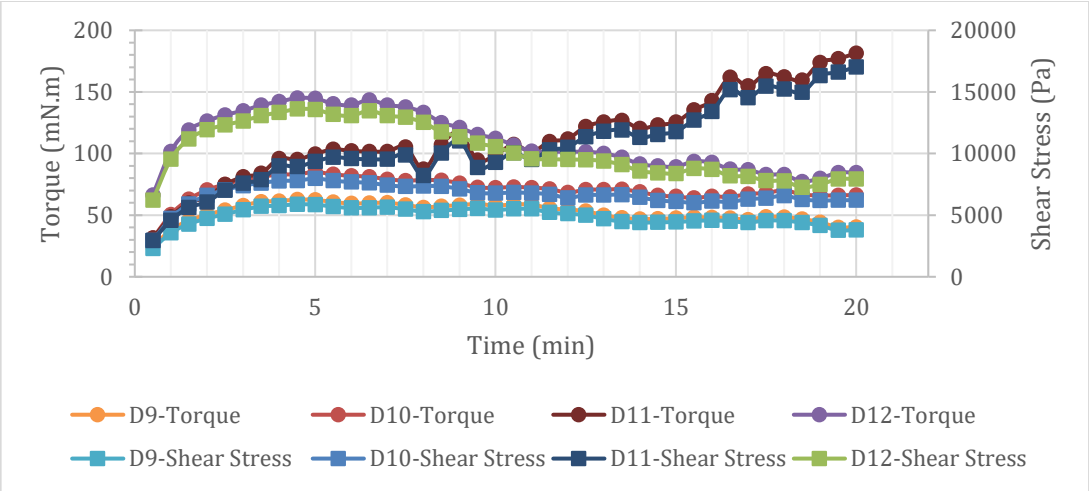

Figure 4.27. Shear stress values of D9, D10, D11 and D12 coded mixtures exposed to constant shear rate.

Table 4.21. Torque and shear stress at yield point and constant region of D9, D10, D11 and D12 coded mixtures and percentage drop between yield and constant values in shear stress

Torque (mN.m)			Shear Stress (Pa)		Drop %
Sample Code	Yield Value (Static)	Constant Region (Dynamic)	Yield Value (Static)	Constant Region (Dynamic)	
D9	62.65	40.33	5879.90	3785.35	35.62
D10	85.01	66.15	7978.10	6207.73	22.19
D11	-	-	-	-	-
D12	145.02	81.57	13611.00	7788.30	42.78

In the D11 sample, the increase in shear stress continued throughout 20 minutes test period. The reason for this could be that the geopolymerization reaction continues continuously and as a result, the sample may start to set over time. However, at first, it was predicted that a possible agglomeration may cause this situation. For this reason, the test was repeated for this sample, but same results were obtained. When other samples were examined, both static and dynamic shear stress values increased with the increasing $Ca(OH)_2$ usage rate as usual (Temuujin et al. 2009; Guo et al. 2010; Hardjito et al., 2008; Wattimena et al., 2017). D12 was the mixture with the highest drop performance with a drop percentage of 42.78%. It has been observed that the utilization of 4% $Ca(OH)_2$ reduces this drop performance.

4.2.4. Various Constant Shear Rate Test Method

The standards of this experiment were determined regarding the research of Lapasin et al. (1983) and Erdem et al. (2009). The samples placed in the measuring cup of the rheometer were subjected to four different constant shear rates, 0.2, 0.3, 0.4 and 0.5 s^{-1} respectively, determined within the scope of the thesis, for 2 minutes after resting time of 5 minutes. As a result, an initial stress for each rate and the equilibrium stress of mixtures that reach equilibrium over time (usually after 1 minute) were recorded. While initial stress represents static stress, equilibrium stress represents dynamic stress. From these results, it was interpreted how the used activators changed the static and dynamic stress and thixotropy of the material. While interpreting thixotropy, two different curves were drawn using the initial and equilibrium stress values at each velocity, and the area between these two curves was used to calculate the structural breakdown area. It was interpreted

that the greater the structural breakdown area, the better the thixotropy performance of the material. However, in that interpretation method, it was observed that whenever the viscosity of materials increase, breakdown area value was become higher since the number was become greater. To interpret result more precise, ratio of breakdown area to overall area drawn by using initial stress was calculated. In that way, proportion of breakdown area to overall area (under initial stress curve) was used to interpret thixotropy performance of materials. So, it was interpreted in a way that the higher the structural breakdown area ratio, the higher the thixotropy performance of the material. So, under this title, two interpretation technics were used to analyze thixotropy performance of sample.

4.2.4.1. The Effect of NaOH Molarity on Rheology and Thixotropy

The initial and equilibrium stress values at 0.2, 0.3, 0.4 and 0.5 s^{-1} shear rate of samples prepared with single activator as 10, 12.5 and 15 Molar NaOH solution are given in the Table 4.22. The curves drawn according to the data in this table are given in Figure 4.28. The area between these two curves was calculated with the "trapezoidal rule".

Table 4.22. Initial and equilibrium stress values and structural breakdown area and its ratio, at 0.2, 0.3, 0.4 and 0.5 s^{-1} shear rate of D1, D5 and D9 coded mixtures

Sample Code	Shear Stress (Pa)	Shear Rate (1/s)				Structural Breakdown Area	Structural Breakdown Area Ratio (%)
		0.2	0.3	0.4	0.5		
D1	Initial (static) stress	1361.5	1386.6	1157.1	1021.7	69.3	18.55
	Equilibrium (dynamic) stress	1310.8	1052.1	931.5	807.5		
D5	Initial (static) stress	3034.2	2997.0	2402.7	1980.4	196.5	24.85
	Equilibrium (dynamic) stress	2563.5	2092.0	1764.0	1609.2		
D9	Initial (static) stress	5668.8	5708.2	4157.5	4112.7	482.7	32.71
	Equilibrium (dynamic) stress	4993.3	3588.9	2669.1	2349.0		

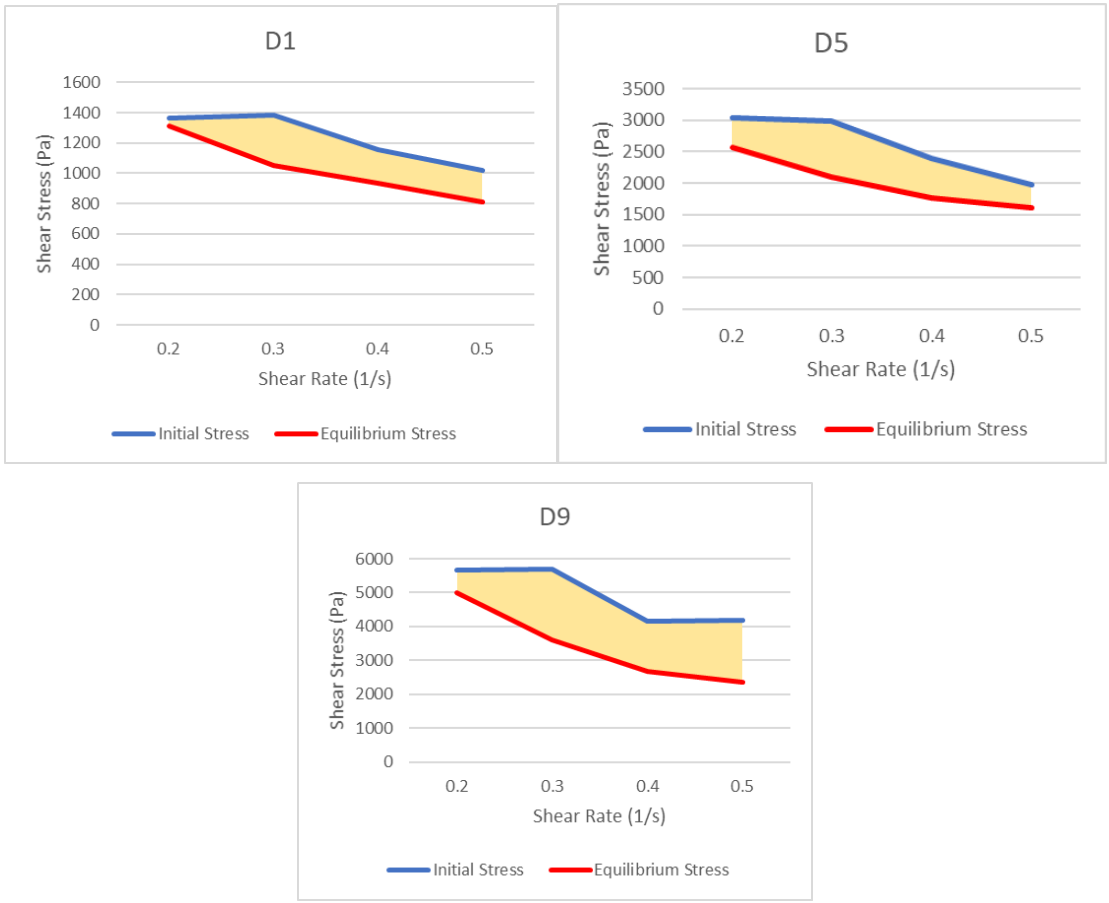

Figure 4.28. Initial and equilibrium stress values and structural breakdown area at 0.2, 0.3, 0.4 and 0.5 s^{-1} shear rate of D1, D5 and D9 coded mixtures

When the results were examined, the initial and equilibrium stress values increased for each shear rate value with increasing molarity (Memon et al., 2013b; Varaprasad et al., 2010; Li et al., 2013). It has been observed that this increase was numerically higher in the transition from 12.5 M to 15 M. As the shear rate augmented, a decrement was observed in the equilibrium stress value at all molarities, while the 0.2 and 0.3 shear rate performed similarly at the initial stresses. However, a decrease was observed in the initial stresses at transition to 0.4 and 0.5 shear rate. When the results of the structural breakdown area were examined, this area was increased as the molarity increased. This shows that the thixotropy of the material increases with increasing molarity. As a result, the fact that the material prepared with 15M NaOH solution had both high static shear stress and high thixotropy. If the static (initial) stress value is too high, it is thought that it will cause trouble in terms of workability, and this issue should be considered. Apart from this, high static stress is another parameter that should be considered as it increases the carrying capacity of the material and thus its buildability. In addition to these

interpretations, when the results of the structural breakdown area ratios were examined, ratio was increased as the molarity increased. This showed that the thixotropy of the material increased with increasing molarity.

4.2.4.2 The Effect of $Ca(OH)_2$ Addition on Rheology and Thixotropy

The effect of $Ca(OH)_2$ on rheology and thixotropy has been studied by applying steady shear rate of 0.2, 0.3, 0.4 and 0.5 s^{-1} to mixtures containing various addition rate of $Ca(OH)_2$ prepared with 10, 12.5 and 15 M NaOH solutions. The initial and equilibrium stress values of the samples prepared with 10M NaOH at four different rates and the structural breakdown areas calculated with the help of these values are given in Figure 4.29 and in the Table 4.23.

Table 4.23. Initial and equilibrium stress values, structural breakdown area and its ratio, at 0.2, 0.3, 0.4 and 0.5 s^{-1} shear rate of D1, D2, D3 and D4 coded mixtures

Sample Code	Shear Stress (Pa)	Shear Rate (1/s)				Structural Breakdown Area	Structural Breakdown Area Ratio (%)
		0.2	0.3	0.4	0.5		
D1	Initial (static) stress	1361.5	1386.6	1157.1	1021.7	69.3	18.55
	Equilibrium (dynamic) stress	1310.8	1052.1	931.5	807.5		
D2	Initial (static) stress	1929.9	1927.6	1428.6	1124.0	106.4	21.79
	Equilibrium (dynamic) stress	1837.1	1310.6	1085.0	1010.6		
D3	Initial (static) stress	3684.8	3438.8	2408.4	2039.2	219.8	25.24
	Equilibrium (dynamic) stress	3175.0	2240.2	1874.6	1618.4		
D4	Initial (static) stress	6726.4	6670.8	5019.9	4383.0	354.0	20.53
	Equilibrium (dynamic) stress	6323.1	4662.0	4035.5	3692.0		

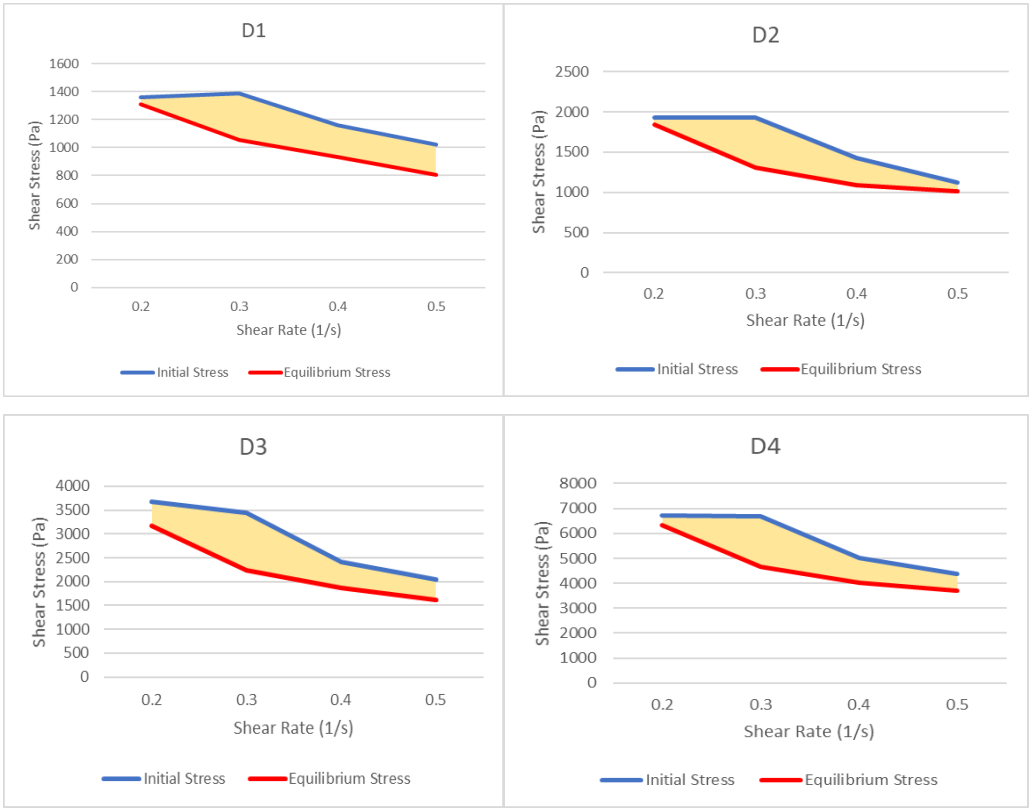

Figure 4.29. Initial and equilibrium stress values and structural breakdown area at 0.2, 0.3, 0.4 and 0.5 s^{-1} shear rate of D1, D2, D3 and D4 coded mixtures

When looking at the results in general, both the initial and equilibrium stress of the materials increased increasingly with increasing $Ca(OH)_2$ ratio (Hardjito et al., 2008; Wattimena et al., 2017). When the structural breakdown area was examined, as the $Ca(OH)_2$ addition rate increased, the structural breakdown area increased which means thixotropic performance of materials increased. The influence of $Ca(OH)_2$ could be clarified in way that significant contributor to the increment in yield stress, which led to higher initial stress value and therefore a higher thixotropy (Salem T.M., 2002). A very serious increase has been observed in the transition from 4% to 8% and from 8% to 12%. When all results were examined, it is seen that increasing $Ca(OH)_2$ addition improves static and dynamic stress (Zhang et al., 2019; Temuujin et al. 2009; Guo et al. 2010).

In addition to these interpretations, when the results of the structural breakdown area ratios were examined, it was observed that $Ca(OH)_2$ addition up to 8% increased the breakdown area ratio for mixtures activated with 10 M. Transition $Ca(OH)_2$ usage from 8% to 12%, breakdown area ratio was decreased, hence decrement in thixotropy performance. Thixotropy performance of samples were showed an alteration in

accordance with interpretation technics. Although, according to first technics, $Ca(OH)_2$ addition increase thixotropy continuously. After 8% $Ca(OH)_2$ usage, thixotropy performance of sample showed decrement according to second technics. To verify which technics results are more reliable, results will be compared in later section with other test methods.

Samples, which were activated with 12.5 M NaOH solution and four addition rates of $Ca(OH)_2$, were tested at four different preset shear rates. The data obtained from the tests are given in Figure 4.30 and Table 4.24.

Table 4.24. Initial and equilibrium stress values, structural breakdown area and its ratio, at 0.2, 0.3, 0.4 and 0.5 s^{-1} shear rate of D5, D6, D7 and D8 coded mixtures

Sample Code	Shear Stress (Pa)	Shear Rate (1/s)				Structural Breakdown Area	Structural Breakdown Area Ratio (%)
		0.2	0.3	0.4	0.5		
D5	Initial (static) stress	3034.2	2997.0	2402.7	1980.4	196.50	24.85
	Equilibrium (dynamic) stress	2563.5	2092.0	1764.0	1609.2		
D6	Initial (static) stress	5432.1	5218.5	3648.6	2887.6	389.70	29.91
	Equilibrium (dynamic) stress	4593.7	3342.4	2429.2	2124.0		
D7	Initial (static) stress	6168.7	6396.1	5085.6	4190.8	410.50	24.64
	Equilibrium (dynamic) stress	5473.2	4396.7	3724.4	3397.0		
D8	Initial (static) stress	7627.7	7129.5	5562.0	4659.8	426.60	22.65
	Equilibrium (dynamic) stress	6663.9	5181.9	4217.4	3675.1		

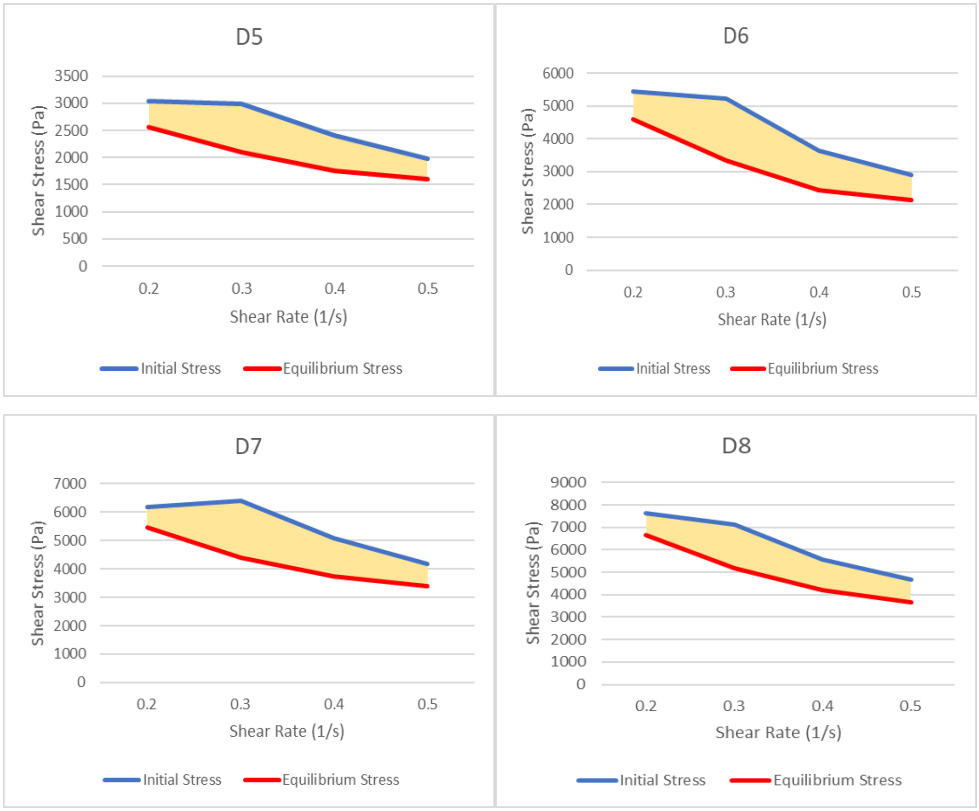

Figure 4.30. Initial and equilibrium stress values and structural breakdown area at 0.2, 0.3, 0.4 and 0.5 s^{-1} shear rate of D5, D6, D7 and D8 coded mixtures

As the content of $Ca(OH)_2$ increased, an increment in the initial and equilibrium stresses was observed in the mixtures prepared with 12.5 M, as in the 10 M activated mixtures. When the results of the structural breakdown area were examined, a decreasingly growing was observed. Especially in the transition from 0% to 4% $Ca(OH)_2$ addition rate, the structural breakdown area was increased dramatically and then the increment was decreased very rapidly. D6, D7 and D8 have very similar structural breakdown areas. Although $Ca(OH)_2$ addition increased the static and dynamic stress at this molarity, using $Ca(OH)_2$ above the 4% addition did not increase thixotropy much. In addition to these interpretations of thixotropy, when the results of the structural breakdown area ratios were examined, it was observed that only 4% $Ca(OH)_2$ addition had a positive effect on thixotropy. Remaining addition percentage affected thixotropy negatively.

Finally, the initial and equilibrium stresses depending on the shear rate of the material in increasing $Ca(OH)_2$ ratios with a constant 15M NaOH concentration were examined. D12 sample could not be tested because it exceeded the torque limit of the rheometer device. The data obtained as a result of the test are given in Figure 4.31 and Table 4.25.

Table 4.25. Initial and equilibrium stress values, structural breakdown area and its ratio, at 0.2, 0.3, 0.4 and 0.5 s^{-1} shear rate of D9, D10 and D11 coded mixtures

Sample Code	Shear Stress (Pa)	Shear Rate (1/s)				Structural Breakdown Area	Structural Breakdown Area Ratio (%)
		0.2	0.3	0.4	0.5		
D9	Initial (static) stress	5668.8	5708.2	4157.5	4112.7	482.70	32.71
	Equilibrium (dynamic) stress	4993.3	3588.9	2669.1	2349.0		
D10	Initial (static) stress	6855.2	7437.9	5975.5	4872.7	461.90	23.96
	Equilibrium (dynamic) stress	6593.0	5121.8	4279.1	3921.7		
D11	Initial (static) stress	10730.0	10014.0	8452.5	7274.5	653.30	23.78
	Equilibrium (dynamic) stress	9380.6	7108.2	6243.0	5787.8		

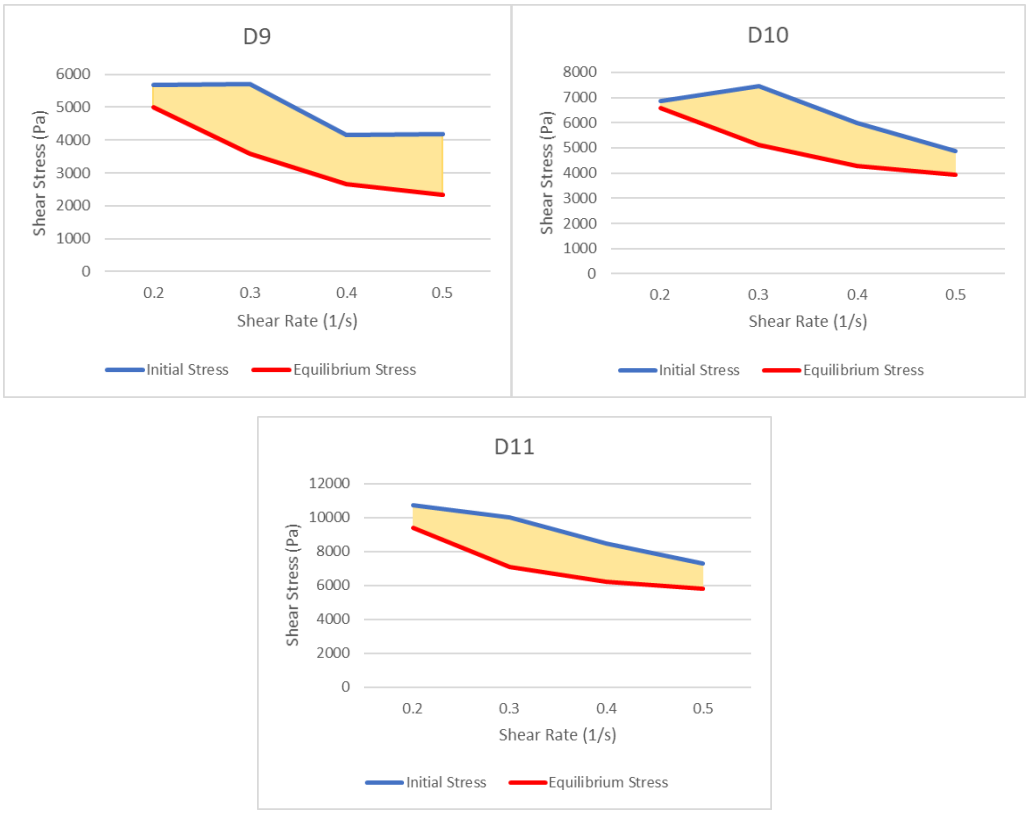

Figure 4.31. Initial and equilibrium stress and structural breakdown area at 0.2, 0.3, 0.4 and 0.5 s^{-1} shear rate of D9, D10 and D11 coded mixtures

With the augmenting usage of $Ca(OH)_2$, initial and equilibrium stress values increased as in other molarities. The logic behind these findings were already discussed in upper section, therefore, not discussed in here.

With the addition rate of 4% $Ca(OH)_2$, slightly decrement was observed in the areas of structural breakdown. However, utilization of %8 $CaOH_2$ showed increment in breakdown area. When breakdown area ratio results were examined, it was seen that $Ca(OH)_2$ usage had a negative effect on thixotropy for mixture prepared with 15 M solution, since breakdown ratio was suddenly decreased with %4 $Ca(OH)_2$ and was remain steady with the usage of %8 $Ca(OH)_2$. Since it is difficult to reach a general conclusion about thixotropy performance of mixtures based on the structural breakdown areas in this series, it was necessary to re-analyze the same samples based on the "Three Interval Thixotropy Test Method" results.

4.2.5. Three Interval Thixotropy Test Method - 3ITT

The rheological and thixotropy behavior of mortar mixtures with 0.39 w/b ratio was also examined by using this test method. The important point here was how much the material can recover its viscosity after being exposed to a high shear rate. The percentage of return/recover belonging each sample was examined while evaluating performance of mixtures. Also, how viscosity changes with activator usage was discussed under this title.

4.2.5.1. The Effect of NaOH Molarity on Rheology and Thixotropy

The results of the experiment belonging to the samples prepared with 10, 12.5 and 15 M NaOH solution are given in Figure 4.32. For better understanding of the plot, the final viscosities of the samples at initial, under shear and equilibrium are given in Table 4.26. In the light of the information obtained from the literature, the value to be looked at here, the relationship between the initial and equilibrium state (after shear force), they regard it as recovery. How much the material has recovered itself was determined by using the parameters that should be checked for interpretation of thixotropy.

According to these results, we can make an interpretation that as the amount of Sodium hydroxide increased (molarity), the recovery feature of the system increased. This could be explained in way that significant contributor to the increment in yield stress, which led

to higher initial stress value and therefore a higher thixotropy (Salem T.M., 2002). D1 showed a 65.00% recovery performance, while D5 and D9 showed slightly higher recovery performance, 71.10% and 75.44%, respectively. In addition to recovery performance, drop percentage in viscosity of the material with shear force were studied. Since the viscosities decreased too much under shear, the values were very close to each other, but while D1 and D5 showed a similar decrease performance, the decrease in D9 was a little less with a difference of 0.1%. In addition to all these, comments can be made regarding the consistency of the material as a result of this experiment. As can be seen, D9 has by far the highest viscosity both at the beginning and after shearing. As the molarity increased, the resistance of the material against flowing, viscosity, increased steadily (Memon et al., 2013b; Varaprasad et al., 2010; Li et al., 2013). This indicates that as the molarity increases, the consistency regularly becomes denser and solid.

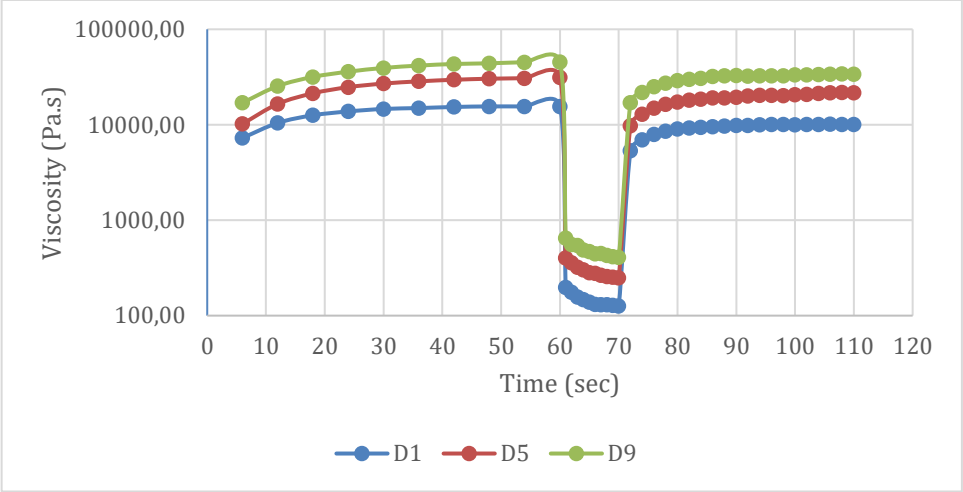

Figure 4.32. Three-Interval Thixotropy test results D1, D5 and D9 coded mixtures

Table 4.26. Viscosity values of D1, D5 and D9 coded mixtures at initial, shear and equilibrium state, and the drop and recovery performance regarding shear rate changes

Viscosity					
Sample Code	Initial (Pa.s)	Shear State (Pa.s)	Equilibrium State (Pa.s)	Drop %	Recover %
D1	15549	128.29	10107	99.17	65.00
D5	30750	252.76	21864	99.18	71.10
D9	45212	416.60	34110	99.08	75.44

4.2.5.2. Effect of $Ca(OH)_2$ Addition on Rheology and Thixotropy

For a more detailed examination, the impacts of $Ca(OH)_2$ addition on rheology and thixotropy at each molarity was examined one by one. The results of the experiment belonging to the samples initially activated with a 10 M NaOH solution are plot in Figure 4.33. For better understanding, the viscosities of the samples at initial, under shear and at equilibrium are given in Table 4.27.

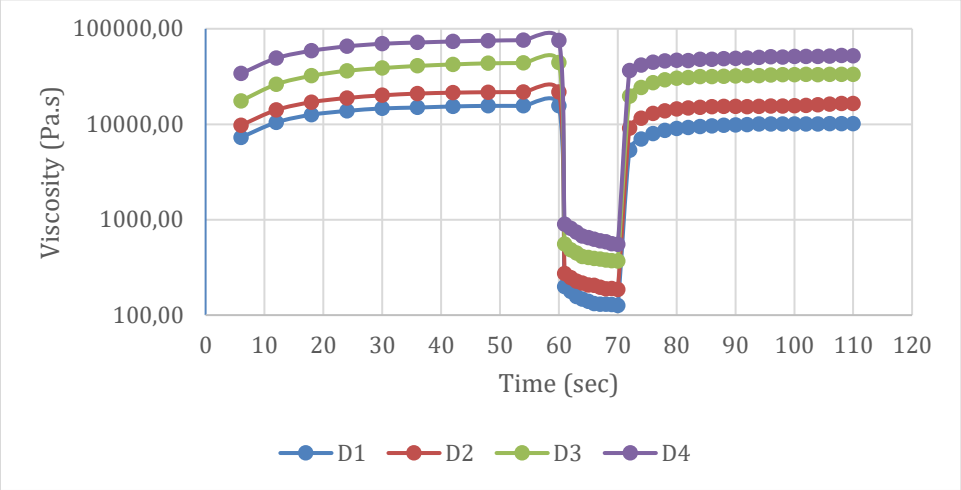

Figure 4.33. Three-Interval Thixotropy test results of D1, D2, D3 and D4 coded mixtures

Table 4.27. The viscosity values at the initial, shear and equilibrium state and the drop and recovery performances of the D1, D2, D3 and D4 coded mixtures

	Viscosity				
	Initial (Pa.s)	Shear State (Pa.s)	Equilibrium State (Pa.s)	Drop %	Recover %
D1	15549	128.29	10107	99.17	65.00
D2	21695	190.07	16442	99.12	75.79
D3	43774	371.76	33291	99.15	76.05
D4	75274	557.79	52490	99.26	69.73

When the results were examined, it was understood from the increasing viscosity values that as the amount of $Ca(OH)_2$ augmented, the materials turn into a more viscous form. Although the transition from D1 to D2 was not much compared to the others, when the amount of addition rate was 8% and 12%, the increase in viscosity was quite higher (Hardjito et al., 2008; Wattimena et al., 2017). This situation shows that as the content of $Ca(OH)_2$ augmented, the viscosity exhibited an increasing behavior. By considering recovery performances, $Ca(OH)_2$ addition dramatically increased recovery at once. D2 and D3 behave similarly, while D4 showed a decline in recovery performance, this could be explained in way that the overabundance lime will interrupt the optimal structure of

the geopolymer gel binder and inhibit the growth of strength (Khater, H. M., 2012). Similar recovery performance was observed in the mixtures using 4% and 8% $Ca(OH)_2$, and higher values were obtained than the mixture without $Ca(OH)_2$.

Samples coded as D5, D6, D7 and D8 prepared with 12.5 M NaOH solution were tested. The results of the experiment are given in Figure 4.34. For better understanding of the plot, the viscosities of the samples at initial, under shear and at equilibrium are given in Table 4.28.

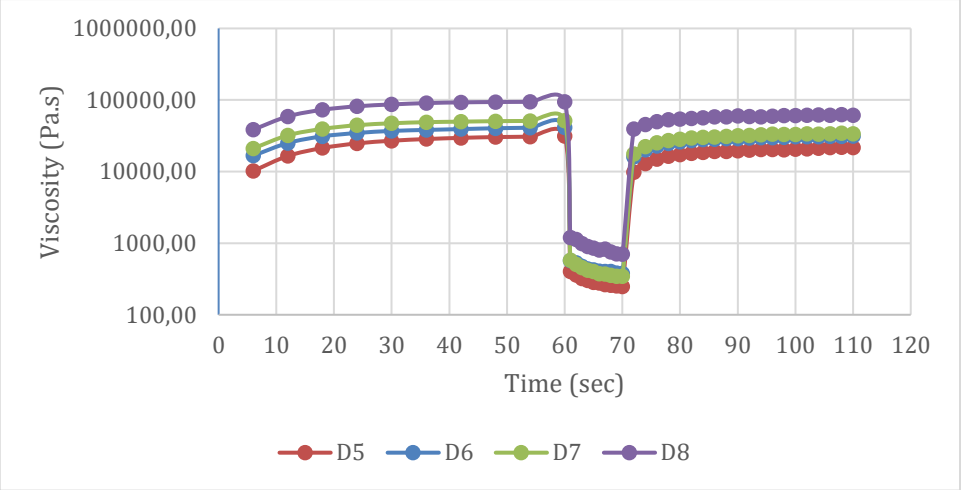

Figure 4.34. Three-Interval Thixotropy test results of D5, D6, D7 and D8 coded mixtures

Table 4.28. The viscosity values at the initial, shear and equilibrium state and the drop and recovery performances of the D5, D6, D7 and D8 coded mixtures

Viscosity					
Sample Code	Initial (Pa.s)	Shear State (Pa.s)	Equilibrium State (Pa.s)	Drop %	Recover %
D5	30750	252.76	21864	99.18	71.10
D6	40983	383.43	31018	99.06	75.69
D7	50959	346.44	34414	99.32	67.53
D8	94015	713.39	62549	99.24	66.53

When the results were examined, the viscosity increased as the content of $Ca(OH)_2$ enhanced, as in 10M (Granizo et al., 2004). This increase in viscosity continued linearly up to 8%, yet viscosity dramatically increased transition from 8% to 12% addition rate of $Ca(OH)_2$. Regarding the recovery performance, although 4% $Ca(OH)_2$ addition improved thixotropy performance, 8% and 12% $Ca(OH)_2$ addition negatively affected thixotropy performance of mixtures activated with 12.5 M NaOH.

Finally, samples encoded with the D9, D10, D11 and D12 activated with 15 M NaOH were tested. The results of the experiment are given in Figure 4.35. For better understanding of the plot, the viscosity of the samples at initial, under shear and equilibrium are given in Table 4.29.

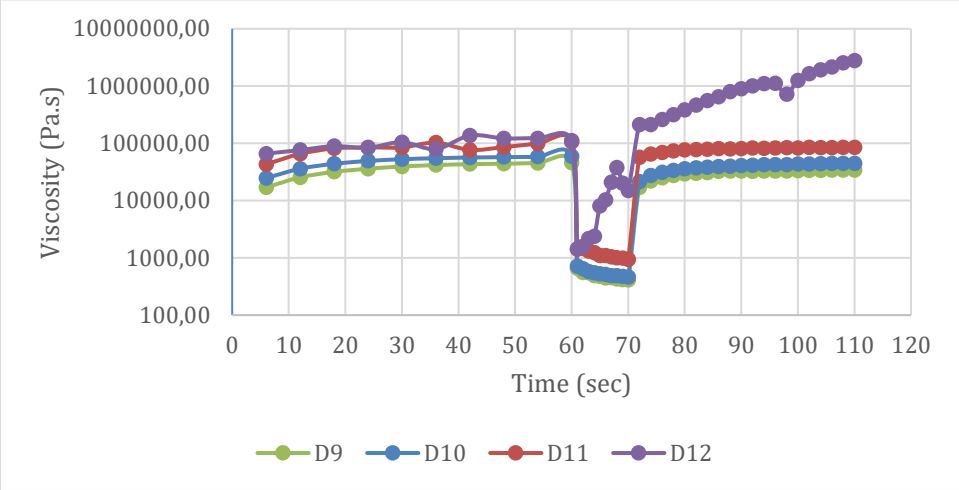

Figure 4.35. Three-Interval Thixotropy test results of D9, D10, D11 and D12 coded mixtures

Table 4.29. The viscosity values at the initial, shear and equilibrium state and the drop and recovery performances of the D9, D10, D11 and D12 coded mixtures

Viscosity					
Sample Code	Initial (Pa.s)	Shear State (Pa.s)	Equilibrium State (Pa.s)	Drop %	Recover %
D9	45212	416.60	34110	99.08	75.44
D10	58066	475.30	44560	99.18	76.74
D11	98644	983.76	80868	99.00	81.98
D12	122120	-	-	-	-

Although the viscosity value can be recorded at the beginning for the D12 coded mixture, as it can be seen from the graph, a meaningful result could not be obtained during test period because it exceeded the torque capacity values of the device when exposed to high shear rate. When the initial viscosity values were examined, a high increase was observed as the content of $Ca(OH)_2$ augmented, as in other molarities. Especially in the transition from 4% to 8% and from 8% to 12%, a very high viscosity increase was observed. When subjected to high shear stress, the drops were higher in the D10 sample than in the others.

When thixotropy performance was examined, as the $Ca(OH)_2$ addition ratio increased, an increasing recovery performance was obtained. The D11 has showed the highest performance among the samples tested so far.

In general, at low molarity (10 M), 4% and 8% performed well, while only 4% $Ca(OH)_2$ addition at 12.5 M increases thixotropy, at high molarity (15 M), 8% Ca $(OH)_2$ addition performed better in terms of recovery performance. In addition, with the enhancing amount of $Ca(OH)_2$ in all molarities, the viscosity values in the first case increased, but the most significant increases were always experienced at the transition between 8% and 12%. If there was a general comment; for binary uses, the influence of the $Ca(OH)_2$ utilization on rheological performance has been to increase continuously viscosity, but not valid for thixotropy.

4.2.6. Open Time Performance of Three Interval Thixotropy Method

Open Time performance of mixtures in terms of thixotropy behavior were tested at 30^{th}, 60^{th} and 90^{th} minutes with 3ITT method. Results are represented in the Table 4.30.

Table 4.30. Open Time Thixotropy Performance of mixtures

Mixture Code	Recover Performance (%)			
	Initial	30 min	60 min	90 min
D1	65.00	61.66	63.20	60.43
D2	75.79	75.24	78.65	66.79
D3	76.05	77.35	72.85	65.04
D4	69.73	68.55	68.41	61.36
D5	71.10	70.96	66.03	68.21
D6	75.69	76.45	77.15	78.69
D7	67.53	61.24	X	X
D8	66.53	X	X	X
D9	75.44	66.65	X	X
D10	76.74	X	X	X
D11	81.98	X	X	X
D12	X	X	X	X

In general, except D6 coded sample, with passing time, thixotropy performance of materials started to decrease, especially transition of 60 to 90 minutes for the mixture activated with lower molarity (Zhang et al., 2019). However, for the sample prepared with higher concentration, this decrement on thixotropy performance was observed at transition from 0 to 30 minutes (Görhan and Kürklü, 2014). This decrement could be explained in a way that materials losing its elastic behavior and could not get back its initial shape after the deformation load. The reason why higher molarity shows sudden losing in thixotropy performance could be attached to fast setting performance as a result of high alkalinity (Görhan and Kürklü, 2014). It could be concluded that, materials activated with lower molarity show high performance in terms of thixotropy for at least 60 minutes. However, this was not valid for the materials activated with high concentration as a result of rapid setting behavior. When the influence of $Ca(OH)_2$ usage on open performance thixotropy behavior was examined, it was observed that $Ca(OH)_2$ usage was decreased thixotropy performance with passing time since it accelerates the geopolymerization reaction and so makes matrix more rigid in a short time (Davidovits, 2015; Leong et al., 2016; Temuujin et al. 2009; Guo et al. 2010; Khater, H. M., 2012).

4.3. Rheometer Test Results of CDW and Different Mineral Additive based Geopolymer

In the light of results obtained from section 4.2 (mortar mixture design), rheometer test was conducted on selected mixtures prepared with CDW and different mineral additive. While selecting mixtures, it was considered that high buildability performance (>4), low vane shear results (<3-4), proper flowability index (>1) and high mechanical performance. During selecting mixtures, it was aimed to reach feasibility of geopolymer on general usage considering high workability, wide open time for processing, high mechanical performance, low yield point to flow materials. In that context, A23, A26, A28, P6, P11, P15 and P21 coded sample (defined in section 4.2) was selected. In that section, the aim was not to investigate effects of each pozzolan addition on rheological performance, instead, it was aimed to demonstrate selected materials' rheological performance measured by rheometer. So, for detailed information about effects of pozzolan addition on rheological performance measured by rheometer, another study should be conducted. To performed test, selected samples were prepared with 0.39 w/b ratio due to concerns previously described.

4.3.1. Up and Down Test Method

Results of selected sample tested on Up and Down method with an open time are given in the Table 4.31. In general, for each mixture, pre-loading shear value increased with passing time, although, yield stress value did not increase regularly. As explained before, pseudo setting was observed on geopolymer and increment in preloading was interpreted to this pseudo setting also, such increment could be attributed to load history of geopolymer occurred during loading of mixture to the cup. When yield stress values of mixtures were examined, it could be concluded that except to A28 and P6, each mixture was workable even after 60 minutes from preparation. In general, it could be concluded that there has not been observed significant increase on yield stress between 0 to 60 minutes except A28 and P6 coded sample. Especially, P15 and P21 coded samples showed better performance on open time in terms of lower increment, and also these sample showed lower pre-loading shear stress value with passing time.

Table 4.31. Up-Down test results of selected mixtures prepared with CDW and different mineral additives

Sample Code	Open Time (min)	Pre-Loading Maximum Shear Stress Value (Pa)	Bingham Yield Stress Value (Pa)
A23	0	5540.60	942.86
	20	5023.30	936.32
	40	5088.00	1012.70
	60	5457.40	1128.20
A26	0	3813.60	855.08
	20	8097.20	1013.40
	40	10731.00	1017.60
	60	8976.50	962.00
A28	0	7804.50	1152.40
	20	18525.00	1346.40
	40	18770.00	X
	60	X	X
P6	0	5145.40	1244.30
	20	13591.00	1505.40
	40	15801.00	1411.20
	60	18770.00	X
P11	0	4241.60	1342.20

	20	5732.60	1307.50
	40	9817.40	1351.02
	60	15125.00	1329.20
P15	0	2614.80	878.56
	20	2613.40	916.68
	40	3633.20	920.74
	60	3336.10	890.25
P21	0	3014.70	966.59
	20	3693.30	1012.40
	40	3799.30	1014.10
	60	3045.40	998.03

4.3.2. Constant Shear Rate Test Method

Results of selected samples tested on Constant Shear Rate method are given in the Table 4.32. When yield value (static stress) and constant region (dynamic stress) were examined, it was observed that, A28 and P6 showed higher stress and torque value than remaining mixtures which means that they would require more energy/force to yield that was not preferable in most case since in such case energy consumption could be increased. Especially, A23, P15 and P21 coded samples show lower viscosity to flow under shear rate which could provide benefit for several application. Although, thixotropy performance could not obtained from this test methods directly, by using drop percentage (as explained before), it could be concluded that, A28, P15 and P21 showed higher thixotropy performance.

Table 4.32. Constant Shear Rate test results of selected mixtures prepared with CDW and different mineral additives

Torque (mN.m)			Shear Stress (Pa)		Drop %
Sample Code	Yield Value (Static)	Constant Region (Dynamic)	Yield Value (Static)	Constant Region (Dynamic)	
A23	36.97	24.80	3469.20	2327.20	32.92
A26	60.62	47.16	5689.00	4426.37	22.19
A28	177.26	106.12	16636.00	9959.43	40.13
P6	117.02	83.56	10982.00	7842.27	28.59
P11	78.24	54.59	7342.50	5123.40	30.22
P15	28.70	11.17	2693.50	1611.53	40.17
P21	37.70	23.42	3537.90	2198.27	37.87

4.3.3. Various Constant Shear Rate Test Method

Results of selected mixtures tested on Various Constant Shear Rate method are given in the Table 4.33. According to results, A28 and P6 showed higher shear stress during both initial and equilibrium region on each given shear rate, while P15 and P21 showed lower shear stress during both initial and equilibrium region. To analyze thixotropy performance of samples by using obtained data, structural breakdown area and its ratio to overall area were used. For the first technics (structural breakdown area), A28 and P6 showed higher performance as the breakdown areas were higher, however, P15 and P21 showed lower performance. For the second technics, while A26 showed highest thixotropic performance, P15 and P21 showed lowest thixotropic performance as in the first technics.

Table 4.33. Various Constant Shear Rate test results of selected mixtures prepared with CDW and different mineral additives

Sample Code	Shear Stress (Pa)	Shear Rate (1/s)				Structural Breakdown Area	Structural Breakdown Area Ratio (%)
		0.2	0.3	0.4	0.5		
A23	Initial (static) stress	4576.6	4029.6	2862.5	2482.6	246.50	23.65
	Equilibrium (dynamic) stress	3932.1	2671.8	2301.8	2034.7		
A26	Initial (static) stress	4011.4	4264.0	2859.6	2213.9	319.20	31.18
	Equilibrium (dynamic) stress	3511.2	2522.5	1899.8	1733.1		
A28	Initial (static) stress	11790.0	11929.0	9780.9	7579.2	838.10	26.69
	Equilibrium (dynamic) stress	10960.0	8229.7	6641.6	5324.9		
P6	Initial (static) stress	7759.9	8572.8	7674	6161.8	518.10	22.33
	Equilibrium (dynamic) stress	7420.8	6606.1	5303.9	4811.6		
P11	Initial (static) stress	3699.5	4056.6	3074.9	2663.7	248.40	24.08
	Equilibrium (dynamic) stress	3450.5	2703.7	2348.1	2105.1		
P15	Initial (static)	2690.2	2797.5	2395.7	2107.7	124.90	16.45

	stress						
	Equilibrium (dynamic) Stress	2561.8	2204.4	1983.7	1748.6		
P21	Initial (static) stress	2638.9	2536.2	2057.9	1820.2	115.00	16.85
	Equilibrium (dynamic) stress	2373.3	1925.7	1760.3	1602.5		

4.3.4. Three Interval Thixotropy Test Method - 3ITT

Results of selected mixtures tested on 3ITT method with an open time are given in the Table 4.34. According to results, A23, A28, P15 and P21 showed higher thixotropic performance at the initial time. However, A28 could not give a thixotropic performance at 30 min test time. This could be attributed to fast geopolymerization reaction process since during geopolymerization, matrix started to lose its plasticity and gets harden which means thixotropic ability of matrix started to be destroyed. At 60 min test time, P6 also did not give recovery performance. For the 90 min, A26 and P11 did not show recovery performance. In general aspect, A23 and P21 showed similar performance during the open time, and did not showed thixotropy reduction over time, although remaining mixtures showed reduction in terms of thixotropy performance.

Table 4.34. Open-time 3ITT test results of selected mixtures prepared with CDW and different mineral additives

Viscosity				
Sample Code	Recovery Performance (%)			
	Initial	30 min	60 min	90 min
A23	73.44	71.95	78.65	79.50
A26	68.25	62.45	60.24	-
A28	72.15	-	-	-
P6	68.39	66.07	-	-
P11	66.75	59.30	57.24	-
P15	73.45	72.89	71.29	69.35
P21	76.80	73.50	75.91	77.55

4.4. Empirical Test and Rheometer

Within the scope of thesis, empirical tests such as flow table, buildability and vane shear test and rheometer test methods such as Up and Down Curve, Constant Shear Rate,

Various Constant Shear Rate, Three Interval Thixotropy test methods, were conducted to analyze effects of activator type, rate and combination on rheological and workability performance of geopolymer mortar.

When the empirical test results were examined, it was observed that the shear vane experiment was related with static yield stress, the flow table experiment was associated with dynamic yield stress, and in the buildability test, it was associated with static yield stress. Although quite important data about consistency and workability were obtained with empirical experiments, it was insufficient to obtain information about thixotropy directly.

The results showed that the small changes in the results obtained from empirical experiments actually corresponded to a rather large increase or decrease in the shear stress (yield point) of the mixtures measured by the rheometer. However, empirical experiments have generally been successful at catching the trend at low molarities (10-12.5 M). But when the molarity was 15 M, the flow table test method was somewhat incapable of interpreting the situation. However, even at high molarity, buildability and vane shear test yielded better results. To summarize briefly, although the empirical results at low molarities give a general information about the consistency and workability of the material, it is useful to use a rheometer for more detailed results. However, at high molarity, measuring the material with a rheometer rather than empirical experiments gave more meaningful and interpretable results, as the material turned into a more sticky form. In addition, empirical results were insufficient to understand thixotropic behavior.

4.4.1. Thixotropy Assessment from Empirical Test Results

Since empirical test could not give a detailed and precise information about thixotropy performance of materials, correlation between flowability, buildability and vane shear stress with rheometer data was made. When all data obtained from the empirical test methods were plotted in a graph as Figure 4.36, the accurate region for high thixotropy performance ability was determined by limiting test results. During limiting test results, high buildability values were preferred since it represented static yield stress of materials, adequate range of vane shear stress value were preferred as it demonstrate lowest required load to flow materials, and high flowability value were preferred since it represent dynamic shear yield stress value. Because, whenever the difference between static and

dynamic shear stress increased, it could be interpreted as high thixotropy performance, as explained in the rheometer test methods. So, by considering these parameters, the first region was drawn. In that region which represent high thixotropy performance, A1-A6-A9-A13 coded samples (defined in Section 4.2) were recorded. It has been observed that recipes with the same formula as these mixtures but with a w/b ratio of 0.39 performed high thixotropy performance in their rheometer tests.

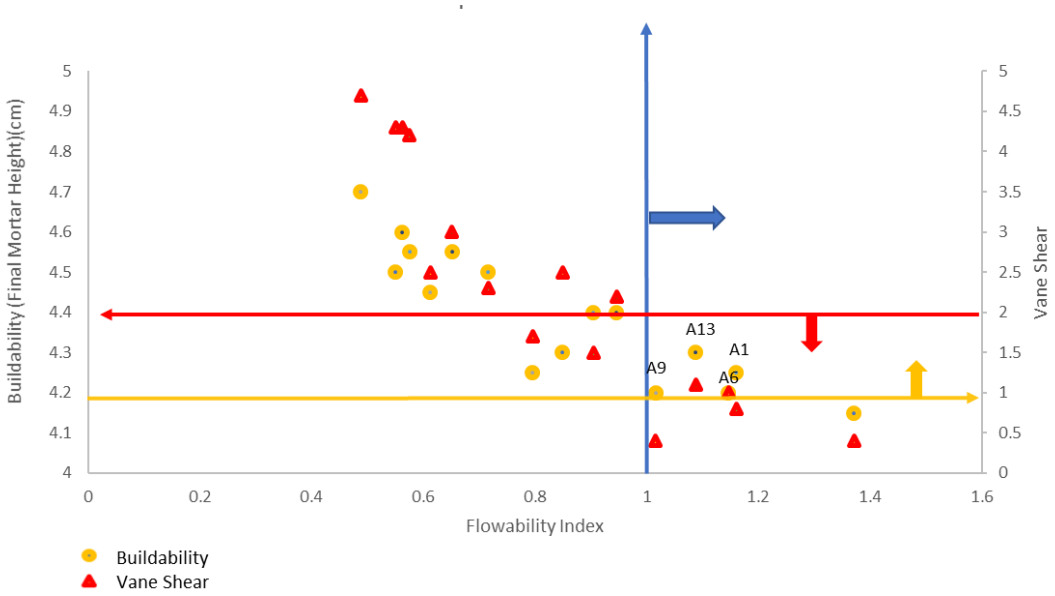

Figure 4.36. Adjusted Zone for High Thixotropy Performance (mixtures defined in Section 4.2)

However, there were some other samples that showed high thixotropy performance as these listed materials in rheometer test. Therefore, to find out general region for high thixotropy performance ability of samples, these regions was enlarged as in the Figure 4.37. In the enlarged region, in addition to A1-A6-A9-A13, A2-A7-A10-A14 coded samples (defined in Section 4.2) were recorded. It has been observed that recipes with the same formula as these mixtures but with a w/b ratio of 0.39 performed high thixotropy performance in their rheometer tests. These adjusted zones included almost each mixture that has high thixotropy performance determined in 3ITT test method conducted on rheometer. So, for the CDW based geopolymer, by using the empirical test method conducted in this study, it was possible to make a comment on thixotropy performance of mixtures if results obtained from empirical test methods standardize with rheometer. To do that, test results should be analyzed by limiting flowability index value higher than

0.8, vane shear indicator value lower than 3, and buildability value higher than 4.2 as shown in the Figure 4.37.

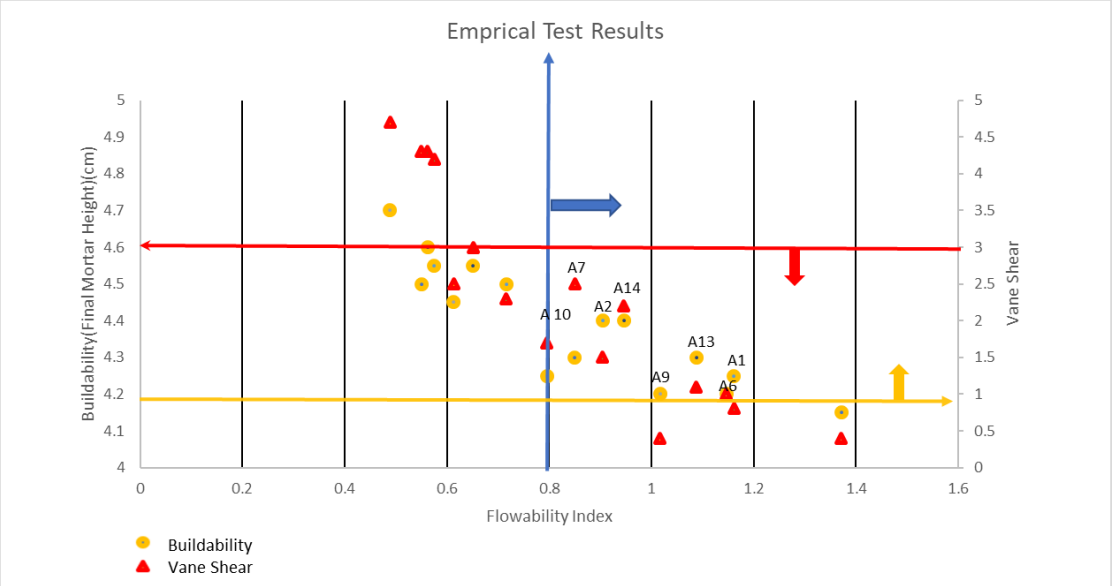

Figure 4.37. Ultimate Adjusted Zone for High Thixotropy Performance (mixtures defined in Section 4.2)

Specified zone was created as result of interpretation of data by comparing empirical and rheometer equipment test results. By using adjusted limitation criteria, materials having a high thixotropic performance could be determined with accurately was not possible for the each geopolymer matrix that were prepared with various type of activators and binders. After testing and analyzing matrix via both empirical test methods and rheometer, and interpreting obtained data, this zone could be created and utilized for the mix design according to desired application, but content of binders and used activator types should be similar to tested materials.

4.5. Comparison of Rheometer Test Methods

By using rheometer, four different test methods were conducted as defined in section 4.3 on mixtures prepared with %100 CDW based materials to analyze the rheological and thixotropic properties of mixtures. Each method had a unique working principle that's why obtained results values were different than each other.

4.5.1. Consistency and Workability Aspect

Results obtained from four different test methods were analyzed and it could be concluded that, similar trend was observed in each test method in terms of rheological properties especially for yield stress. In general, it was observed that, as molarity increased gradually from 10 M to 15 M, static and dynamic shear stress value increased for each test methods. For the $Ca(OH)_2$ addition on mixtures prepared with 10, 12.5 and 15 M NaOH solution, in each increment on usage amount, shear stress values increased for each test methods.

4.5.2. Thixotropy Performance Aspect

To measure thixotropy performance of mixtures, 3ITT test method was used primarily as the main objective of this test method was focusing thixotropy performance assessment. However, by interpreting of data obtained from Constant Shear Rate and Various Constant Shear Rate method, thixotropy performance of mixtures were analyzed. During interpreting the data obtained from various constant shear rate test method, 2 technics were used as explained in the section 4.3.4. Results obtained from the test methods to interpret thixotropy are represented in the Table 4.35.

Table 4.35. Results of three different test methods (four interpretation methods) for interpretation of thixotropic performance of mixture

Sample Code	Constant Shear Rate	Various Constant Shear Rate		3ITT
	Drop % (Method 1)	Structural Breakdown Area (Method 2)	Structural Breakdown Area Ratio (%) (Method 3)	Recovery (%) (Method 4)
D1	33.49	69.30	18.55	65.00
D2	45.80	106.40	21.79	75.79
D3	41.94	219.80	25.24	76.05
D4	51.26	354.04	20.53	69.73
D5	27.38	196.50	24.85	71.10
D6	40.82	389.70	29.91	75.69
D7	45.37	410.50	24.64	67.53
D8	44.66	426.60	22.65	66.53
D9	35.62	482.70	32.71	75.44

D10	22.19	461.90	23.96	76.74
D11	-	653.34	23.78	86.49
D12	42.78	-	-	-

To understand the influence of NaOH activator on the thixotropy performance, first, D1, D5 and D9 coded specimens were compared. According to results, Method 2,3 and 4 gave the similar trend to each other, although method 1 showed different trend. To examine effects of $Ca(OH)_2$ addition on thixotropy, D1-D2-D3-D4 coded samples prepared with 10M NaOH and 0%,4%,8% and 12% $Ca(OH)_2$ were examined. Results showed that although method 1 and 2 gave incoherent information, method 3 and 4 gave similar increase/decrease trend in terms of thixotropy performance. When D5-D6-D7-D8 coded samples prepared with 12.5 M examined, as 10 M activated samples, Method 3 and 4 gave similar results. As a final, D9-D10-D11 and D12 coded samples were analyzed, but there has not been observed similarity between samples increase/decrease trend in terms of thixotropy performance. This could be attributed to mixture consistence since samples prepared with 15 M NaOH solution showed high viscosity which could hinder precise data to interpret. In general, it could be concluded that method 3 and 4 showed similar results in terms of thixotropy performance assessment. Since, primary target of methods of 1, 2 and 3 were not to measure thixotropy performance of materials directly, interpretation of data and used method could be reason of various findings regarding thixotropy. However, primary aim of 3ITT test method was to understand thixotropic performance of mixture, that's why this method was preferred to analyze thixotropic performance of mixtures in this thesis study.

5. CONCLUSION

Within the scope of the thesis study, it was aimed to analyze effects of activators type, usage rates and combinations on rheological and workability performance of CDW based geopolymer matrix composed of RT, HB, RCB, CW and GW. In the study, feasibility of application of CDW based geopolymer in the various application area was considered, hence know-how about rheological and workability performance of CDW based geopolymer was created as well as mechanical performance. Thus, influences of activators on performance of CDW based geopolymer matrix could be known and according to requirement of application, activators selection could be possible by using results of the thesis study. According to results of experimental researches predefined in upper section, following outcomes have been obtained;

- For mortar phase, recycled aggregate was used as filler materials with a maximum size of 2 mm. According to empirical test methods, molarity of NaOH from 7.5M to 10M, flowability was increased, buildability and vane shear stress values were decreased. Although, afterwards, buildability and vane shear values continued to increase with small deviation as molarity increase, flowability values decreased first then increased. Influence of $Ca(OH)_2$ addition was investigated and results showed that flowability started to decrease, buildability and vane shear stress results started to increase as Ca(OH)2 addition rate to mixtures in which NaOH was also utilized as an activator, was increased. Only mixtures activated with 10M NaOH were showed 2 hours workable time, remaining mixtures were lost their workability and harden at the end of 1 hour resting time. The highest compressive strength of mixtures that was activated binary usage of NaOH and $Ca(OH)_2$ was 17.9 MPa. Effects of w/b ratio was also investigated, results showed that, as ratio increase, flowability was increased, buildability and vane shear stress were decreased. Also, compressive strength was decreased as in the OPC based mortar. Influence of Na_2SiO_3 was also investigated and results showed that increment in flowability, decrement in buildability, vane shear yield stress and workable time. However, compressive strength was enhanced and reached 35.8 MPa at the end of 28-day. Effect of w/b ratio also investigated, but, similar results were observed. 20% substitution of BFS was also investigated in terms of both rheological and mechanical aspects. BFS addition was found to favorable in terms of both aspects.

Since, it increased the flowability and workable time and compressive strength. Maximum compressive strength was reached with 20% substitution of BFS activated with binary usage of NaOH and $Ca(OH)_2$ was 25.8 MPa at 28-day ambient curing. Effect of w/b ratio also investigated, but, similar results were observed. Influence of Na_2SiO_3 was investigated in that matrix and results showed that Na_2SiO_3 increased flowability, however, decreased buildability, vane shear stress and workable time dramatically. In terms of strength development, Na_2SiO_3 was pronounced since it increased compressive strength and maximum value was reached as 42.8 MPa. Afterwards, combination of BFS, FA, and SF were investigated. Each mineral additive was found as favorable regarding rheological performance. Since they increased flowability and open time performance of mixtures. Also, adequate buildability performance and vane shear stress values were obtained. The maximum compressive strength value of 34.7 MPa was reached with the combination of 5%BFS +10%SF +5%FA mineral additives activated with 10M NaOH and %8 $Ca(OH)_2$ addition rate. Effects of w/b ratio was also investigated, but similar outcomes were recorded.

- In the scope of thesis study, to investigate rheological performance of CDW based geopolymer, 4 different test methods were conducted by using the rheometer in addition to empirical test methods. Results obtained from the 4 test methods showed that as molarity increased from 10M to 15M, viscosity and yield stress of mixtures were decreased gradually. For the addition of $Ca(OH)_2$, results showed that mixtures become more viscous as addition rate was increased, yet, influence of addition rate was changed regarding with NaOH molarity. Also, thixotropy performance of mixtures were investigated, and it was found that as molarity increased thixotropy performance of mixture was improved. Also, it was found that addition of 4% and 8% $Ca(OH)_2$ was favorable regarding increment in thixotropy performance of mixtures. In addition to 100% CDW based geopolymer, selected mixtures from the CDW and mineral additive used geopolymer matrix were subjected to these test methods. Results showed that A23 and P21 coded mixtures were found to be more favorable in terms of having high thixotropy, although P15 and P21 coded mixtures showed lowest viscosity and yield stress value and better open time performance according to test results.
- Empirical test results and rheometer test results were compared. Results showed that although flow table test method gave different results than rheometer in a case

of alkalinity changes, buildability and vane shear test results were compatible with rheometer results. Since, thixotropy measurement with empirical test methods were not conducted, to identify high thixotropy performance by using empirical test results, thixotropy zone was developed by using rheometer test data and limiting empirical test results. The zone was covered the mixtures that showed high thixotropy performance in rheometer measurement.

- With the increment in usage of CDW based geopolymer in order to make world green again by using waste materials as raw materials in concrete technology, knowledge about rheology of geopolymer will be become more essential for different advanced construction application such as self-leveling, shotcrete, 3D additive manufacturing, isolation application etc. Therefore, to apply geopolymer in a work area as wide as concrete, rheology of geopolymer must be known down to the last detail. By enlarging application area of CDW based geopolymer by means of enhancing its properties with the knowledge of its rheological and mechanic properties in details, requirement for new landfill area, contamination of earth and groundwater resource, CO_2 emission, hazardous dust and greenhouse gasses will be reduced. Therefore, in that thesis, investigation about workability and rheological properties of CDW-based geopolymer systems together with mechanical properties are addressed.

REFERENCES

Aboulayt, A., Riahi, M., Anis, S., Ouazzani T. M., and Moussa, R. (**2014**). "Rheological behavior of a fresh geopolymer based on metakaolin: effect of the introduction of calcium carbonate," International Journal of Innovation and Applied Studies, vol. 7, no. 3, pp. 1170–1177.

ACI 233R-95. (**1996**) Ground granulated blast-furnace slag as a cementitious constituent in concrete. ACI manual of concrete practice. Part 1. Materials and general properties of concrete. American Concrete Institute;.

ACI Committee 226 (**1987**) Ground granulated blast-furnace slag as a cementitious constituent in concrete. ACI Materials Journal, 84, 327–342.

Adam, A. & Maricar, S. & Ramadhan, B. (**2019**). The Effects of Water to Solid Ratio, Activator to Binder Ratio, and Lime Proportion on the Compressive Strength of Ambient-Cured Geopolymer Concrete. 10.22146/jcef.43878.

Ahmari, S., Ren, X., Toufigh, V. and Zhang, L. (**2012**). 'Production of geopolymeric binder from blended waste concrete powder and fly ash', Const Build Mater 35, 718–729.

Aiello R, Crea F, Nastro A, Subotic´ B, Testa F. (**1991**). Influence of cations on the physicochemical and structural properties of aluminosilicate gel precursors. Part 1. Chemical and thermal properties, Zeolites, Volume 11, Issue 8, Pages 767-775, ISSN 0144-2449, https://doi.org/10.1016/S0144-2449(05)80054-5.

Aïtcin, P. (**2000**). Cements of yesterday and today. Cement and Concrete Research, 30(9), 1349-1359. doi:10.1016/s0008-8846(00)00365-3

Aitcin, P. C., Lachemi, M., Adeline, R., and Richard, P. (**1998**) "The Sherbrooke reactive powder concrete dootbridge," Structural Engineering International 8(2), 140–144.

Al Bakri, A.M., et al. (**2012**), Effect of Na2SiO3/NaOH ratios and NaOH molarities on compressive strength of fly-ash-based geopolymer. ACI Materials Journal,. 109(5): p. 503-508.

Alfani, R., & Guerrini, G. L. (**2005**). Rheological test methods for the characterization of extrudable cement-based materials - A review. Materials and Structures, 38(276), 239-247. doi:10.1617/14191

Aliabdo, A. A., Abd Elmoaty, A. E. M., & Salem, H. A. (**2016**). Effect of water addition, plasticizer and alkaline solution constitution on fly ash based geopolymer concrete

performance. Construction and Building Materials, 121, 694–703. doi:10.1016/j.conbuildmat.2016.06.062

Allahverdi, A. & Najafi, E. (**2009**). Construction Wastes as Raw Materials for Geopolymer Binders. International Journal of Civil Engineering. 7. 154-160.

Allahverdi, A. L. I., Kani, E. N., & Yazdanipour, M. (**2011**). Effects of blast-furnace slag on natural pozzolan-based geopolymer cement. Ceramics-Silikáty, 55(1), 68-78.

Allahverdi, A., & Kani, E. (**2013**). Use of construction and demolition waste (CDW) for alkali-activated or geopolymer cements. Handbook Of Recycled Concrete And Demolition Waste, 439-475. doi: 10.1533/9780857096906.3.439

Angulo-Ramírez, D. E., Gutiérrez, R. M., & Puertas, F. (**2017**). Alkali-activated Portland blast-furnace slag cement: Mechanical properties and hydration. Construction and Building Materials, 140, 119-128. doi:10.1016/j.conbuildmat.2017.02.092

Anton Paar Wiki,. Flow curve and yield point determination with rotational viscometry Retrieved September 23, **2020**, from https://wiki.anton-paar.com/tr-tr/rotasyonel-viskozimetri-ile-akis-egrisi-ve-akma-noktasinin-belirlenmesi/

Atiş, C.D. (**1997**). Design and Properties of High Volume Fly Ash Concrete for Pavements. The University of Leeds, PhD. Thesis, Leeds, U.K., 342p.

Aydın, S., & Baradan, B. (**2014**). Effect of activator type and content on properties of alkali-activated slag mortars. Composites Part B: Engineering, 57, 166-172. doi:10.1016/j.compositesb.2013.10.001

Badogiannis, E., Kakali, G. and Tsivilis, S. (**2005**) Metakaolin as supplementary cementitious material. Optimization of kaolin to metakaolin conversion. Journal of Thermal Analysis and Calorimetry, 81, 457–462. doi: 10.1007/s10973-005-0806-3.

Bahr, B. V., Hanssen, O., Vold, M., Pott, G., Stoltenberg-Hansson, E., & Steen, B. (**2003**). Experiences of environmental performance evaluation in the cement industry. Data quality of environmental performance indicators as a limiting factor for Benchmarking and Rating. Journal of Cleaner Production, 11(7), 713-725. doi:10.1016/s0959-6526(02)00126-9

Bakharev, T., Sanjayan, J. G., & Cheng, Y. (**1999**). Alkali activation of Australian slag cements. Cement and Concrete Research, 29(1), 113-120. doi:10.1016/s0008-8846(98)00170-7

Bakharev, T., Sanjayan, J., & Cheng, Y. (**2001**). Resistance of alkali-activated slag concrete to carbonation. Cement and Concrete Research, 31(9), 1277-1283. doi:10.1016/s0008-8846(01)00574-9

Bakri AMMA, Kareem OAKAA, Myint S. (**2009**). Study on the Effect of Alkaline Activators Ratio in Preparation of Fly Ash-based Geopolymer. Malaysia: University Malaysia Perlis (UniMAP);.

Bao Y, Grutzeck MW, Jantzen CM (**2005**) J Am Ceram Soc 88:3287

Barbosa VFF, MacKenzie KJD, Thaumaturgo C. (**2000**). Synthesis and characterisation of materials based on inorganic polymers of alumina and silica: sodium polysialate polymers. Int J Inorg Mater.2:309–17.

Barnes H. A. (**1997**). Thixotropy-a review. Journal of Non-Newtonian Fluid Mechanics, Vol. 70, pp. 1–33.

Barnes H.A. (**1995**). review of the slip (wall depletion) of polymer solutions, emulsions and particle suspensions in viscometer: its causes, character, and cure J Non-Newton Fluid Mech, 56, pp. 221-251

Ben Haha, M., Lothenbach, B., Le Saout, G., Winnefeld, F. (**2011**). Influence of slag chemistry on the hydration of alkali-activated blast-furnace slag – Part I: effect of MgO. Cem. Concr. Res. 41 (9), 955–963.

Ben Haha, M., Lothenbach, B., Le Saout, G., Winnefeld, F. (**2012**) Influence of slag chemistry on the hydration of alkali-activated blast-furnace slag – Part II: effect of Al 2 O 3 . Cem. Concr. Res. 42 (1), 74–83.

Bernal, S. A., Rodríguez, E. D., de Gutiérrez, R. M., Gordillo, M., & Provis, J. L. (**2011**). Mechanical and thermal characterisation of geopolymers based on silicate-activated metakaolin/slag blends. Journal of materials science, 46(16), 5477-5486.

Bernal, S.A., Provis, J.L., Walkley, B., San Nicolas, R., Gehman, J.D., Brice, D.G., Kilcullen, A., Duxson, P., van Deventer, J.S.J. (**2013**). Gel nanostructure in alkali-activated binders based on slag and fl y ash, and effects of accelerated carbonation. Cem. Concr. Res. 53 , 127–144. doi: 10.1016/j.cemconres.2013.06.007

Bhavsar G. D., Talavia, K. R., Amin, D. P. S. M. B. and Parmar, A. A. (**2014**). "Workability properties of geopolymer concrete using accelerator and silica fume as an admixture," International Journal for Technological Research in Engineering, vol. 1, no. 8.

Bingham, E.C. (**1916**). An Investigation of the Laws of Plastic Flow. US Bureau of Standards Bulletin.

Bingham, E.C. (**1922**). Fluidity and Plasticity. New York: McGraw-Hill.

Björn, A., Segura, P., Karlsson, A., & Ejlertsson, J., Svensson, B. (**2012**). Rheological Characterization. 10.5772/32596.

Boesch, M. E., & Hellweg, S. (**2010**). Identifying Improvement Potentials in Cement Production with Life Cycle Assessment. Environmental Science & Technology, 44(23), 9143-9149. doi:10.1021/es100771k

Boukendakdji, O., Kadri, E. H., & Kenai, S. (**2012**). Effects of granulated blast furnace slag and superplasticizer type on the fresh properties and compressive strength of self-compacting concrete. Cement and concrete composites, 34(4), 583-590.

Boukendakdji, O., Kenai, S., Kadri, E. H., & Rouis, F. (**2009**). Effect of slag on the rheology of fresh self-compacted concrete. Construction and Building Materials, 23(7), 2593-2598.

Bouzoubaâ, N., Zhang, M. H., Malhotra, V. M. and Golden, D. M. (**1999**) Blended fly ash cements – A review. ACI Materials Journal, 96, 641–650.

Brooks, J.J., Megat Johari, M.A., and Mazloom, M. (**2000**). "Effect of admixtures on the setting times of high-strength concrete," Cement and Concrete Composites, Vol. 22, pp. 293-301.

Brough, A.R., Atkinson, A. (**2002**). Sodium silicate-based, alkali-activated slag mortars: Part I. Strength, hydration and microstructure. Cem. Concr. Res. 32 (6), 865–879.

Cagiao, J., Gómez, B., Doménech, J. L., Mainar, S. G., & Lanza, H. G. (**2011**). Calculation of the corporate carbon footprint of the cement industry by the application of MC3 methodology. Ecological Indicators, 11(6), 1526-1540. doi:10.1016/j.ecolind.2011.02.013

Carlos Montes , Di Zang & Erez N. Allouche. (**2012**) Rheological behavior of fly ash-based geopolymers with the addition of superplasticizers, Journal of Sustainable Cement-Based Materials, 1:4, 179-185, DOI: 10.1080/21650373.2012.754568

Cartwright, C., Rajabipour, F., & Radlińska, A. (**2015**). Shrinkage Characteristics of Alkali-Activated Slag Cements. Journal of Materials in Civil Engineering, 27(7). doi:10.1061/(asce)mt.1943-5533.0001058

Casson, N. (**1959**). A flow equation for pigment-oil suspensions of the printing ink type. C.C. Mill, Rheology of disperse systems, New York: Pergamon press, 84–104.

Chen, C., Habert, G., Bouzidi, Y., & Jullien, A. (**2010**). Environmental impact of cement production: Detail of the different processes and cement plant variability evaluation. Journal of Cleaner Production, 18(5), 478-485. doi:10.1016/j.jclepro.2009.12.014

Chen, L. B., Zukoski, C. F., Ackerson B.J., Hanley, H. J. M., Straty, G. C., Barker J., Glinka, C. J., (**1992**), Structural Changes and Orientational Order in a Sheared Colloidal Suspension, Phys. Rev. Lett. 69, 688

Cheng TW, Chiu JP. (**2003**). Fire-resistant geopolymer produced by granulated blast furnace slag. Miner Eng.;16:205–10.

Cheng, A. Chao, S.-J. and Lin, W.-T. (**2013**). "Effects of leaching behavior of calcium ions on compression and durability of cement-based materials with mineral admixtures," Materials, vol. 6, no. 5, pp. 1851–1872.

Chennur, J. R., & Elavenil, S. (**2019**). Performance of Na2SiO3 solution fly ash based geopolymer mortar under ambient curing. Materials Research Express. doi:10.1088/2053-1591/ab0dd1

Chhabra R.P. (**2010**) Non-Newtonian Fluids: An Introduction. In: Krishnan J., Deshpande A., Kumar P. (eds) Rheology of Complex Fluids. Springer, New York, NY. https://doi.org/10.1007/978-1-4419-6494-6_1

Chindaprasirt, P., Chareerat, T., Sirivivatnanon, V. (**2007**). Workability and strength of coarse high calcium fly ash geopolymer, Cement and Concrete Composites, Volume 29, Issue 3, Pages 224-229, ISSN 0958-9465, https://doi.org/10.1016/j.cemconcomp.2006.11.002.

Craven, D.J., Okraglik, H.M., and Eilenberg, I.M. (**1994**). Construction waste and a new design methodology, In: C.J. Kibert (ed.), Proceedings of the First Conference of CIB TG 16 on Sustainable Construction, pp. 89–98, Tampa.

Criado M, Palomo A, Fern´andez-Jim´enez A. (**2005**). Alkali activation of fly ashes. Part 1. Effect of curing conditions on the carbonation of the reaction products. Fuel 84:2048–54

Cui, Y., & Wang, D. (**2019**). Effects of Water on Pore Structure and Thermal Conductivity of Fly Ash-Based Foam Geopolymers. Advances in Materials Science and Engineering, 2019, 1–10. doi:10.1155/2019/3202794

D. Hardjito, C. C. Cheak, and C. H. Lee Ing, (**2008**). Strength and Setting Times of Low Calcium Fly Ash-based Geopolymer Mortar , Mod. Appl. Sci., vol. 2, no. 4, pp. 3±11,.

Dadsetan, S., Siad, H., Lachemi, M., & Sahmaran, M. (**2019**). Construction and Demolition Waste in Geopolymer Concrete Technology: A review. Magazine of Concrete Research, 1–68. doi:10.1680/jmacr.18.00307

Davidovits J. (**1979**). Synthesis of new high temperature geo-polymers for reinforced plastics/composites. In: SPE PACTEC 79 Society of Plastic Engineers, Brookfield Center. p. 151–4.

Davidovits J. (**2008**). Geopolymer chemistry and application. Institute geopolymer 16 rue Galilee F02100 Saint- Quentin, France. p. 585.

Davidovits, J. (**1982**). Minerals polymers and methods of making them. US Patent 4472199.

Davidovits, J. (**1982a**) The need to create a new technical language for the transfer of basic scientific information. Transfer and Exploitation of Scientific and Technical Information, EUR 7716. Luxembourg, Commission of the European Communities.

Davidovits, J. (**1985**) Early high strength mineral polymer. US Patent 45009985.

Davidovits, J. (**1991**) Geopolymers – Inorganic polymeric new materials. Journal of Thermal Analysis, 37, 1633–1656. doi:10.1007/BF01912193.

Davidovits, J. (**1999**). Chemistry of Geopolymeric Systems, Terminology, 2nd International Conference in Geopolymer, pp. 9-40, Saint-Quentin, France.

Davidovits, J. (**2015**). Geopolymer Chemistry and Applications. 4-th edition. J. Davidovits.–Saint-Quentin, France.

Day, L., and McNeil, I. (**1996**) Biographical dictionary of the history of technology, New York: Routledge.

Deb, P. S., Sarker, P. K. and Barbhuiya, S. (**2015**). "Effects of nanosilica on the strength development of geopolymer cured at room temperature," Construction and Building Materials, vol. 101, pp. 675–683.

Deb, P., Nath, P., & Sarker, P. (**2014**). The effects of ground granulated blast-furnace slag blending with fly ash and activator content on the workability and strength properties of geopolymer concrete cured at ambient temperature. Materials & Design (1980-2015), 62, 32-39. doi: 10.1016/j.matdes.2014.05.001

Divoux, T., Barentin, C., Manneville S. (**2013**) Rheological Hysteresis in Soft Glassy Materials ,DOI: 10.1103/PhysRevLett.110.018304

Divoux, T., Barentin, C., Manneville S.(**2011b**). Stress overshoot in a simple yield stress fluid: An extensive study combining rheology and velocimetry, DOI: 10.1039/c1sm05740e

Divoux, T., Barentin, C., Manneville S., (**2011a)**, From stress-induced fluidization processes to Herschel-Bulkley behaviour in simple yield stress fluids, DOI: 10.1039/c1sm05607g.

Dombrowski, K., Buchwald, A., & Weil, M. (**2007**). The influence of calcium content on the structure and thermal performance of fly ash based geopolymers. Journal of Materials Science, 42(9), 3033-3043.

Durairaj, R., Man, L. W., Ekere, N., & Mallik, S. (**2010)**. The effect of wall-slip formation on the rheological behaviour of lead-free solder pastes. Materials & Design, 31(3), 1056 1062. doi:10.1016/j.matdes.2009.09.051

Dutta, D., Thokchom, S., Ghosh, P. and Ghosh, S. (**2010**). "Effect of silica fume additions on porosity of fly ash geopolymers," Journal of Engineering and Applied Sciences, vol. 5, no. 10, pp. 74–79.

Duxson P., Fernández-Jiménez A., Provis J.L., Lukey G.C., Palomo A. and van Deventer J.S.J. (**2007a**), 'Geopolymer technology: the current state of the art', J. Mater. Sci. 42, 2917–2933.

Duxson P., Mallicoat S.W., Lukey G.C., Kriven W.M. and van Deventer J.S.J. (**2007b**), 'The effect of alkali and Si/Al ratio on the development of mechanical properties of metakaolin based geopolymers', Colloids and Surfaces A: Physicochemical and Engineering Aspects 292, 8–20.

Duxson, P., Fernández-Jiménez, A., Provis, J. L., Lukey, G. C., Palomo, A., & Deventer, J. S. (**2006**). Geopolymer technology: The current state of the art. Journal of Materials Science, 42(9), 2917-2933. doi:10.1007/s10853-006-0637-z

Duxson, P., Provis, J., Grant, L., Mallicoat, S., Kriven, W., van Deventer, J.S.J. (**2005**). Understanding the relationship between geopolymer composition, microstructure and mechanical properties, Colloids and Surfaces A: Physicochemical and Engineering Aspects, 269:47-58.

Encyclopaedia Britannica, Inc. (**1991**) The new encyclopaedia Britannica, 15th edition, Chicago, IL: Encyclopaedia Britannica.

Environmental Protection Agency. (**1998**). Characterization of Building-Related Construction and Demolition Debris in the United States, EPA 530-R-98-010.

Erdem, T. K., Khayat, K. H., Yahia, A. (**2009**). "Correlating rheology of self-consolidating concrete to corresponding concrete-equivalent mortar", ACI Materials Journal, 106 (2), 154.

Erdoğan, Y.T. (**2003**). Beton. 1. Baskı, Ankara: ODTÜ Geliştirme Vakfı Yayıncılık ve İletişim A.Ş.

Fan, Y., Yin, S., Wen, Z., & Zhong, J. (**1999**). Activation of fly ash and its effects on cement properties. Cement and Concrete Research, 29(4), 467-472.

Ferna´ndez-Jime´nez A, Palomo A, Sobrados I, Sanz J. (**2006**). " the role played by the reactive alumina content in the alkaline activation of fly ashes", Microp. Mesop, Mater. 91, 111-119

Fernandez.A- Jimenez A.Paloma, Criado.M. (**2005**). Microstructure development of alkali activated cements descriptive model ,Cem .Conc.Res,2005,35,1204-1209.

Fernández-Jiménez A. and Palomo A. (**2003**), 'Characterisation of fly ashes: potential reactivity as alkaline cements', Fuel 82, 2259–2265.

Fernández-Jiménez, A. Palomo A. and Alonso M.M. (**2005b**), 'Alkali activation of fly ashes: mechanisms of reaction', in Congress of Non-Traditional Cement and Concrete II, Ed. V. Bilek and Z. Kersner, Brno University of technology, 1–12.

Formoso, C.T., Soibelman, L., De Cesare, C., and Isatto, E.L. (**2002**). Material waste in building industry: main causes and prevention, J. Cons. Eng. & Manage., 128(4), 316–25.

Garcia-Lodeiro, I., Fernández-Jiménez, A., & Palomo, A. (**2013**). Hydration kinetics in hybrid binders: Early reaction stages. Cement and Concrete Composites, 39, 82-92.

Garcia-Lodeiro, I., Palomo, A., Fern´andez-Jim´enez, A. and Macphee, D. E. (**2011**). "Compatibility studies between NASH and CASH gels. Study in the ternary diagram Na2O–CaO–Al2O3–SiO2– H2O," Cement and Concrete Research, vol. 41, no. 9, pp. 923–93.

Gartner, E. (**2004**), Industrially interesting approaches to "low-CO2" cements, Cement and Concrete Research, Volume 34, Issue 9,Pages 1489-1498, ISSN 0008-8846, https://doi.org/10.1016/j.cemconres.2004.01.021.

Gautefall, O. (**1986**). "Effect of CSF on the diffusion of chloride through hardened cement paste," in Proceedings of the 2nd International Conference on the Use of Fly Ash, Silica Fume, Slag and Natural Pozzolans in Concrete, vol. 2, pp. 991–998, American Concrete Institute, Madrid, Spain, Publication SP-91.

Gesoğlu, M., & Özbay, E. (**2007**). Effects of mineral admixtures on fresh and hardened properties of self-compacting concretes: binary, ternary and quaternary systems. Materials and Structures, 40(9), 923-937.

Glukhovsky, V. D. (**1959**). Soil silicates. Gosstroyizdat, Kiev, 154.

Goberis, S., & Antonovich, V. (**2004**). Influence of sodium silicate amount on the setting time and EXO temperature of a complex binder consisting of high-aluminate cement, liquid glass and metallurgical slag. Cement and concrete research, 34(10), 1939-1941.

Gordon, M., Bell, J. L. and Kriven, W. M. (**2005**) Comparison of naturally and synthetically derived, potassium-based geopolymers. Ceramic Transactions, 165, 95–106.

Görhan, G., & Kürklü, G. (**2014**). The influence of the NaOH solution on the properties of the fly ash-based geopolymer mortar cured at different temperatures. Composites part b: engineering, 58, 371-377.

Granizo, M. L., Alonso, S., Blanco-Varela, M. T., and Palomo, A. (**2004**). "Alkaline activation of metakaolin: Effect of calcium hydroxide in the products of reaction." J. Am. Ceram. Soc., 85(1), 225–231.

Granizo, M. L., Blanco Varela, M. T. and Martínez-Ramírez, S. (**2007**) Alkali activation of metakaolins: Parameters affecting mechanical, structural and microstructural properties. Journal of Materials Science, 42, 2934–2943. doi: 10.1007/s10853-006-0565-y.

Granizo, M. L., Blanco-Varela MT, Puertas F, Paloma A. (**1997**). Alkali, activation of metakaolin: influence of synthesis parameters. In: Proceedings of the tenth international congress on the chemistry of cement, Gothenburg, Sweden, vol. 3.

Granizo, M.L., Blanco-Varela MT, Palomo A. (**2000**). Influence of the starting kaolin on alkali-activated materials based on metakaolin. Study of the reaction parameters by isothermal conduction calorimetry. J Mater Sci ;35:6309–15.

Gruskovnjak, A., Lothenbach, B., Holzer, L., Figi, R., Winnefeld, F. (**2006**). Hydration of alkaliactivated slag: comparison with ordinary Portland cement. Adv. Cem. Res. 18 (3), 119–128.

Guo, X., Shi, H., Chen, L., and Dick, W. A. (**2010**). "Alkali-activated complex binders from class C fly ash and Ca-containing admixtures." J. Hazard. Mater., 173(1–3), 480–486.

Habert, G. (**2014**). Assessing the environmental impact of conventional and 'green' cement production. Eco-efficient Construction and Building Materials, 199-238. doi:10.1533/9780857097729.2.199

Hajimohammadi, A., Provis, J. L. and van Deventer, J. S. J. (**2011**). "The effect of silica availability on the mechanism of geopolymerisation," Cement and Concrete Research, vol. 41, no. 3, pp. 210–216.

Hajimohammadi, A., Provis, J. L., & van Deventer, J. S. J. (**2010**). Effect of Alumina Release Rate on the Mechanism of Geopolymer Gel Formation. Chemistry of Materials, 22(18), 5199–5208. doi:10.1021/cm101151n

Herschel, W.H.; Bulkley, R. (**1926**). Konsistenzmessungen von Gummi-Benzollösungen. Kolloid Zeitschrift, 39(4), 291-300.

Hewlett, P. P. (**1998**). Preface. Lea's Chemistry of Cement and Concrete, Xix-Xxi. doi:10.1016/b978-075066256-7/50009-6

Hos, J. P., McCormick, P. G. and Byrne, L. T. (**2002**) Investigation of a synthetic aluminosilicate inorganic polymer. Journal of Materials Science, 37, 2311–2316. doi:10.1023/A:1015329619089.

Huseien, G. F., Mirza, J., Ismail, M., & Hussin, M. W. (**2016**). Influence of different curing temperatures and alkali activators on properties of GBFS geopolymer mortars containing fly ash and palm-oil fuel ash. Construction and Building Materials, 125, 1229-1240.

I. Kourti, D.A. Rani, D. Deegan, A.R. Boccaccini, C.R. Cheeseman. (**2010**). Production of geopolymers using glass produced from DC plasma treatment of air pollution control (APC) residues, Journal of Hazardous Materials, 176 704–709.

Iotti, M., Gregersen, Ø.W., Moe, S. (**2011**). Rheological Studies of Microfibrillar Cellulose Water Dispersions. J Polym Environ 19, 137–145, https://doi.org/10.1007/s10924-010-0248-2

Ivanova, I. I., Aiello, R., Nagy, J. B., Crea, F., Derouane, E. G., Dumont, N., Nastro, A., Subotic, B., Testa, F. (**1994**). "Influence of Cations on the Physicochemical and Structural Properties of Aluminosilicate Gel Precursors. II. Multinuclear Magnetic Resonance Characterization." Microporous Mater., 3 (3), 245-257.

Jeong, S., (**2019**), Shear Rate-Dependent Rheological Properties of Mine Tailings: Determination of Dynamic and Static Yield Stresses

Jiang, M. Chen, X., Rajabipour,. Hendrickson, C.T. (**2014**) Comparative life cycle assessment of conventional, glass powder, and alkali-activated slag concrete and mortar J. Infrastruct. Syst.

Jithendra, C., & Elavenil, S. (**2019**). Effects of Silica Fume on Workability and Compressive Strength Properties of Aluminosilicate Based Flowable Geopolymer Mortar under Ambient Curing. Silicon. doi: 10.1007/s12633-019-00308-0

Johari, M. M., Brooks, J. J., Kabir, S., & Rivard, P. (**2011**). Influence of supplementary cementitious materials on engineering properties of high strength concrete. Construction and Building Materials, 25(5), 2639-2648.

Jong BHWSD, JR GEB. (**1980**). Polymerization of silicate and aluminate tetrahedra in glasses, melts, and aqueous solutions-I. Electronic structure of H6Si207, H6AlSiO7, and H6A1207-. Geochim Cosmochim Acta. 44(3):491-511.

Josa, A., Aguado, A., Cardim, A., & Byars, E. (**2007**). Comparative analysis of the life cycle impact assessment of available cement inventories in the EU. Cement and Concrete Research, 37(5), 781-788. doi:10.1016/j.cemconres.2007.02.004

Josa, A., Aguado, A., Heino, A., Byars, E., & Cardim, A. (**2004**). Comparative analysis of available life cycle inventories of cement in the EU. Cement and Concrete Research, 34(8), 1313-1320. doi:10.1016/j.cemconres.2003.12.020

Joshi, R. C., & Lohita, R. P. (**1997**). Fly ash in concrete: production, properties and uses (Vol. 2). CRC Press.

Jumrat S, Chatveera B, Rattanadecho P. (**2011**). Dielectric properties and temperature profile of fly ash-based geopolymer mortar. Int Commun Heat Mass Tran,38(2):242–8.

Kalyon D.M. (**2005**). Apparent slip and viscoplasticity of concentrated suspensions J Rheol, 49, pp. 621-640

Keppert, M. et al. (**2018**) 'Red-clay ceramic powders as geopolymer precursors: Consideration of amorphous portion and CaO content', Applied Clay Science, 161, pp. 82–89. doi: 10.1016/j.clay.2018.04.019.

Khater, H. (**2012**). Effect Of Calcium On Geopolymerization Of Aluminosilicate Wastes. Journal Of Materials In Civil Engineering. 24. 92-101. 10.1061/(Asce)Mt.1943-5533.0000352.

Khater, H. M. (**2013**). Effect of silica fume on the characterization of the geopolymer materials. International Journal of Advanced Structural Engineering, vol. 5, no. 1, pp. 1–10.

Khayat, K.H., Omran, A., Neji, S., Billberg, P., Yahia, A. (**2008**). Test Methods to Evaluate Form Pressure of SCC", The Third North American Conference on the Design and Use of Self-Consolidating Concrete, SCC, 308-214.

Kibert, C.J. (**2000**). Deconstruction as an essential component of sustainable construction, In: Proceedings of the Second Southern African Conference on Sustainable Development in the Built Environment, pp. 1-5, Pretoria.

Ko, L. S., Beleña, I., Duxson, P., Kavalerova, E., Krivenko, P. V., Ordoñez, L., Winnefeld, F. (**2013**). AAM Concretes: Standards for Mix Design/Formulation and Early-Age Properties. Alkali Activated Materials RILEM State-of-the-Art Reports, 157-176. doi:10.1007/978-94-007-7672-2_7

Kohno, K., Aihara, F., and Ohno, K. (**1989**). "Relative durability properties and strengths of mortars containing finely ground silica and silica fume," in Proceedings of the 3rd International Conference on Fly Ash, Silica Fume, Slag, andNatural Pozzolans inConcrete, vol. 1, pp. 815–826, Trondheim,Norway.

Kolli, V.G., Gadala-Maria, F., Anderson, R., (**1997)**, Rheological characterisation of solder paste for surface mount applications IEEE Trans Compon, Pack Manufact Technol, B, 20, pp. 416-423

Komljenović, M., Bascarevi´c, Z., Bradi´c, V. (**2010**). "Mechanical and microstructural properties of alkali-activated fly ash geopolymers", Journal of Hazardous Materials, 181, 35–42.

Komnitsas, K., Zaharaki, D., Vlachou, A., Bartzas, G., & Galetakis, M. (**2015**). Effect of synthesis parameters on the quality of construction and demolition wastes (CDW) geopolymers. Advanced powder technology, 26(2), 368-376.

Kotwal AR, Kim YJ, Hu J, Sriraman V. (**2015**). Characterization and early age physical properties of ambient cured geopolymer mortar based on class C fly ash. Int J. Concr. Struct. Mater. 9(1):35–43.

Krivenko PV (**1994**) In: Krivenko PV (ed) Proceedings of the first international conference on alkaline cements, concretes. VIPOL Stock Company, Kiev, Ukraine, pp 11– 129

Krivenko, P. (**1997**) Alkaline cements: terminology, classification, aspects of durability. In: Proceedings of the tenth international congress on the chemistry of cement, Gothenburg, Sweden, vol. 4.

Kruger, J., Zeranka, S., & Zijl, G. V. (**2019**). An ab initio approach for thixotropy characterisation of (nanoparticle-infused) 3D printable concrete. Construction and Building Materials, 224, 372-386. doi:10.1016/j.conbuildmat.2019.07.078

Labanda, J. & Llorens, J. (**2005**). Influence of sodium polyacrylate on the rheology of aqueous Laponite dispersions, Journal of Colloid and Interface Science, Volume 289, Issue 1, Pages 86-93, ISSN 0021-9797, https://doi.org/10.1016/j.jcis.2005.03.055.

Lapasin, R., Papo, A., Rajgelj, S. (**1983**). "Flow Behavior of Fresh Cement Pastes. A Comparison of Different Rheological Instruments and Techniques", Cement and Concrete Research, 13 (3), 349-356

Laskar, A. I., & Talukdar, S. (**2008**). Rheological behavior of high performance concrete with mineral admixtures and their blending. Construction and Building materials, 22(12), 2345-2354.

Lee, N.K., An, G.H., Koh, K.T., Ryu, G.S. (**2016**). "Improved Reactivity of Fly Ash-Slag Geopolymer by the Addition of Silica Fume", Advances in Materials Science and Engineering, vol. 2016, Article ID 2192053, 11 pages. https://doi.org/10.1155/2016/2192053

Leong, H. Y., Ong, D. E. L., Sanjayan, J. G., & Nazari, A. (**2016**). The effect of different Na2O and K2O ratios of alkali activator on compressive strength of fly ash based-geopolymer. Construction and Building Materials, 106, 500-511.

Li, C., Sun, H., Li, L. (**2010**). A review: The comparison between alkali-activated slag (Si+ Ca) and metakaolin (Si + Al) cements, Cem. Concr. Res. 40 (9) 1341–1349.

Li, X., Ma, X., Zhang, S., & Zheng, E. (**2013**). Mechanical properties and microstructure of class C fly ash-based geopolymer paste and mortar. Materials, 6(4), 1485-1495.

Li, Z. (**2011**). Advanced concrete technology. Hoboken, NJ: Wiley.

Li, Z., Mu, B. and Chui, S.N.C. (**1999a**). 'Systematic study of properties of extrudates with incorporated metakaolin or silica fume', ACI Mat. Journal 96 (5), 574-579.

Li, Z., Mu, B. and Chui, S.N.C. (**1999b**). 'Rheology behaviour of short fiber reinforced cement-based extrudate', Journ. Of Engin. Mechanics 125 (5), 530-536.

Liew, Y. M., Heah, C. Y., & Kamarudin, H. (**2016**). Structure and properties of clay-based geopolymer cements: A review. Progress in Materials Science, 83, 595-629.

Lombois-Burger, H. (**2003**). 'Mixing and rheological behaviour of powder pastes in presence of a polymer: application to the extrusion of cement-based formulations' (Malaxage et comportement rhéologique des pâtes granulaires en presence de polymère: application à l'extrusion de formulations cimentaires), Ph Thesis, University of Paris VI.

Low-Carbon Transition in the Cement Industry. (**2018**). IEA Technology Roadmaps. doi:10.1787/9789264300248-en

MacKenzie, K. J. D., Brown, I. W. M., Meinhold, R. H. and Bowden, M. E. (**1985**) Outstanding problems in the kaolinite-mullite reaction sequence investigated by 29Si and 27Al solid-state nuclear magnetic resonance: I. Metakaolinite. Journal of the American Ceramic Society, 68, 293–297. doi: 10.1111/j.1151-2916.1985.tb15228.x.

Mahmoodi O, Siad H, Lachemi M, Dadsetan S, Sahmaran M. (**2020**). Optimization of brick waste-based geopolymer binders at ambient temperature and pre-targeted chemical parameters, Journal of Cleaner Production, doi: https://doi.org/10.1016/j.jclepro.2020.122285.

Malkawi, A., Nuruddin, M., Fauzi, A., Almattarneh, H., & Mohammed, B. (**2016**). Effects of Alkaline Solution on Properties of the HCFA Geopolymer Mortars. Procedia Engineering, 148, 710-717. doi: 10.1016/j.proeng.2016.06.581

Malkin, A. I., & Isayev, A. I. (**2012**). Rheology: Concepts, methods, and applications. Toronto: ChemTec Pub.

Mastali, M., Kinnunen, P., Dalvand, A., Firouz, R. M., & Illikainen, M. (**2018**). Drying shrinkage in alkali-activated binders – A critical review. Construction and Building Materials, 190, 533-550. doi:10.1016/j.conbuildmat.2018.09.125

Melo Neto, A.A., Cincotto, M.A., Repette, W. (**2008**). Drying and autogenous shrinkage of pastes and mortars with activated slag cement. Cem. Concr. Res. 38 , 565–574.

Memon, F. A., Nuruddin, M. F. and Shafiq, N. (**2013**). "Effect of silica fume on the fresh and hardened properties of fly ash-based self-compacting geopolymer concrete," International Journal of Minerals, Metallurgy and Materials, vol. 20, no. 2, pp. 205–213.

Memon, F. A., Nuruddin, M. F., Khan, S., Shafiq, N., & Ayub, T. (**2013b**). Effect of sodium hydroxide concentration on fresh properties and compressive strength of self-compacting geopolymer concrete. Journal of Engineering Science and Technology, 8(1), 44-56.

Metwally A. Abd Elaty & Mariam F. Ghazy (**2012**) Flow properties of fresh concrete by using modified geotechnical Vane shear test. HBRC Journal. 8:3. 159-169. DOI: 10.1016/j.hbrcj.2012.07.001

Mezger, T. G. (**2011**). The Rheology Handbook. 3rd revised ed. Hanover: Vincentz Network.

Mezger, T.G. (**2006**). The Rheology Handbook, 3rd edn, Hannover: Vincentz Network.

Miyazawa, S., Yokomuro, T., Sakai, E., Yatagai, A., Nito, N., & Koibuchi, K. (**2014**). Properties of concrete using high C3S cement with ground granulated blast-furnace slag. Construction and Building Materials, 61, 90-96. doi:10.1016/j.conbuildmat.2014.03.008

Najafi Kani E, Allahverdi A, Provis JL. (**2012**). Efflorescence control in geopolymer binders based on natural pozzolan. Cem. Concr. Compos. 34:25–33

Nematollahi, B., Vijay, P., Sanjayan, J., Nazari, A., Xia, M., Naidu Nerella, V., & Mechtcherine, V. (**2018**). Effect of polypropylene fibre addition on properties of geopolymers made by 3D printing for digital construction. Materials, 11(12), 2352.

Newman, J. (**2003**). Advance concrete technology: Constituent material. Butterworth: Heineman.

Oikonomou, N. D. (**2005**). Recycled concrete aggregates. Cement and concrete composites, 27(2), 315-318.

Okoye F. N., Durgaprasad, J. and Singh, N. B. (**2016**). "Effect of silica fume on themechanical properties of fly ash based-geopolymer concrete," Ceramics International, vol. 42, no. 2, pp. 3000–3006.

Olivier JGJ, Janssens-Maenhout G, Peters JAHW. (**2012**). Trends in global CO2 emissions; 2012 report. Rep., PBL Neth. Environ. Assess. Agency, The Hague

Pacheco-Torgal, F. Labrincha, A., Leonelli, C., Palomo, A., & Chindaprasirt P. (**2017**). Handbook of alkali-activated cements, mortars and concretes. Place of publication not identified: WOODHEAD.

Pacheco-Torgal, F., Castro-Gomes, J. P., & Jalali, S. (**2008**). Investigations on mix design of tungsten mine waste geopolymeric binder. Construction and Building Materials, 22(9), 1939-1949.

Palacios, M & Banfill, P & Puertas, F. (**2008**). Rheology and setting of alkali-activated slag pastes and mortars: Effect of organ admixture. ACI Materials Journal. 105. 140-148.

Pallagi, A., Tasi, Á., Gácsi, A., Csáti, M., Pálinkó, I., Peintler, G., & Sipos, P. (**2012**). The solubility of Ca(OH)2 in extremely concentrated NaOH solutions at 25°C. Open Chemistry, 10(2). doi:10.2478/s11532-011-0145-0

Palomo, A., Grutzeck, M. W., & Blanco, M. T. (**1999**). Alkali-activated fly ashes: A cement for the future. Cement and concrete research, 29(8), 1323-1329.

Palomo, J.I & López, D F .(**2003**). Alkali-activated cementitous materials: Alternative matrices for the immobilisation of hazardous wastes: Part I. Stabilisation of boron, Cement and Concrete Research, Volume 33, Issue 2, 2003, Pages 281-288, ISSN 0008-8846, https://doi.org/10.1016/S0008-8846(02)00963-8.

Panda B., Unluer, C.,Tan, M.J., (**2018a**), Investigation of the rheology and strength of geopolymer mixtures for extrusion-based 3D printing, Cement and Concrete Composites, Volume 94, Pages 307-314, ISSN 0958-9465, https://doi.org/10.1016/j.cemconcomp.2018.10.002.

Panda, B. & Tan, M.J., (**2018b**), Experimental study on mix proportion and fresh properties of fly ash based geopolymer for 3D concrete printing, Ceramics International, Volume 44, Issue 9, Pages 10258-10265, ISSN 0272-8842, https://doi.org/10.1016/j.ceramint.2018.03.031.

Panda, B., Ruan, S., Unluer C., Tan, M.J., (**2020**), Investigation of the properties of alkali-activated slag mixes involving the use of nanoclay and nucleation seeds for 3D printing, Composites Part B: Engineering, Volume 186,107826, ISSN 1359-8368, https://doi.org/10.1016/j.compositesb.2020.107826.

Papo, A. & Piani, L.(**2004**). Effect of various superplasticizers on the rheological properties of Portland cement pastes, Cement and Concrete Research, Volume 34, Issue 11, Pages 2097-2101, ISSN 0008-8846, https://doi.org/10.1016/j.cemconres.2004.03.017.

Patankar, S. & Jamkar, S. & Ghugal, Y. (**2013**). Effect of Water-to-Geopolymer Binder Ratio on the Production of Fly ash Based Geopolymer Concrete.. Journal. 2. 10.13140/2.1.4792.1284.

Patankar, S. V., Ghugal, Y. M., & Jamkar, S. S. (**2014**). Effect of Concentration of Sodium Hydroxide and Degree of Heat Curing on Fly Ash-Based Geopolymer Mortar. Indian Journal of Materials Science, 2014, 1–6. doi:10.1155/2014/938789

Phoo-ngernkham, T., Chindaprasirt, P., Sata, V., Hanjitsuwan, S., & Hatanaka, S. (**2014**). The effect of adding nano-SiO2 and nano-Al2O3 on properties of high calcium fly ash geopolymer cured at ambient temperature. Materials & Design, 55, 58-65.

Phoo-ngernkham, T., et al. (**2015**). Effects of sodium hydroxide and sodium silicate solutions on compressive and shear bond strengths of FA–GBFS geopolymer. Construction and Building Materials, 91: p. 1-8.

Poulesquen, A., Frizon, F., Lambertin D. (**2011**). Rheological behavior of alkali-activated metakaolin during geopolymerization, Journal of Non-Crystalline Solids, Volume 357, Issue 21, 2011, Pages 3565-3571, ISSN 0022-3093,https://doi.org/10.1016/j.jnoncrysol.2011.07.013.

Provis JL, Lukey GC, van Deventer JSJ (**2005a**) Do geopolymers actually contain nanocrystalline zeolites? A reexamination of existing results. Chem Mater 17:3075–3085

Provis JL, Yong CZ, Duxson P, van Deventer JSJ. (**2009**). Correlating mechanical and thermal properties of sodium silicate–fly ash geopolymers. Colloids Surf. A 336:57–63

Provis, J. L. (**2006**). Modelling the formation of geopolymers. PhD thesis, Chemical & Biomolecular Engineering, University of Melbourne.

Provis, J. L. (**2013**). Geopolymers and other alkali activated materials: Why, how, and what? Materials and Structures, 47(1-2), 11-25. doi:10.1617/s11527-013-0211-5

Provis, J. L., & Van Deventer, J. S. (Eds.). (**2013**). Alkali activated materials: state-of-the-art report, RILEM TC 224-AAM (Vol. 13). Springer Science & Business Media.

Provis, J. L., Van Deverten J.S.J. (**2009**). Geopolymers: Structures, Processing, Properties and Industrial Applications, Woodhead Publishing, 2009, Pages xi-xiv, ISBN 9781845694494, https://doi.org/10.1016/B978-1-84569-449-4.50022-9.

Provis, J., & Van Deventer, J. (**2014**). Alkali Activated Materials: State-of-the-Art Report, RILEM TC 224-AAM. 10.1007/978-94-007-7672-2.

Provis, J., Yong, S., & Duxson, P. (**2009b**). Nanostructure/microstructure of metakaolin geopolymers. Geopolymers, 72-88. doi: 10.1533/9781845696382.1.72

Provis, J.L., Duxson, P., Van Deventer, J.S.J., Lukey, G.C. (**2005b**). The Role of Mathematical Modelling and Gel Chemistry in Advancing Geopolymer Technology, Chemical Engineering Research and Design, Volume 83, Issue 7, Pages 853-860, ISSN 0263-8762, https://doi.org/10.1205/cherd.04329.

Provis, J.L., van Deventer, J.S.J. (**2007**). Direct measurement of the kinetics of geopolymerisation by in-situ energy dispersive X-ray diffractometry. J Mater Sci 42, 2974–2981 https://doi.org/10.1007/s10853-006-0548-z

Puertas, F., González-Fonteboa, B., González-Taboada, I., Alonso, M., Torres-Carrasco, M., Rojo, G., & Martínez-Abella, F. (**2018**). Alkali-activated slag concrete: Fresh and hardened behaviour. Cement and Concrete Composites, 85, 22-31. doi:10.1016/j.cemconcomp.2017.10.003

Puertas, F., Palacios, M., Manzano, H., Dolado, J.S., Rico, A., Rodríguez, J. (**2011**). A model for the C-A-S-H gel formed in alkali-activated slag cements. J. Eur. Ceram. Soc. 31 (12), 2043– 2056.

Puertas, F., Varga, C., & Alonso, M. (**2014**). Rheology of alkali-activated slag pastes. Effect of the nature and concentration of the activating solution. Cement and Concrete Composites, 53, 279-288. doi:10.1016/j.cemconcomp.2014.07.012

Qiu, J., Zhao, Y., Xing, J., & Sun, X. (**2019**). Fly Ash/Blast Furnace Slag-Based Geopolymer as a Potential Binder for Mine Backfilling: Effect of Binder Type and Activator Concentration. Advances In Materials Science And Engineering, 2019, 1-12. doi: 10.1155/2019/2028109

Rahier, H., Simons W, van Mele B, Biesemans M. (**1997**). Recent literature in geopolymer science and technology. Journal of Master Science; 32(9):2237–47.

Rahier, H., Van M, B., Biesemans, M. et al. (**1996**).Low-temperature synthesized aluminosilicate glasses. Journal of materials science 31, 71–79. https://doi.org/10.1007/BF00355128

Rakhimova, N. R. and Rakhimov, R. Z. (**2015**) 'Alkali-activated cements and mortars based on blast furnace slag and red clay brick waste', Materials and Design, 85, pp. 324–331. doi: 10.1016/j.matdes.2015.06.182.

Rashad, A. M. (**2013**). A comprehensive overview about the influence of different additives on the properties of alkali-activated slag – A guide for Civil Engineer. Construction and Building Materials, 47, 29-55. doi:10.1016/j.conbuildmat.2013.04.011

Reig, L., Tashima, M.M., Soriano, L., Borrachero, M. V., J. Monzó, J. Payá. (**2013**). Alkaline Activation of Ceramic Waste Materials, Waste and Biomass Valorization, 4,729–736.

Richard, P. and Cheyrezy M. (**1995**) "Composition of reactive powder concretes," Cement and Concrete Research 25(7), 1501–1511.

Richardson, I. G. (**2004**) Tobermorite/jennite- and tobermorite/calcium hydroxide-based models for the structure of C-S-H: applicability to hardened pastes of tricalcium silicate,

-dicalcium silicate, Portland cement, and blends of Portland cement with blast-furnace slag, metakaolin, or silica fume. Cement and Concrete Research, 34, 1733–1777. doi:10.1016/j.cemconres.2004.05.034.

Rifaai Y., Yahia A., Mostafa, A., Aggoun S., Kadri, E. (**2019**). Rheology of fly ash-based geopolymer: Effect of NaOH concentration, Construction and Building Materials, Volume 223, Pages 583-594, ISSN 0950-0618, https://doi.org/10.1016/j.conbuildmat.2019.07.028.

Risdanareni, P., J.J. Ekaputri, and Triwulan. (**2015**). The Influence of Alkali Activator Concentration to Mechanical Properties of Geopolymer Concrete with Trass as a Filler. Materials Science Forum. 803: p. 125-134.

Robayo-Salazar, R.A.; Rivera, J.F.; Mejía De Gutiérrez, R. (**2017**). Alkali-activated building materials made with recycled construction and demolition wastes, Construction and Building Materials, 149, 130–138.

Rocha, J. and Klinowski, J. (**1990**) Solid-state NMR studies of the structure and reactivity of metakaolinite. Angewandte Chemie – International Edition, English, 29, 553–554. doi: 10.1002/anie.199005531.

Rovnaník, P. et al. (**2018**) 'Rheological properties and microstructure of binary waste red brick powder/metakaolin geopolymer', Construction and Building Materials, 188, pp. 924–933. doi: 10.1016/j.conbuildmat.2018.08.150.

Rovnaník, P.; Ěezník, B.; Rovnaníková, P. (**2016**). Blended alkali-activated fly ash/brick powder materials, Procedia Engineering, 151, 108–113.

Rowles, M., O'connor, B. (**2003**). Chemical optimisation of the compressive strength of aluminosilicate geopolymers synthesised by sodium silicate activation of metakaolinite. Journal of Materials Chemistry, 13(5), 1161-1165. doi:10.1039/b212629j

Sabir, B. B., Wild, S. and Bai, J. (**2001**) Metakaolin and calcined clays as pozzolans for concrete: a review. Cement and Concrete Composites, 23, 441–454. doi:10.1016/ S0958-9465(00)00092-5.

Sathonsaowaphak, A., Chindaprasirt, P., Pimraksa, K. (**2009**). Workability and strength of lignite bottom ash geopolymer mortar, Journal of Hazardous Materials, Volume 168, Issue 1, Pages 44-50, ISSN 0304-3894, https://doi.org/10.1016/j.jhazmat.2009.01.120.

Scrivener K.L., & Kirkpatrick RJ. (**2008**). Innovation in use and research on cementitious material. Cem. Concr. Res. 38:128–36

Sellevold EJ. (**1987**). The function of condensed silica fume in high strength concrete. In: Holand I, Helland S, Jakobsen B, Lenschow R, editors. Proceedings of the symposium on utilization of high strength concrete. Stavanger, Norway; p. 39–49.

Serag Faried, A., Sofi, W. H., Taha, A. Z., El-Yamani, M. A., & Tawfik, T. A. (**2020**). Mix design proposed for geopolymer concert mixtures based on ground granulated blast furnace slag. Australian Journal of Civil Engineering, 1-14.

Serpell, A., and Labra, M. (**2003**). A study on construction waste in Chile, In: G., Ofori and F.Y.Y., Ling (ed.), Proceedings, Joint Symposium of CIB W55, W65 and W107 on Knowledge Construction, pp. 102-111, Singapore.

Shi C. (**1996**). Strength, pore structure and permeability of alkali-activated slag mortars. Cem. Concr. Res. 26:1789–99

Shi C., Fernández-Jiménez A. and Palomo A. (**2011**), 'New cements for the 21st century: the pursuit of an alternative to Portland cement', Cem. Concr. Res. 41, 750–763.

Simonson, J. M., Mesmer, R. E. and Rogers, P. S. Z. (**1989**) The enthalpy of dilution and apparent molar heat capacity of NaOH(aq) to 523 K and 40 MPa. Journal of Chemical Thermodynamics, 21, 561–584. doi:10.1016/0021-9614(89)90172-9

Siyal, A. A., Azizli, K. A., Man, Z., & Ullah, H. (**2016**). Effects of Parameters on the Setting Time of Fly Ash Based Geopolymers Using Taguchi Method. Procedia Engineering, 148, 302–307. doi:10.1016/j.proeng.2016.06.624

Skvara, F.; Kopecky, L.; Nimeeek, J.; Bittnar, Z (**2006**): Microstructure of geopolymer materials based on fly ash. Ceramics Silikaty 50, 208–215

Sofi M, Van Deventer JSJ, Mendis PA, Lukey GC. (**2006**). J Mater Sci (this issue)

Srinivasan, R., DeFord, D. and Shah, S.P. (**1999**). 'The use of the extrusion rheometer in the development of extruded fiberreinforced cement composites', Concrete Science and Engineering 1 (1), 26-36.

Stokoe, M.J., Kwong, P.Y., and Lau, M.M. (**1999**). Waste reduction: a tool for sustainable waste management for Hong Kong, In: A. Barrage and Y. Edelmann (ed.), Proceedings of R'99 World Congress, pp. 165–70, Geneva.

Sum, W., Zhang, Y., Lin, W., Liu Zhi-yong. (**2004**). In situ monitoring of the hydration process of K-PS geopolymer cement with ESEM. Cem Concr Res. 34:935–40.

Sun, Z. et al. (**2013**), Synthesis and thermal behavior of geopolymer-type material from waste ceramic, Construction and Building Materials, 49, 281–287.

Swaddle, T. W., Salerno, J., & Tregloan, P. A. (**1994**). Aqueous aluminates, silicates, and aluminosilicates. Chemical Society Reviews, 23(5), 319. doi:10.1039/cs9942300319

Swaddle, T.W. (**2001**) Silicate complexes of aluminum(III) in aqueous systems, Coord. Chem. Rev., vols. 219–221, pp. 665–686.

Taylor M, Tam C, Gielen D. (**2006**). Energy efficiency and CO2 emissions from the global cement industry. Presented at Workshop, Energy Efficiency and CO2 Emission Reduction Potentials and Policies, Int. Energy Agency, Paris, Sept. 4–5.

Temuujin, J., van Riessen, A., & Williams, R. (**2009**). Influence of calcium compounds on the mechanical properties of fly ash geopolymer pastes. Journal Of Hazardous Materials, 167(1-3), 82-88. doi: 10.1016/j.jhazmat.2008.12.121

Thokchom, S., Dutta, D. and Ghosh, S. (**2011**). "Effect of incorporating silica fume in fly ash geopolymers," World Academy of Science,Engineering and Technology, vol. 60, pp. 243–247.

Thormark, C. (**2001**). Conservation of energy and natural resources by recycling building waste, Resources, Conserv. & Recycl., 33, 113–130.

Toker, O. S., Karasu, S., Yilmaz, M. T., & Karaman, S. (**2015**). Three interval thixotropy test (3ITT) in food applications: A novel technique to determine structural regeneration of mayonnaise under different shear conditions. Food Research International, 70, 125-133. doi:10.1016/j.foodres.2015.02.002

Tossavainen, M., Engstrom, F., Yang, Q., Menad, N., Larsson, M. L., & Bjorkman, B. (**2007**). Characteristics of steel slag under different cooling conditions. Waste Management, 27(10), 1335-1344. doi:10.1016/j.wasman.2006.08.002

Toutou, Z., Lanos, C. and Laquerbe, M. (**2002**). 'Vers un BHP extrudable: Rhéologie des pâtes et mortiers', Proceedings of the ' XXèmes Rencontres Universitaires de Génie Civil: Innovation et développement en génie civil et urbain', Toulouse (France).

Valderrama, C., Granados, R., Cortina, J. L., Gasol, C. M., Guillem, M., & Josa, A. (**2012**). Implementation of best available techniques in cement manufacturing: A life-cycle assessment study. Journal of Cleaner Production, 25, 60-67. doi:10.1016/j.jclepro.2011.11.055

Van Deventer, J. S. J., Provis, J. L., Duxson, P., & Lukey, G. C. (**2007**). Reaction mechanisms in the geopolymeric conversion of inorganic waste to useful products. Journal of hazardous materials, 139(3), 506-513.

Van Jaarsveld, J. G. S., Van Deventer, J. S. J., & Lukey, G. C. (**2002**). The effect of composition and temperature on the properties of fly ash-and kaolinite-based geopolymers. Chemical Engineering Journal, 89(1-3), 63-73.

Van Wazer JR (**1970**) Inorg Macromol Rev 1:89

Vance, K & Dakhane, A & Sant, G & Neithalath, N. (**2014**). Observations on the rheological response of alkali activated fly ash suspensions: the role of activator type and concentration. Rheologica Acta. 53. 843-855. 10.1007/s00397-014-0793-z.

Varaprasad, B. S. K. R. J., & Reddy, K. N. K. (**2010**). Strength and workability of low lime fly-ash based geopolymer concrete. Indian Journal of Science and Technology, 3(12).

Wang, S.-D., Scrivener, K. L., & Pratt, P. L. (**1994**). Factors affecting the strength of alkali-activated slag. Cement and Concrete Research, 24(6), 1033–1043. doi:10.1016/0008-8846(94)90026-4

Wang, S.D., Scrivener, K.L. (**1995**). Hydration products of alkali-activated slag cement. Cem. Concr. Res. 25 (3), 561–571.

Wang, W., Wang, H., & Lo, M. (**2015**). The fresh and engineering properties of alkali activated slag as a function of fly ash replacement and alkali concentration. Construction And Building Materials, 84, 224-229. doi: 10.1016/j.conbuildmat.2014.09.059

Wattimena, O. K., Antoni, & Hardjito, D. (**2017**). A review on the effect of fly ash characteristics and their variations on the synthesis of fly ash based geopolymer. In AIP Conference Proceedings (Vol. 1887, No. 1, p. 020041). AIP Publishing LLC.

Wiedema B. (**2008**). Avoiding co-product allocation in life-cycle assessment. J. Ind. Ecol. 4:11–33

Xiao, R., Ma, Y., Jiang, X., Zhang, M., Zhang, Y., Wang, Y., & He, Q. (**2020**). Strength, microstructure, efflorescence behavior and environmental impacts of waste glass geopolymers cured at ambient temperature. Journal of Cleaner Production, 252, 119610.

Yang, W., Yu, G.,Tan, S.K., and Wang, H., (**2014)**, Rheological properties of dense natural cohesive sediments subject to shear loadings, International Journal of Sediment Research 29, 454-470

Yang, Z.X., Ha, N.R., Hwang, K.H. and Lee, J.K. (**2009b**). 'A study of the performance of a concrete sludge-based geopolymer', J Ceram Process Res 10, s72–s74.

Yang, Z.X., Ha, N.R., Jang, M.S. and Hwang, K.H. (**2009a**). 'Geopolymer concrete fabricated by waste concrete sludge with silica fume', Mater Sci Forum 620–622, 791–794.

Yang, Z.X., Ha, N.R., Jang, M.S., Hwang, K.H. and Lee, J.K. (**2009c**). 'The effect of SiO2 on the performance of inorganic sludge-based structural concretes', J Ceram Process Res 10, 266–268.

Yıldırım, G., Kul, A., Özçelikci, E., Şahmaran, M., Aldemir, A., Figueira, D., & Ashour, A. (**2020**). Development of alkali-activated binders from recycled mixed masonry-originated waste, Journal of Building Engineering, doi: https://doi.org/10.1016/j.jobe.2020.101690.

Yip C.K., Lukey G.C., van Deventer J.S.J., (**2005**). The coexistence of geopolymeric gel and calcium silicate hydrate at the early stage of alkaline activation. Cement Concrete Res. 2005;35:1688-1697.

Yip, C. K., & van Deventer, J. S. J. (**2003**). Journal of Materials Science, 38(18), 3851 3860. doi:10.1023/a:1025904905176

Yunsheng, Z., We, S., Zuquan, J., Hongfa, Y., Jia, Y. (**2007**). In situ observing the hydration process of K-PSS geopolymeric cement with environment scanning electron microscopy. Mater Lett.61:1552–7.

Zaharaki, D.; Galetakis, M.; Komnitsas, K. (**2016**). Valorization of construction and demolition(C&D) and industrial wastes through alkali activation, Construction and Building Materials, 121, 686–693.

Zhang C., Hou Z., Chen C., Zhang Y., Viktor Mechtcherine, Zhengming Sun. (**2019b**). Design of 3D printable concrete based on the relationship between flowability of cement paste and optimum aggregate content, Cement and Concrete Composites, Volume 104, 103406, ISSN 0958-9465, https://doi.org/10.1016/j.cemconcomp.2019.103406.

Zhang YS, Sun W, Li ZJ. (**2005**). Hydration process of potassium polysialate (K-PSDS) geopolymer cement. Adv Cem Res;17(1):23–8.

Zhang, B., MacKenzie Kenneth JD, Brown Ian WM. (**2009**) Crystalline phase formation in metakaolinite geopolymers activated with NaOH and sodium silicate. Journal of Master Science; 44:4668–76.

Zhang, J., Li, S., Li, Z., Zhang, Q., Li, H., Du, J., & Qi, Y. (**2019**). Properties of fresh and hardened geopolymer-based grouts. Ceramics–Silikáty, 63(2), 164-173.

Appendix 6 – Thesis Originality Report

Şablona uygun olarak hazırlanan "Orijinallik Raporu"nun imzalı hali bu bölümde verilmelidir.